A Unique Role for Sarcolemmal Membrane Associated Protein Isoform 1 (SLMAP1) as a Regulator of Cardiac Metabolism and Endosomal Recycling.

By:

Aaraf Dewan

A thesis submitted to the Faculty of Graduate and Postdoctoral Studies in partial fulfillment of the requirements of the M.Sc. degree in Cellular and Molecular Medicine

Department of Cellular and Molecular Medicine

Faculty of Medicine

University of Ottawa,

Ottawa, Ontario, Canada

Abstract:

Altered glucose metabolism is the underlying factor in many metabolic disorders, including diabetes. A novel protein recently linked to diabetes through animal and clinical studies is Sarcolemmal Membrane Associated Protein (SLMAP) but its role in metabolism remains undefined. The data here reveals a novel role for SLMAP isoform1 in glucose metabolism within the myocardium. Neonatal cardiomyocytes (NCMs) harvested from hearts of transgenic mice expressing SLMAP1, presented with increased glucose uptake, glycolytic rate, as well as glucose transporter 4 (GLUT4) expressions with minimal impact on lipid metabolism. SLMAP1 expression markedly increased the machinery required for endosomal trafficking of GLUT4 to the membrane within NCMs, accounting for the observed effects on glucose metabolism. The data here indicates SLMAP1 as a unique regulator of glucose metabolism through endosomal regulation of GLUT4 trafficking and suggests it may uniquely serve as a target to limit cardiovascular disease in metabolic disorders such as diabetes.

Table of Contents

LIST OF TABLES

LIST OF FIGURES

LIST OF ABBREVIATIONS

2DG	2-Deoxy glucose
AGE	Advanced glycated end product
ALDH2	Aldehyde dehydrogenase 2
AMP	Adenosine monophosphate
AMPK	AMP-activated protein kinase
ATP	Adenosine triphosphate
BCA	Bicinchoinic acid
BSA	Bovine serum albumin
CAD	Coronary artery disease
CAMKII	Calcium calmodulin kinase II
CD36	Cluster differentiation 36
CPT-1	Carnitine palmitoyltransferase-1
DAPI	4',6-Diamidino-2-phenylindole
DMEM	Dulbecco's modified eagle medium
ECAR	Extracellular acidification rate
EE	Early endosome
EEA1	Early endosome antigen 1
ER	Endoplasmic reticulum
ERC	Endosomal recycling compartment
ETC	Electron transport chain
FBS	Fetal bovine serum
FFA	Free fatty acid
GLUT	Glucose transporter
GSV	GLUT4 storage vesicle
GTP	Guanine triphosphate
HBSS	Hank's balanced salt solution
IKKβ	Inhibitor of nuclear factor kappa-beta kinase subunit beta
IRS	Insulin receptor substrate
NMCM	Neonatal mouse cardiomyocytes
OCR	Oxygen consumption rate
PBS	Phosphate buffered saline
PDK	Phosphoinostide-dependant kinase
P-I3K	Phosphoinositide 3-kinase
PIP3	Phosphotidylinositol 3, 4, 5-triphosphate
PKCβ2	Protein kinase C beta 2
PPAR	Peroxisome proliferator-activated receptor
qPCR	Quantitative polymerase chain reaction
ROS	Reactive oxygen species
SLMAP	Sarcolemmal membrane associated protein
SNAP	Synaptosomal-associated protein
SNARE	Soluble N-ethylmaleimide-sensitive factor activating protein receptor
SR	Sarcolemmal reticulum
TBST	Tris-buffered saline with Tween20
TCA	Tricarboxylic Acid

TfR	Transferrin receptor
TGN	Trans-golgi network
VAMP	Vesicle associated membrane protein

ACKNOWLEDGEMENTS:

I would like to thank my supervisor Dr. Balwant Tuana for always reminding me to focus. His mentorship has helped me grow as a person and the lessons I have learned under his supervision have helped nurture my love for science and innovation. Through his support and guidance, I learned the importance of protecting scientific ideas through intellectual property and how crucial a role that plays in the field of science, helping me in deciding to pursue a career in law to protect the interests of scientists as an intellectual property lawyer.

I would like to give my sincere gratitude to all members of the Tuana lab, for their time and help with completing this project. After these last three years, I think of my fellow lab members like family. Maysoon Salih was always like a mother, looking out for us and always being there to give advice and help troubleshoot our problems. Jennifer Major was like an older sister, sharing her wisdom with me about all the ins and outs of graduate school having recently completed it all herself. Finally, Taha Rehmani was like a brother, laughing and celebrating with me when times were great, and helping to pick me up when times were rough. I would also like to acknowledge Dr. Mary-Allen Harper and her lab for allowing me the use of their Seahorse XF^e24 Flux Bioanalyzer.

I would also like to thank my best friend and girlfriend, Niki Dignard, for always being the supportive rock I need to be able to get through anything, my strength and resilience comes from the love that she has given me. Finally, and most important, I would like to thank my mom, Quamrunnesa Dewan, who loved, supported, and pushed me to succeed. Growing up she taught me the importance of hard work through her own strength, resolve, and work ethic. I would not be where I am today if not for her.

CHAPTER 1: Introduction

1.1 Heart function in the healthy and diabetic heart

The cardiovascular system is often referred to as the body's "highway" for nutrient and hormone delivery, with the heart at the center of this system. In Canada, heart disease is the second leading cause of death (Statistics Canada, 2014) and has taxed the healthcare system through increased hospitalization (Public Health Agency of Canada, 2009) and drug prescription rates (IMS Brogan, 2011). Diabetes is one of the greatest risk factors for cardiovascular disease and is the 6th leading cause of death (Statistics Canada, 2014). Between the years of 2008 and 2009, 2.4 million Canadian patients were diagnosed with diabetes, with this number having grown since (Public Health Agency of Canada, 2011). With this rising epidemic, research into the underlying mechanisms involved in diabetes is becoming crucial. By further understanding the mechanisms causing the onset of pathology in diabetes, we can potentially reveal new molecular targets for treating or preventing the disease.

Type I diabetes is characterized by loss of pancreatic β-cell function, leading to a hypoinsulineamic and hyperglycemic state. In contrast, Insulin resistance, hyperglycemia, and glucose intolerance characterize type II diabetes. Following insulin resistance, the pancreatic β-cells in type II diabetes compensate by increasing insulin production, creating a hyperinsulinemic state. Following this, the β-cells either sustain the hypersulinemia, or begin to deteriorate from over-stimulation, leading to decreased insulin production and insulin-dependent diabetes (McGarry, 2002). Type II diabetes is the most prevalent form of the disease, largely due to its link with obesity, another disease plaguing 2.1 billion people worldwide (U.S. Department of Agriculture and U.S. Department of Health and Human Services, 2011). The hormonal and metabolic changes associated with both type I and II diabetes eventually cause complications in

various organs which can lead to death. The most common organ complication is diabetic heart disease (Boudina & Adel, 2007).

The systemic environment in diabetes creates many risk factors for heart disease like hypertension and coronary artery disease (CAD). Although, these comorbidities are not the sole cause of heart disease in patients as diabetics without hypertension or CAD still present with heart failure (Rubler, et al., 1972). The risk for heart disease is also greater in diabetic patients than patients with hypertension and CAD alone (de Simone, et al., 2010). These findings suggest that there are underlying factors in diabetes outside of hypertension and CAD that lead to the development of diabetes. Due to this phenomenon, the term "diabetic cardiomyopathy" was coined in order to define the ventricular dysfunction that is unattributed to hypertension or CAD.

Diabetic cardiomyopathy causes structural and functional alterations which impact cardiac physiology. The heart cycles through two states, systole and diastole. During systole the heart ventricles are in a state of contraction, pumping blood out to the entire body. In diastole, the ventricles are in a state of relaxation, filling up with blood prior to systole. Cycling through these two states allows the heart to meet the blood supply demand for the whole body. In diabetic heart disease, both systolic and diastolic functions are compromised, leading to the inadequate cardiac output. Diastolic dysfunction, characterized by muscle stiffness, normally presents early in diabetic cardiomyopathy (Devereux, et al., 2000). Systolic dysfunction (depressed contraction) will normally present later on in the disease progression, although slight alterations in systolic function present early in 24% of diabetic patients without CAD (Fang, et al., 2005). These efficiency deficits in heart function activate compensatory heart remodelling processes known as cardiac hypertrophy.

Cardiac hypertrophy is commonly found in diabetic patients (Devereux, et al., 2000), characterized most commonly as a thickening of the left ventricular walls. Chronic persistence of systolic and diastolic dysfunction lead to pathological hypertrophy where the heart's ability to pump blood steadily declines until heart failure ensues. Left ventricular hypertrophy accompanied by heart failure is typically the end result of diabetic cardiomyopathy, which precedes death. Understanding the molecular mechanisms leading to onset of this pathology will provide for better outcomes for those afflicted.

The Framingham study reported that glycaemic control correlated with cardiac hypertrophy in diabetic patients (Kannel & McGee, 1979). This correlation was independent of hypertension, suggesting that the hyperglycemic environment brought on by diabetes may play a role in the onset of cardiomyopathy. In order to understand how hyperglycemia can lead to onset of cardiomyopathy, a systematic approach to investigating the changes in cellular and molecular signalling which impact cardiac metabolism has been implemented. .

1.2 Metabolism plays a pivotal role in pathological states

Accounting for ~10% of systemic metabolism and burning ~400kcal/kg/day (McClave & Snider, 2001), the heart is one of the most metabolically demanding organs. This makes metabolic regulation of great importance to cardiovascular health. The energy expenditure of a healthy heart is derived 70% from fatty acid oxidation and 30% coming from glucose metabolism (Stanley, et al., 2005). Myocardium metabolic regulation is impaired in disease states such as diabetes, leading to various pathological outcomes including diabetic cardiomyopathy. In diabetic patients a shift in metabolism occurs which leads to a suppression of glycolysis and an increase of fatty acid oxidation (Scheuermann-Freestone, et al., 2003). This leads to decreased cardiac efficiency and an increase in toxic metabolites formed during fatty acid oxidation,

contributing to the onset of diabetic cardiomyopathy (How, et al., 2006). The shift in metabolism, inevitably leads to oxidative stress, a common symptom of most cardiac pathologies (Elahi, et al., 2009) and ultimately causes cellular and molecular changes like impaired calcium handling, hypertrophy, apoptosis, and fibrosis which impair heart function (Bugger & Abel, 2014; Hafstad, et al., 2013; Ungvári, et al., 2005).

Antioxidant therapy was originally believed to be protective against oxidative damage in cardiac pathologies, although recent data indicates that these therapies produce no therapeutic benefit (Hafstad, et al., 2013). Further, lacking spatio-temporal knowledge of reactive oxygen species (ROS) makes it difficult to produce more directed therapies to combat oxidative damage (Hafstad, et al., 2013). Thus focus on providing therapy in these pathologies shifts to a preventative approach, targeting and modulating the underlying impaired cardiac metabolism in order to prevent oxidative damage from accumulating.

1.2.1 Cardiac metabolism

In order for fatty acids to enter cardiomyocytes, they must be in a "free fatty acid" (FFA) state, which is a monomer form not conjugated to glycerol. While glucose can only enter cardiomyocytes through facilitative transporters, FFAs can enter passively or through a facilitative transporter known as cluster of differentiation 36 (CD36). Deletion of CD36 leads to a 50%-60% reduction in FFA uptake, suggesting that the majority of FFA enters the cell through this transporter (Kuang, et al., 2004). Following cell entry, FFAs in the cytosol must become conjugated with acyl-CoA and carnitine by acyl-CoA synthase and carnitine palmitoyltransferase-1 (CPT-1) respectively in order to be utilized by the cell (Wisneski, et al., 1987). Carnitine addition is a key rate limiting step for the entry of FFAs into the mitochondria and their subsequent oxidation (Kerner & Hoppel, 2000) and thus is tightly regulated by the

energy sensor AMP-activated protein kinase (AMPK) (Dyck & Lopaschuk, 2006). Carnitine addition is regulated indirectly via CPT-1 inhibitor malonyl-CoA (Paulson, et al., 1984). When ATP is abundant in the cell, malonyl-Coa is actively synthesized by acytel-CoA carboxylase (ACC), which inhibits CPT-1 from allowing entry of FFAs into the mitochondria. When ATP levels are scarce, AMP accumulates, activating AMPK, which inhibits malonyl-CoA synthesis by ACC, leading to the activation of CPT-1, and FFA entry into the mitochondria.

Upon entry into the mitochondria, FFAs undergo β-oxidation, a process which produces NADH and $FADH_2$, which are reducing equivalents used to generate ATP through the electron transport chain (ETC) (Houten & Wanders, 2010). Acetyl-CoA is also produced by this process and is fed into the tricarboxylic acid (TCA) cycle to further produce reducing equivalents for ATP production. Approximately 60-90% of mitochondrial acetyl-CoA is produced through β-oxidation, while 10%-40% is generated through pyruvate metabolism (Stanley, et al., 1997; Gertz, et al., 1988; Wisneski, et al., 1985). CD36, CPT-1, and enzymes involved in β-oxidation are regulated by the presence of FFAs through highly expressed nuclear receptors known as peroxisome proliferator-activated receptors (PPARs) (Yang & Li, 2007; Huss & Kelly, 2004).

Unlike FFAs, glucose can't passively diffuse across the cell membrane and can only enter cardiomyocytes through facilitative glucose transporters (GLUTs). Upon entry into the cell, glucose immediately becomes phosphorylated through hexokinase (Ren, et al., 1993), a rate-limiting step which prevents it from being recognized by GLUTs, and thus limiting exit from the cell. Following this, glucose-6-phosphate undergoes multiple enzymatic steps for conversion to pyruvate, the final product of glycolysis. Within the cytosol, pyruvate undergoes fermentation through lactate dehydrogenase into lactic acid, but within the mitochondria, pyruvate is converted to Acetyl-CoA to enter the TCA cycle (Heather & Clarke, 2011). The anaerobic nature

of glycolytic metabolism serves a very important purpose for energy generation when blood flow to the heart is obstructed in conditions like ischemia or CAD, two very common co-morbidities often noted in diabetic patients.

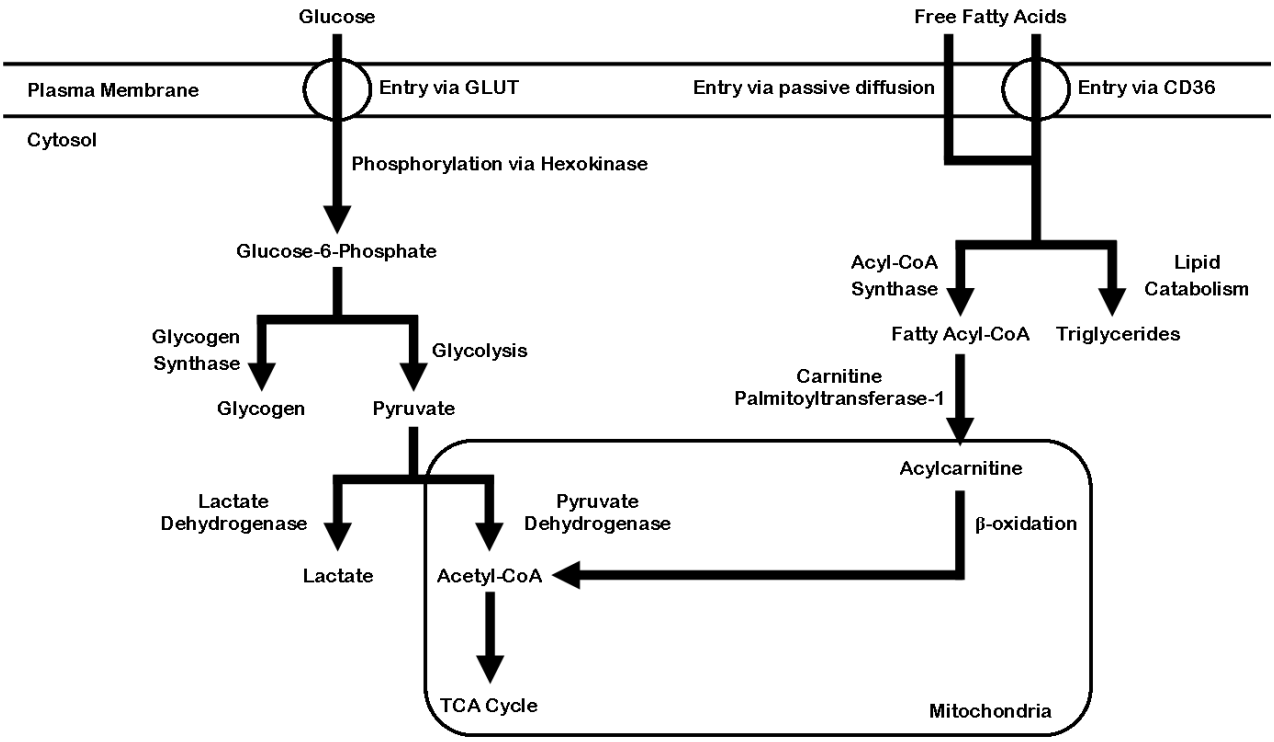

Figure 1. *Overview of glucose and fatty acid metabolism in cardiomyocytes.* Glucose enters via GLUT1 or GLUT4 and undergoes conversion into pyruvate through glycolysis in the cytosol. Pyruvate is then transported into the mitochondria and is converted into Acetyl CoA for feeding into the TCA cycle and subsequent generation of reducing equivalents for the ETC. Fatty acids enter the cell through passive diffusion or via CD36 and then undergo β-oxidation for the generation of Acetyl-CoA for feeding into the TCA cycle.

1.2.2 Metabolic complications in diabetes

The importance of metabolic balance between lipid and glycolytic metabolism is exemplified in diabetes, where enhanced lipid oxidation and impaired glucose metabolism ultimately lead to the generation of ROS and oxidative damage. Type II diabetic patients present with increased H_2O_2 production, depleted glutathione, and mitochondrial dysfunction within atrial tissue (Anderson, et al., 2009). These patients also show a decrease in their maximal ability to oxidize fatty acids and glutamate (Anderson, et al., 2009). Further, when comparison of diabetic patients and obese patients revealed that both presented with atrial contractile dysfunction, but only diabetic patients presented with mitochondrial dysfunction and oxidative stress (Montaigne, et al., 2014). This suggests that hyperglycemia and insulin resistance may be an important contributor for oxidative stress present in diabetic.

1.2.3 Effects of hyperglycemia in pathology

The hyperglycemia in diabetes leads to molecular alterations, which eventually cause the functional changes associated with diabetic cardiomyopathy. Within the diabetic heart, not only is glucose uptake decreased, so is glucose metabolism. This leads to build up of glucose, which when unutilized, can lead to non-enzymatic glucose-mediated modifications (Singh, et al., 2001). These glucose modifications can continue to propagate and form many by-products, ultimately leading to the formation of compounds known as advanced glycated end products (AGEs) (Singh, et al., 2001). AGEs are proteins that have undergone glycation multiple times. Proteins that are turned into AGEs typically become non-functional, although there are many other properties about AGEs which lead to impacts on cell biology. AGEs can form cross-links between proteins, leading to aggregation and a subsequent impairment of degradation of these proteins (Goldin, et al., 2006). Pharmaceutical inhibition of AGEs aid the prevention of cardiac fibrosis and stiffening in diabetic animals (Norton, et al., 1996; Candido, et al., 2003).

Furthermore, glucose mediated modifications to calcium transporters and CAMKII, a major regulator of calcium in the heart, have been implicated in the impairment of calcium handling seen in diabetic hearts (Kranstuber, et al., 2012; Erickson, et al., 2013; Ai, et al., 2005)**.**

Another link between hyperglycemia and CAMKII activation is through the activation of the Na^+/H^+ exchanger by lactic acid production (Nakamura, 2004). When this transporter activates, the influx of sodium forces the Na^+/Ca^{2+} exchange to expel sodium from the cell in order to maintain the sodium gradient, leading to a subsequent influx of Ca^{2+}, which then activates CAMKII (Williams & Howard, 1994). Interestingly, the effects of hyperglycemia on membrane ion transporters also have also been linked to oxidative damage through the sodium/glucose co-transporter (SGLT1). Hyperglycemic conditions mediate the generation of ROS, but upon treatment with the SGLT1 inhibitor phrolizin ROS generation is prevented (Balteau, et al., 2011). It should be noted the ROS prevention was not achieved through the inhibition of glucose influx, as the inhibition of other glucose transporters through phloretin did not prevent ROS generation (Balteau, et al., 2011). Rather, the inhibition of sodium influx is the culprit, which as discussed previously, ultimately leads to the activation of Na^+/Ca^{2+} exchanger, increasing intracellular calcium and activating CAMKII. The link between CAMKII and ROS generation is hypothesized to be mediated through PKCβ2 (Liao, et al., 2013), a kinase which activates a potent superoxide generator, NADPH oxidase (Nox2), under hyperglycemic conditions (Balteau, et al., 2011; Serpillon, et al., 2009; Wang, et al., 2013).

1.2.4 Oxidative damage in pathology

In addition to cytosolic ROS, mitochondrial ROS may be responsible for the majority of oxidative damage present in diabetes and is present in many patients and animal models. In support of mitochondrial ROS, the inhibition of ETC complexes I and II led to a complete

reduction of excess ROS in diabetic cardiomyocytes (Ye, et al., 2004). Further, cardiac overexpression of catalase, an antioxidant enzyme involved in the elimination of mitochondrial ROS, protected diabetic hearts from morphological and contractile changes (Ye, et al., 2004). Interestingly, hyperglycemia-mediated cytosolic ROS can drive mitochondrial ROS via the inhibition of mitochondrial aldehyde dehydrogenase 2 (ALDH2) (Wang, et al., 2011), an enzyme which prevents oxidative stress through the conversion of reactive aldehydes into unreactive carboxylic acids (Choi, et al., 2011). These findings suggest hyperglycemia to have a two-pronged effect on myocardial oxidative stress through generation of both cytoplasmic and mitochondrial ROS.

One of the major causes for the decreased glucose metabolism in diabetes is due to a decrease in glucose uptake (Desrois, et al., 2004). Glucose is unable to cross the cell membrane without the aid of glucose transporters (GLUT). The primary carrier of glucose in muscle and heart cells is glucose transporter 4 (GLUT4) and its expression and localization is altered in the diabetic myocardium (Ménard, et al., 2010; Chen & Ding, 2011). The GLUT4 content in the cell membrane is a rate limiting step in glucose uptake (Liu, et al., 1993). Loss of function (ie. deletion of GLUT4) in muscle leads to insulin resistance and impaired glucose tolerance (Zisman, et al., 2000), while overexpression of GLUT4 results in increased insulin sensitivity and protection against insulin resistance (Tozzo, et al., 1997; Ikemoto, et al., 1995). It is believed that upregulation of GLUT4 levels would beneficially impact glucose metabolism and could be used to treat diabetes and other metabolic diseases.

1.3 Regulation of GLUT4 trafficking through endocytic and exocytic functions

GLUT4 is trafficked within the cell through various compartments. Under basal conditions, less than 10% of GLUT4 resides in the plasma membrane (Huang & Czech, 2007), where it allows

for facilitative transport of glucose. The majority of GLUT4 resides within the endosomal recycling compartment (approximately 40-50%) (Martin, et al., 1996), and the Trans-Golgi network and GLUT4 storage vesicles (GSV) (approximately 50-60%) (Zeigerer, et al., 2002). Due to the large retention of GLUT4 in the endosome, recycling of GLUT4 is of great importance in cellular regulation of GLUT4 levels. A variety of proteins are involved in the intracellular trafficking and membrane fusion of these vesicles with the plasma membrane (Bryant, et al., 2002). In muscle cells, endocytosis of GLUT4 has been demonstrated to be mediated by both clathrin-dependant and clathrin-independent-cholesterol-dependant internalization mechanisms (Antonescu, et al., 2008). In the context of the cardiomyocyte, endosomal GLUT4 sorting has yet to be extensively studied but may provide us with novel mechanisms of regulation of glucose metabolism in the myocardium.

1.3.1 The internalization of GLUT4 at the plasma membrane

Endocytosis is a fundamental process for the maintenance of cell size, as well as balancing intracellular and extracellular pools of membrane proteins. Endocytosis occurs through one of two routes: Clathrin-mediated or clathrin-independant pathways involving lipid domains with or without caveolin or flotillin (Doherty & McMahon, 2009). Endocytic routes of GLUT4 differs between cell types, adipocytes predominantly undergo endocytosis through cholesterol mediated pathways (Blot & McGraw, 2006) whereas muscle cells favour clathrin or interleukin receptor (IL-2Rβ) endocytosis (Antonescu, et al., 2009; Antonescu, et al., 2008). Specific amino acid sequences on the cytosolic tail of GLUT4 have been identified which control its internalization. The LL^{490} motif encodes for the clathrin-mediated endocytosis of GLUT4 and variants expressed in muscle cells without this motif can only undergo endocytosis through the interleukin pathway (Planas, et al., 2000). The F^{5}QQI motif is also present on the cytosolic tail and shares sequence

homology to other motifs which are responsible for clathrin mediated endocytosis (Antonescu, et al., 2009). This motif also regulates the post-golgi/endosomal sorting of GLUT4 into insulin sensitive compartments (Bernhardt, et al., 2009).

Regulation of GLUT4 endocytic rates also differs between cell types. In adipocytes, insulin stimulation reduces GLUT4 endocytosis by inhibiting cholesterol endocytic routes and diverting traffic to the lesser used clathrin endocytic route (Shigematsu, et al., 2003; Jhun, et al., 1992). In contrast, GLUT4 internalization rates are unaltered by insulin in muscle cells (Foster, et al., 2001; Wijesekara, et al., 2006) or cardiomyocytes (Yang & Holman, 2005), but insulin does increase the cell surface localization of GLUT4 through increased exocytosis. Although, it should be noted that other stimuli which effect GLUT4 cell surface localization do have effects on GLUT4 internalization in muscle. Membrane depolarization during muscle contraction elevates membrane GLUT4 content through a large reduction of endocytosis, with only a small increase in exocytosis (Wijesekara, et al., 2006). Hypertonicity disrupts the organization of clathrin pits at the plasma membrane, thereby inhibiting clathrin mediated endocytosis of GLUT4 (Antonescu, et al., 2008). Further, changes in oxidative metabolism also reduces the rate of GLUT4 endocytosis through the IL-2Rβ route in through the activation of AMPK (Yang & Holman, 2005; Patel, et al., 2001).

1.3.2 Intracellular GLUT4 trafficking

Much like most membrane proteins, GLUT4 is extremely stable, with a half-life of 48 hours (Sargeant & Pâquet, 1993). Thus, each GLUT4 molecule will be recycled multiple times prior to lysosomal sorting and subsequent degradation. Under basal conditions, GLUT4 accumulates in peripheral vesicle and perinuclear regions (Ploug, et al., 1998; Schertzer, et al., 2009). These two regions represent the two major compartments by which GLUT4 is sorted into: GLUT4 storage

vesicles (GSVs) and the endosomal recycling compartment (ERC) respectively. GSVs are an insulin responsive compartment (Zeigerer, et al., 2002) and common vesicle markers for this compartment are Vesicle-associated membrane protein 2 (VAMP2) (Martin, et al., 1996), Insulin regulated aminopeptidase (IRAP) (Subtil, et al., 2000), sortilin (Shi, et al., 2005), tether containing a UBX domain for GLUT4 (TUG) (Yu, et al., 2007), and low-density lipoprotein receptor-related protein 1 (LRP1) (Jedrychowski, et al., 2010). Another hallmark trait of this compartment is the absence of transferrin receptor (TfR) (Zeigerer, et al., 2002), in contrast to GLUT4 compartments in the ERC which do contain TfR, Rab5, and Rab11 (Zeigerer, et al., 2002; Aledo, et al., 1997). Finally, a small portion of GLUT4 is also found in the Trans-Golgi Network (TGN) which also contains Syntaxin-6 and Syntaxin-16 (Zeigerer, et al., 2002; Shewan, et al., 2003) Interestingly this compartment does not contain other common TGN markers like furin or TGN38, suggesting its presence as a unique TGN subcompartment.

GLUT4 containing compartment	Compartment protein markers	References
GLUT4 storage vesicles (GSVs)	Vesicle-associated membrane protein 2 (VAMP2)	(Martin, et al., 1996)
	Insulin regulated aminopeptidase (IRAP)	(Subtil, et al., 2000)
	Sortilin	(Shi, et al., 2005)
	Tether containing a UBX domain for GLUT4 (TUG)	(Yu, et al., 2007)
	Low-density lipoprotein receptor-related protein 1 (LRP1)	(Jedrychowski, et al., 2010)
	Rab8a Rab8b Rab10 Rab14	(Ishikura & Klip, 2008)
Endosomal Recycling Compartment (ERC)	Transferrin receptor (TfR)	(Zeigerer, et al., 2002)
	Rab5 Rab11	(Aledo, et al., 1997)
Trans-golgi network (TGN)	Syntaxin-6 Syntaxin-16	(Shewan, et al., 2003)

Table 1. *Overview of intracellular GLUT4 containing compartments.* Protein markers used for the identification of these compartments are listed.

1.3.3 Theoretical models for GLUT4 trafficking

Under basal conditions, GLUT4 is dynamically trafficked through intracellular compartments, with a small percentage recycling to the plasma membrane at any given time, insulin stimulation increases this rate. Two theoretical models are used to describe this GLUT4 distribution maintenance: the static retention model and the dynamic recycling model.

The static retention model states that under basal conditions, GLUT4 resides mainly within GSVs and the TGN acts as the primary intermediate compartment for its intracellular sorting and idle plasma membrane recycling. Indeed, the $TE^{499}LE^{501}Y$ motif of GLUT4 acts as a molecular signal for its transition from endosomes to a specialized TGN subcompartment (Shewan, et al.,

2003). This model also assumes that a portion of GLUT4 is sequestered and does not cycle into the plasma membrane without a stimulus like insulin or membrane depolarization. Supporting this model, single molecule imaging of GLUT4 within adipocytes revealed statically retained compartments under basal conditions (Fujita, et al., 2010), supporting this model. Further, kinetic analysis of basal GLUT4 plasma membrane content revealed only 10% of GLUT4 in adipocytes reached the plasma membrane while 61% incorporated in muscle cells (Fazakerley, et al., 2010). This study is limited by the timeframe used for imaging which (180 minutes) may have been too short for the completion of slow recycling processes, but these studies do suggest that the static retention model may be more representative for adipocyte GLUT4 trafficking than for muscle GLUT4 trafficking.

The dynamic recycling model states that the intermediate compartment for intracellular GLUT4 trafficking is the ERC and that all GLUT4 molecules can slowly be recycled to the plasma membrane under resting conditions. This model is supported by experimental data revealing that intracellular GLUT4 vesicles continually undergo fusion and fission with the ERC, allowing for slow plasma membrane recycling under basal conditions (Karylowski, et al., 2004). Further, while internalization of GLUT4 is unaffected by insulin stimulation, the recycling traffic through the ERC is greatly accelerated in muscle cells (Foster, et al., 2001). The conflicting results between these two models may be attributed to differences in experimental conditions such as cell confluence (Muretta, et al., 2008), in truth, physiological GLUT4 trafficking most likely utilizes both models such that traffic can dynamically pass through both the TGN and ERC as needed.

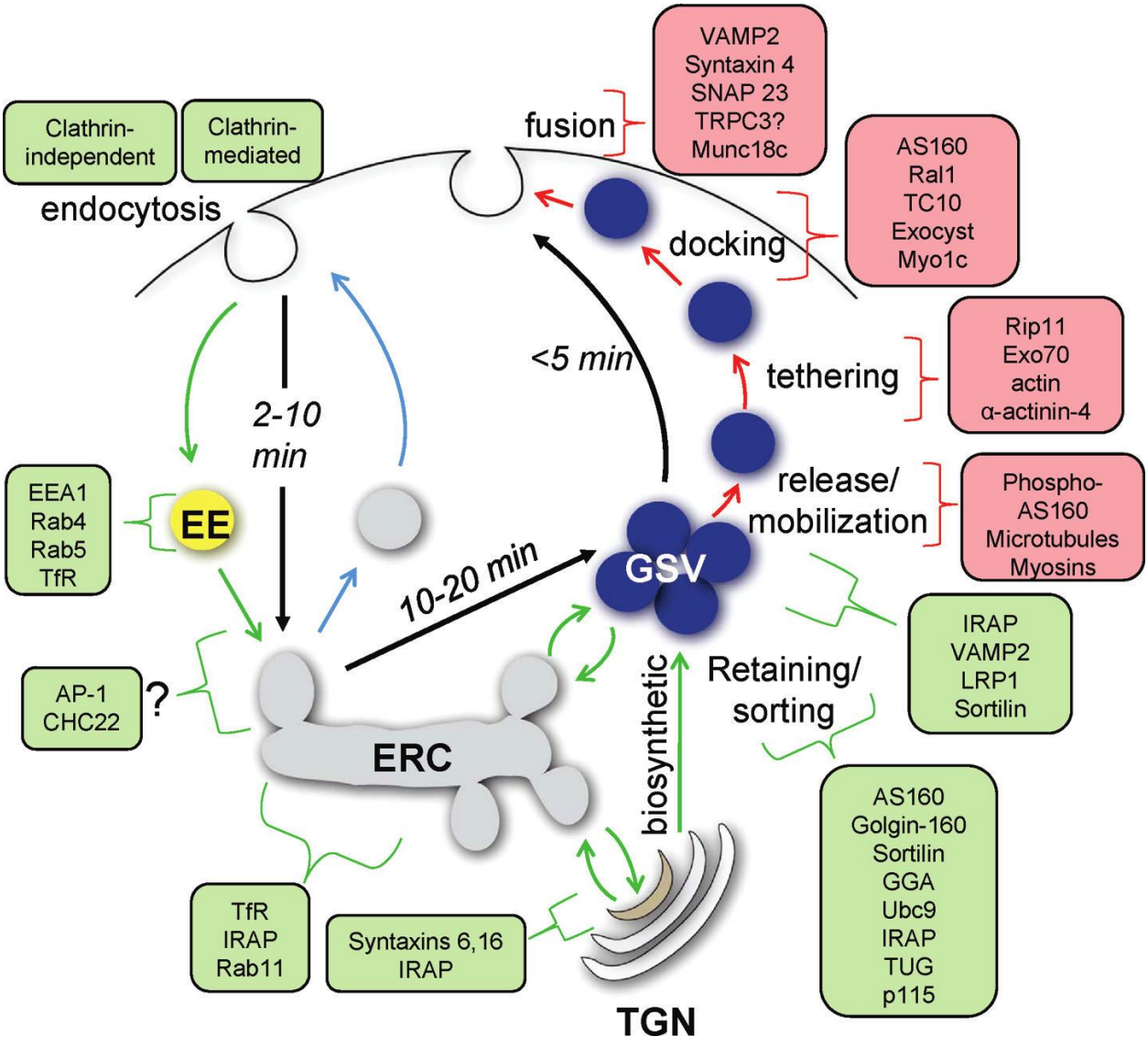

Figure 2. *Overview of proteins involved in the recycling of GLUT4 traffic.* Newly synthesized GLUT4 is delivered fro the trans-golgi network (TGN), directly to GLUT4 storage vesicles (GSV), where they then mobilize to the plasma membrane upon insulin stimulation. Following endocytosis via clathrin or cholesterol mediated mechanisms, vesicles are sorted into sorting endosomes (EE) and then recycled directly to the plasma membrane or sent to the ERC for slow recycling to the plasma membrane, or redirection into GSVs. Figure reprinted with permission from (Foley, et al., 2011). Copyright (2011) American Chemical Society.

1.3.4 Role of Rab proteins in GLUT4 trafficking

Intracellular GLUT4 traffic and sorting is regulated through the Rab superfamily of GTPases (Stenmark, 2009; Kaddai, et al., 2008; Foley, et al., 2011). Rabs act as molecular switches which, when bound to GTP, recruit effector proteins to mediate fusion, fission, and trafficking. Upon internalization of GLUT4, vesicles fuse with Rab5 and early endosome antigen 1 (EEA1) containing early endosomes within two minutes (Foster, et al., 2001; Aledo, et al., 1997), suggesting that at least the initial destinations may be similar between different internalization routes. Interestingly, Rab5 inhibition increased cell surface GLUT4 content with no noted effects on the insulin-stimulated release of GLUT4 (Huang, et al., 2001). Taken together these findings suggest the involvement of Rab5 in early endosomal sorting of GLUT4. Further, insulin stimulation inhibits Rab5 activation (Huang, et al., 2001) in order to redirect GLUT4 traffic from endosomal sorting pathways into secretory pathways.

Early endosomes continually fuse with one another in order to become sorting endosomes, where incoming cargo is accepted approximately 5-10 minutes following internalization (Presley, et al., 1997; Johnson, et al., 1993). . Rabaptin-5, a Rab5 effector protein, begins the early endosomal fusion process by binding to Rab5 on two different vesicles, allowing for the tethering of the two endosomes to one another (Zhu, et al., 2004). Next, Rab5 recruits early endosomal antigen 1 (EEA1), an endosomal tether, which allows for endosomal docking and recruitment of the SNARE family of fusion proteins fusion proteins (Christoforidis, et al., 1999). Within endosomes, the proteins involved in forming these SNARE complexes are SNAP23, Syntaxin-4, and VAMP-2 (Chen & Whiteheart, 1999; Band, et al., 2002; Ramm, et al., 2000). Most notably, these proteins play a pivotal role in the translocation of GLUT4 into the plasma membrane (Kupriyanova, et al., 2002). These sorting endosomes target molecules to one of three

destinations: the plasma membrane, the ERC, or the late endosome. While plasma membrane internalization of GLUT4 is directed by motifs present at the cytosolic tail, sorting endosome traffic is determined predominantly through the geometry of the early endosomal organelle (Dunn, et al., 1989) (Mayor, et al., 1993), not signaling sequences. Vesicles containing proteins targeted for recycling destinations (the plasma membrane or the ERC) undergo fission as narrow tubules which have a higher membrane surface area to lumen ratio (Dunn, et al., 1989; Mayor, et al., 1993). This mechanism of sorting, provides GLUT4, and other membrane proteins, with long half-lives, as most membrane lipids and proteins are conserved during each round of sorting. Vesicles which bud from these sorting endosomes can either undergo fast recycling directly to the plasma membrane through Rab4 (Ward, et al., 2005), or indirect slow recycling via Rab11 with transit through the ERC as an intermediate step (Moore, et al., 2004). In some cell types, like neurons and cardiomyocytes, the ERC is a collection of tubular organelles associated with microtubules contained at the microtubule-organization centre (Grant & Donaldson, 2009). Most molecules in the ERC eventually return to the plasma membrane, although the ERC can direct traffic to alternate routes as well. Rab11 and EH-domain containing protein 1 (EHD1) are important proteins which regulate transport from the ERC and alterations to these proteins effect transport to the TGN and plasma membrane (Lin, et al., 2001; Caplan, et al., 2000). Interestingly, GLUT4 becomes sequestered to the ERC and is incapable of transitioning onto GSVs when the activities of either Rab11 (Zeigerer, et al., 2002) or IRAP (Jordens, et al., 2010) are impaired. Knockout of golgin-160, a TGN membrane protein, also prevents internalized GLUT4 from transitioning into GSVs (Williams, et al., 2006), thereby supporting an intermediary role for the TGN in ERC to GSV sorting.

1.3.5 Role of Akt in GLUT4 translocation

In order for insulin-stimulated GLUT4 plasma membrane translocation to occur, protein kinase B (Akt), needs to be activated via phosphorylation (Cho, et al., 2001; Czech & Corvera, 1999). There are three different Akt isoforms, each of which plays different roles within the cell. Akt1 is largely involved in cell growth, proliferation, and has been shown to lead to hypertrophy in the myocardium (Condorelli, et al., 2002). Akt2 is involved in insulin signalling and GLUT4 vesicle translocation (Zhou, et al., 2004). Akt3 is not found in insulin responsive tissues (Masure, et al., 1999) and its role is not well understood.

During insulin signalling, insulin binding to its receptor causes the receptor to autophosphorylate. This recruits and activates insulin receptor substrate (IRS) is recruited. Which goes on to activate phosphoinositide 3-kinase (P-I3K) resulting in the production of phosphotidylinositol 3, 4, 5-triphosphate (PIP3). Akt2 must dock on a PIP3 lipid raft on the plasma membrane in order for phosphorylation by phosphoinositide-dependent kinase 1 (PDK1) and phosphoinositide-dependent kinase 2 (PDK2) to occur (Fukuda, 2011). Activation of Akt2 allows it to phosphorylate AS160, thereby inactivating its inhibitory function on Rab proteins (Kane, et al., 2002), and allowing Rab proteins to facilitate GSV targeting to the membrane (Zerial & McBride, 2001). Knockout studies of Akt2 in mice show development of insulin resistance and type 2 diabetes (Cho, et al., 2001), indicating a crucial role of this protein in the onset of disease.

Following the insulin stimulated release of GSVs, most intracellular GLUT4 is trafficked to recycling endosomes, but in the absence of insulin, GLUT4 is transported from ERC to the GSVs (Zeigerer, et al., 2002; Lampson, et al., 2001). Under resting conditions, the GLUT4 in ERC and GSVs are evenly distributed, with the GSVs being a “ready to deploy” compartment

upon insulin stimulation via Rab8a, Rab10, and Rab13 (Sun, et al., 2010). Interestingly, insulin also activates GTP binding of Rab4 (Shibata, et al., 1997) and Rab11 (Schwenk & Eckel, 2007), in order to increase the recycling and release of GLUT4 from endosomal compartments to the plasma membrane. The remaining membranes, proteins, and intravesicular lumen contents within the sorting endosome are targeted for degradation, as the sorting endosome matures into a late endosome, followed by lumen pH acidification and subsequent maturation into a lysosome (Van-Weert, et al., 1995; Aniento, et al., 1996).

1.3.6 Molecular motors and vesicle trafficking

Vesicular traffic is directed and carried to their destinations along actin filaments by molecular motor proteins, typically belonging to the myosin family of proteins. Motors in the myosin V class are most heavily implicated in vesicle traffic. Myosin V motors move along actin filaments in a processes fashion, taking multiple consecutive steps prior to disassociation from the actin filament (Mehta, et al., 1999; Sakamoto, et al., 2000). Movement of GSVs to the plasma membrane is mediated by Myosin Va and Myosin Vb. Akt2 phosphorylates Myosin Va upon insulin stimulation, allowing it to bind to actin filaments and translocate GSVs to the plasma membrane (Yoshizaki, et al., 2007). Disruption of Myosin Va activity through siRNA or dominant-negative mutant expression inhibits GSV movement to the plasma membrane (Yoshizaki, et al., 2007). The role of Myosin Vb in GSV translocation has been implicated through its interactions with Rab8A, one of the Rab proteins involved in GSV movement. Interestingly overexpression of the Myosin Vb fragment involved in Rab8a binding attenuated insulin GLUT4 translocation and altered the distribution of Rab8a within the cell (Ishikura & Klip, 2008). Further, Myosin Vb also plays a role in the Rab11-mediated recycling of vesicles from the ERC to the plasma membrane (Schafer, et al., 2014), suggesting this protein may be

involved in multiple branches of GLUT4 trafficking. Interestingly, the presence of Myosin Vb does not seem to be crucial to the trafficking of endosomes, as depletion does not produce swollen endosomes within the cell, suggesting that there is no block in trafficking. Myosin VI is an actin-motor capable of movement toward the minus end of actin (Wells, et al., 1999). This retrograde movement allows this protein to move early endosome traffic to the ERC. Depletion of Myosin VI leads to development of swollen early endosomes and a block in traffic from early endosomes to the ERC (Chibalina, et al., 2007), supporting a crucial role for Myosin VI in this trafficking step.

1.4 Tail anchored proteins are involved in multiple cell functions and novel disease targets

Regulation of recycling, degradation, and intracellular cargo is of the utmost importance due to the multitude of cellular processes occurring at the plasma membrane which lead to wear and tear over time which need to be controlled in order to preserve cellular function. Various pathological states such as cystic fibrosis (Gadsby, et al., 2006; Birault, et al., 2013) and diabetes (Morgan, et al., 2011; Bogan, 2012) disrupt this balance through effects on membrane proteins, such as genetic alterations or disruption of their trafficking, leading to impaired cellular function or cell death (Cobbold, et al., 2003). Due to the role these membrane trafficking events play in cell health, understanding the machinery and mechanisms involved in trafficking events has played a crucial role in understanding disease states and discovering therapeutic targets. As discussed previously, Rab proteins play a large role in trafficking events, although another class of proteins which play an equally crucial role are tail anchored membrane proteins. These proteins are defined by a C-terminal hydrophobic transmembrane domain which may also be flanked with hydrophilic residues (Kutay, et al., 1993; Borgese, et al., 2003). These tail-anchored domains allow for targeting to various cellular subcompartments based on the hydrophobic

profile of the tail anchored domain (Byers, et al., 2009). One example such proteins are the soluble N-ethylmaleimide-sensitive factor activating protein receptors (SNAREs). These proteins aid membrane trafficking events by forming protein scaffolds to mediate membrane fusion events (Haucke, et al., 2011). SNAREs are required in order for vesicle-membrane fusion events to occur.

1.4.1 Protein structure of SNAREs

The protein scaffold produced by these tail anchors are hetero-oligomeric complexes (Sollner, et al., 1993; Sollner, et al., 1993). These complexes are formed through interactions between coiled-coil regions known as SNARE motifs which typically span the length of approximately 60 residues (Jahn & Su¨dhof, 1999). Further, C-terminal regions anchor these proteins into the lipid bilayer of various membranes within the cell (Jahn & Su¨dhof, 1999). SNAREs utilize a highly conserved "zipper" mechanism where SNAREs on opposing membranes bind one another, forming protein bridges between membranes, this is followed by a decrease in the distance in between the two membranes, which eventually leads to the fusion of the two membranes (Hanson, et al., 1997; Hay & Scheller, 1997). Protein bridges formed by SNARE proteins are created through a conformational transition from an unstructured monomeric states to complexed heteromeric states with many α-helical regions which allow for the lowering of the energy gap required for membrane fusion (Fasshauer, et al., 1997).

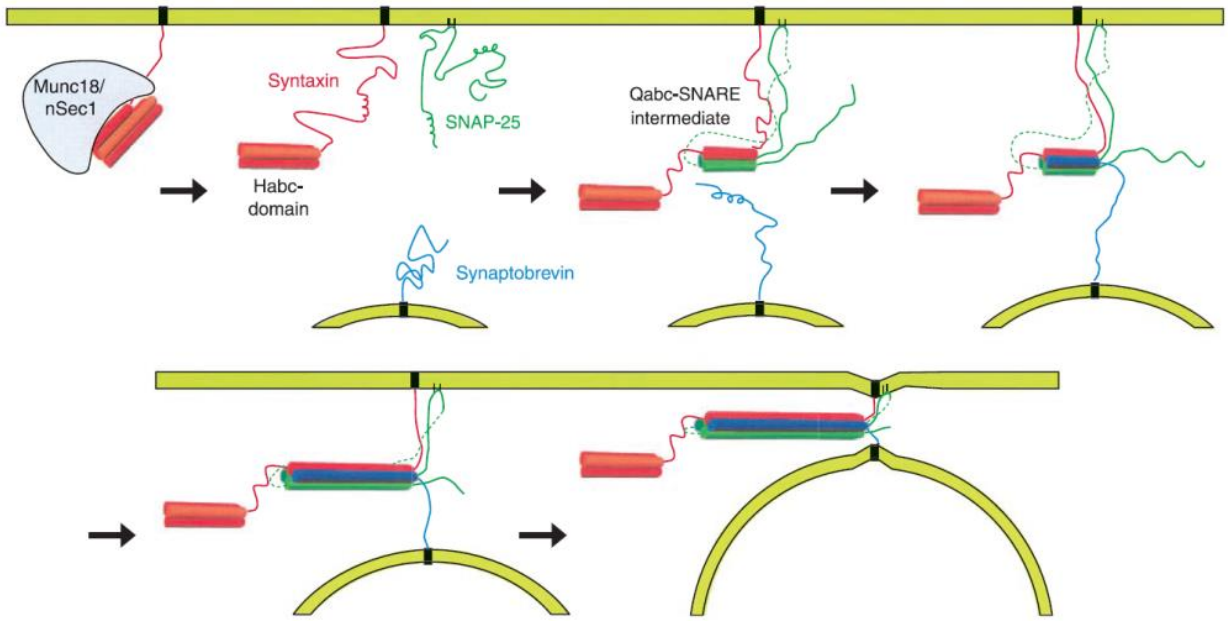

Figure 3. *Mechanism of syntaxin-mediated GLUT4 vesicle fusion into the plasma membrane.* Syntaxin proteins are normally inactive when bound to their inhibiting proteins such as Munc18. When unbound, Syntaxin can become activated by SNAP-25 which allows for binding to Synaptobrevin to form the SNARE complex. This complex is "zippered" further inorder to bring the two membranes closer together in order to mediate vesicle fusion. Figure reprinted with permission from (Fasshauer, 2003). Copyright (2003) of Biochimica et Biophysica Acta (BBA) – Molecular Cell Research.

The most well characterized SNAREs are those involved during neurotransmitter release in neurons: VAMP-2, SNAP-25, and Syntaxin-1a (Sollner, et al., 1993). These SNAREs have structurally similar isoforms present in other cell types in order to mediate other membrane fusion processes. VAMP-2 and Syntaxin-1a contain a C-terminal tail anchored transmembrane domain and a SNARE motif directly adjacent to this tail anchor. Conversely, SNAP-25 contains two SNARE motifs connected by a linker region which is palmitoylated in order to allow for

anchoring into the plasma membrane. SNAREs are categorized by which membrane they reside in prior to fusion. SNAP-25 and Syntaxin-1a are known as target SNAREs (t-SNAREs) due to their localization at the plasma membrane, the location which intracellular vesicles will fuse into, while VAMP-2 is known as the vesicle SNARE (v-SNARE) as it resides in vesicle membranes (Rothman, 1994).

1.4.2 SNAREs and membrane trafficking

While contributing to the fusion and targeting dynamics of membrane fusion, SNAREs also play an important role in the specificity of these events as well (Sudhof & Rothman, 2009), allowing them to regulate other specialized membrane fusion events, such as the insulin-stimulated translocation of GLUT4 to the plasma membrane. While VAMP-2 is still the v-SNARE VAMP-2 involved in this process, there are alternate t-SNARE isoforms present to mediate membrane fusion events: SNAP23 and Syntaxin-4 (Bryant & Gould, 2011). VAMP2 is present within an insulin sensitive compartment known as GLUT4 storage vesicles (GSVs) and has been implicated as the v-SNARE most important to GSV translocation. Syntaxin-4 and SNAP23 were identified as the t-SNAREs involved in this process. Disruption of protein expression through siRNA knockdown in adipocytes revealed SNAP23 and Syntaxin-4 to both be necessary for tethering and fusion of GSVs into the plasma membrane (Kawaguchi, et al., 2010). Conversely, VAMP2 knockdown, while preventing fusion, did not have significant impact on tethering of vesicles (Kawaguchi, et al., 2010). Further, VAMP2 has been implicated in not only the fusion of GSV to the plasma membrane, but also the sorting of vesicles from the endosomal recycling compartment (ERC) into GSVs (Williams & Pessin, 2008). Insulin stimulation mediates fusion of GSVs into the plasma membrane by increasing the number of hetero-oligomeric SNARE complexes formed between Syntaxin-4, SNAP23, and VAMP-2 (Kioumourtzoglou, et al., 2014).

Further, presence of Syntaxin-4 and SNAP23 is required for the constitutive recycling of GLUT4 through the endosomal pathway (Kioumourtzoglou, et al., 2014). Due to these profound effects these tail anchors play in insulin-stimulated GLUT4 trafficking, it is hypothesized they may act as potentially therapeutic targets in diabetes. Not only is Syntaxin-4 expression significantly reduced in human diabetic β-cells, overexpression of Syntaxin-4 significantly increases the insulin release (Oh, et al., 2014). It should also be noted that post-translational modifications to these proteins are also important in a disease context. Cysteine S-nitrosylation of Syntaxin-4 allows for glucose-induced insulin release by increasing binding of VAMP-2 to Syntaxin-4 (Wiseman, et al., 2011). Further, dysfunctional cytokine-mediated release, which precedes cell death in inflammatory diseases, also greatly correlated with the S-nitrosylation of Syntaxin-4 (Wiseman, et al., 2011). Phosphorylation of SNAP23 have also been implicated in platelet secretion within the circulatory system (Karim, et al., 2013). It was also noted that tail bleed times increased upon inhibition of IKKβ, the kinase responsible for phosphorylating Syntaxin-4 (Karim, et al., 2013).

1.4.3 Sarcolemmal Membrane Associated Proteins (SLMAPs): Novel tail anchored proteins involved in cardiovascular health

A novel class of coiled-coil tail anchored membrane proteins known as Sarcolemmal Membrane Associated Proteins (SLMAPs) share structural homology to the SNARE proteins Syntaxin-4 and SNAP23. SLMAP isoforms (35, 45, 63, and 83-91 kDa) are a product of alternative splicing of the SLMAP gene and expressed in a tissue specific manner. These isoforms have shown to be involved in a variety of different functions in the cell including microtubule organization (Guzzo, et al., 2004), myoblast fusion (Guzzo, et al., 2004), and excitation-contraction coupling (Guzzo, et al., 2005). These isoforms each contain conserved transmembrane domains (TM1 and TM2) which serve to target SLMAPs to various subcellular membranes within the cell. The TM2

domain possesses a unique hydrophobic profile, which provides it with the promiscuous nature to be able to transverse into various membranes including the sarcolemma, sarcoplasmic/endoplasmic reticulum (SR/ER) and the mitochondria (Byers, et al., 2009). A conserved coiled-coil leucine zipper domain is also present which allows homo- and hetero-dimerization of SLMAPs, allowing it to form complexes, which may aid in membrane trafficking events, similar to SNAREs.

Recent data support a role for SLMAP in trafficking events involved in Brugada Syndrome, a cardiac pathology brought on by the disrupted shuttling of the sodium channel hNav1.5 (Ishikawa, et al., 2012). Proteomic screens noted complexes formed between SLMAPs and Rabaptin-5/RABEP1 (Hauri, et al., 2013), a coiled-coil protein regulator of endosomal fusion (Stenmark, et al., 1995). Myosin VI, a motor protein involved in Rab11 mediated recycling (Chibalina, et al., 2007), was also noted to be present in complex with SLMAPs (Hauri, et al., 2013). Furthermore, SLMAPs are critical during myoblast fusion (Guzzo, et al., 2004), a membrane fusion event necessary for the differentiation and development of muscle fibers (Hindi, et al., 2013).

Interestingly, recent data on diabetic populations suggest that mutations in the SLMAP gene were linked with patients' susceptibility to diabetic retinopathy (Upadhyay, et al., 2015). SLMAPs are expressed in a tissue specific manner, in particular, a splice variant of SLMAP known as SLMAP Isoform 1 (SLMAP1) is predominantly expressed in the myocardium and was found to be upregulated in dysfunctional micro-vessels and adipose tissue of diabetic mice (Ding, et al., 2005; Chen & Ding, 2011). Our lab has generated a transgenic mouse line in which SLMAP1 (the 35kDa isoform) is overexpressed within the cardiomyocytes of the heart. In this model, we use an α-MHC promoter in order to overexpress SLMAP1 within post-natal mouse

hearts. We tagged this overexpressed protein with Myc so that we can track its expression within the cell. Overexpression of this protein leads to structural and functional changes within the heart, presenting with mild cardiac dysfunction, SR/ER membrane remodelling, and increased vesicle formation within the myocardium (Nader, et al., 2012). Interestingly, knockdown of SLMAP1 in adipocytes lead to reduced glucose uptake (Chen & Ding, 2011), suggesting a unique role for this protein in glucose metabolism.

1.5 Statement of the problem

Diabetic cardiomyopathy can arise due to hyperglycemia, resulting in defective metabolism and heart failure. Muscle tissue, including the myocardium, can profoundly effect whole body systemic metabolism (Lee, et al., 2014; Grueter, et al., 2012; Baskin, et al., 2014). Recent efforts in the development of therapeutic strategies for metabolic disease such as diabetes are aimed at targeting systemic metabolism at the level of skeletal and cardiac muscle specific regulation of metabolism (Baskin, et al., 2015). Thus the discovery of novel modulators of glucose uptake and metabolism within muscle tissue would greatly impact treatment of metabolic diseases. SLMAPs belong to the superfamily of tail anchored membrane proteins which regulate vesicle transport and proteomic screens reveal that it is present in complex with Rabaptin-5 and Myosin VI (Hauri, et al., 2013). SLMAPs are linked to diabetes and GLUT4 expression. We hypothesize SLMAP1 is a novel regulator of GLUT4 expression and endosomal trafficking. Further, SLMAP1-mediated changes to GLUT4 trafficking will lead to enhanced myocardial glucose metabolism and uptake. In order to test this hypothesis, we examined cardiomyocytes from transgenic mice with cardiac specific expression of SLMAP1 to evaluate any impact on glucose uptake and metabolism. Using Western Blot and qPCR we evaluated expression levels of proteins involved in the trafficking of GLUT4 and immunofluorescence microscopy to track the effects of SLMAP1 on membrane trafficking events. Finally, we performed extracellular flux bioanalysis in order to evaluate the role of SLMAP1 in glucose and fatty acid metabolism.

CHAPTER 2: Materials and Methods:

2.1 SLMAP-Transgenic mice

a) *Mouse line*: Transgenic lines previously established (Nader, et al., 2012) were used and bred with B6C3F1 mice. The transgenic line was developed for cardiac specific overexpression of SLMAP1-TM2 with a 6 myc tag under an α-MHC promoter. All animals were handled according to protocols approved by the Institutional Animal Care and Use Committee.

b) *Genotyping*: Mice were genotyped blindly by extracting genomic DNA was extracted from the from tail clips using 180μL of 50mM NaOH per tail followed by a 10 minute heat shock at 95^0C. DNA solution was then neutralized using 20μL of 1M Tris-Cl pH 8.0. Transgenic mice were identified by polymerase chain reaction (PCR) using Terra PCR Direct (Clontech) for the PCR mix. The forward primer was: 5`-GAG AGC CAT AGG CTA CGG TG-3` corresponding to exon α-MHC promoter sequence and reverse primer: 5`-CAT AGC TTA TCG ATA CCG TCG-3` corresponding to the myc tag sequence. This resulted in a PCR product of ~152 bp for transgenic 6-myc-tagged SLMAP1-TM2 mice and no product for wildtype mice. PCRs were visualized by Red Safe (Sigma) staining on a 1.2% agarose gel. Genotyping was routinely verified at the protein level by western blot using an anti-Myc antibody to detect 6-Myc-tagged SLMAP1-TM2.

2.2 Protein isolation from mouse heart

Hearts of adult mice (male mice at 9 weeks of age) were collected after CO_2 euthanasia, and immediately frozen in -80^0C. Each single heart was later washed with ice-cold 1X phosphate buffered saline (PBS), and homogenized using Fisher handheld Maximzer homogenizer in ice-cold lysis buffer (1mM ethylene glycol tetraacetic acid (EGTA), 1 mM ethylenediaminetetraacetic (EDTA), 20 mM Tris base, 1% Triton, 150 mM sodium chloride, 1X

complete mini EDTA-free protease inhibitor cocktail (Roche), and 1X PhosSTOP (Roche)). The suspension was centrifuged for 15 min at 12,000g to separate the proteins from cell debris. The supernatant containing protein was collected in eppendorf tubes and stored in freezer at -80^{o}C. In immunoblotting experiments, proteins from each heart were used in a single lane of 10% sodium dodecyl sulfate polyacrylamide gel electrophoresis (SDS-PAGE).

2.3 Neonatal Mouse Cardiomyocytes (NMCM) Culture

Hearts from 1-day old pups were collected by decapitation euthanasia. The hearts were immediately washed with ice-cold Hank's Buffer (HBSS) containing no calcium or magnesium, and transferred to tubes containing HBSS with 0.1% trypsin. The tubes were left overnight on a slow shaker at 4^{o}C. The tails collected from each pup were used for genotyping to identify transgenic and wildtype mice.

The transgenic and wildtype hearts were pooled in separate 15 mL falcon tubes containing HBSS solution. The hearts were washed twice with HBSS solution at room temperature. Following complete aspiration of HBSS solution from the tubes, the hearts were digested at 37^{o}C in 0.1% collagenase II dissolved in HBSS. Digestion process was done three times for 12 min each with gentle shaking. Each time the supernatant containing predominantly cardiomyocytes and fibroblasts was collected and centrifuged at 600g for 3 min. The supernatant after centrifugation was discarded and the pellet was resuspended in Dulbecco's Modified Eagle Medium (DMEM) containing 10% fetal bovine serum (FBS), 1% non-essential amino acid (NEAA) and 1% pen/strep (hereinafter referred as cardio media). The resuspended cells were kept at 37^{o}C and 5% CO_2. The suspension resulting from three digestions was pooled together in 15 mL falcon tube and centrifuged at 600g for 3 min. The pellet was resuspended in desired amount of cardio media. The media was plated on uncoated culture dishes and incubated for 45 minutes at 37^{o}C

and 5% CO_2. This media was then transferred to a second plate for 45 minutes and incubated under the same conditions. Media from this dish was then transferred to a 1% gelatin coated plate and incubated for 48 hours at 37^{o}C and 5% CO_2. Fibroblast adhered to uncoated plates whereas cardiomyocytes adhered to the gelatin coated plate.

2.4 Protein Extraction

After incubation period, the media from culture dishes was completely aspirated and the dishes were washed with PBS, and followed by freezing at -80^{o}C. The culture dishes were scraped using Lysis Buffer (Cell Signalling). The cells in the suspension were lysed by syringing at least 10 times and centrifuged for 15 min at 12000g to separate the proteins from cell debris. The supernatant containing proteins was collected in Eppendorf tubes and stored in freezer at -80^{o}C. Heart tissue protein was also extracted in this way prior to homogenization using an electric tissue homogenizer. Protein measurements were performed with Bicinchoninic acid (BCA) protein assay kit (Pierce) as per the manufacturer's protocol.

2.5 Glucose Uptake Assay

Cardiomyocytes were isolated from neonatal mouse hearts at day 1 and allowed to adhere for 48 hours in cardiomyocyte media. On day of experiment, cells were starved in a DMEM solution containing 2mM glutamine without glucose or FBS for one hour followed by treatment with 2-deoxy-glucose (2DG) for 20 minutes. Cells were then flash frozen in liquid nitrogen and 2DG was extracted and detected using the Glucose Uptake Assay Kit (Colorimetric) from Abcam.

2.6 Glycolysis Measurement

Neonatal cardiomyocytes were isolated from one day old mouse hearts and then seeded on XF^{e}24 plates at a concentration of ~300,000 cells per well. Cells were allowed 48 hours to adhere to plates prior to assay. On day of assay, media was replaced with bicarbonate and

glucose free DMEM containing 2mM glutamine. The extracellular acidification rate (ECAR) of the media was measured using an XF^{e}24 Extracellular Flux Analyzer. ECAR measurements were presented as the percent increase from the baseline measurement (ECAR prior to any injection). Cardiomyocytes were sequentially treated with 20mM glucose (Gibco), 2mg/mL oligomycin (Sigma), and 100mM 2-deoxy-glucose (Sigma) and the three corresponding ECAR measurements were taken with the representative mean measurements for each treatment being presented.

2.7 Fatty Acid Oxidation Measurement

Neonatal cardiomyocytes were isolated from one day old mouse hearts and then seeded on XF^{e}24 plates at a concentration of ~300,000 cells per well. Cells were allowed 48 hours to adhere to plates. Cells were subsequently starved for 24 hours in Substrate Limited Medium (DMEM (Corning 17-207), 0.5mM glucose, 1.0mM Glutamine, 0.5mM L-carnitine, 1% FBS) for 24 hours prior to assay. On day of assay, Substrate Limited Medium was replaced with fatty acid oxidation (FAO) assay medium (111mM NaCl, 4.7mM KCl, 1.25mM $CaCl_2$, 2.0mM $MgSO_4$, NaH_2PO_4, 2.5mM glucose, 0.5mM L-carnitine, and 5mM HEPES) prior to assay. Cells were separated into groups which were either treated or untreated with 40µM etomoxir for 15 minutes prior to assay in order to inhibit fatty acid transport into mitochondria. The oxygen consumption rate (OCR) of the media was measured using an XF^{e}24 Extracellular Flux Analyzer. OCR measurements were presented as the percent increase from the baseline measurement (OCR prior to any injection). Cardiomyocytes were sequentially treated with 100 µM palmitate (Sigma) conjugated to 17µM BSA or 17µM BSA (Sigma), 2mg/mL oligomycin (Sigma), 1uM Carbonyl cyanide-4-(trifluoromethoxy)phenylhydrazone (FCCP) (Sigma), and

1µM Antimycin A (Sigma). Three corresponding OCR measurements following each treatment with the representative mean measurements for each treatment being presented.

Parameter	Equation used for calculation
Basal Respiration	$= (Palmitate\ or\ Vehicle) - (Antimycin\ A)$
Proton Leak	$= (Oligomycin) - (Antimycin\ A)$
ATP Production	$= (Palmitate\ or\ Vehicle) - (Oligomycin)$
Maximal Respiration	$= (FCCP) - (Antimycin\ A)$
Spare Capacity	$= (FCCP) - (Palmitate\ or\ Vehicle)$
Non-mitochondrial Respiration	$= (Antimycin\ A)$
Oxygen Consumption due to uncoupling by FFA	$= (Oligomycin\ of\ Palmitate\ without\ Eto) - (Oligomycin\ of\ BSA\ without\ Eto)$
Basal Respiration due to utilization of exogenous FAs	$= (Basal\ Respiration\ of\ Palmitate\ without\ Eto) - (Basal\ Respiration\ of\ BSA\ without\ Eto) - (Oxygen\ consumption\ due\ to\ uncoupling\ by\ FFA)$
Maximal Respiration due to utilization of endogenous FAs	$= (Maximal\ Respiration\ of\ Palmitate\ without\ Eto) - (Maximal\ Respiration\ of\ BSA\ without\ Eto) - (Oxygen\ consumption\ due\ to\ uncoupling\ by\ FFA)$
Basal Respiration due to utilization of endogenous FAs	$= (Basal\ Respiration\ of\ BSA\ without\ Eto) - (Basal\ Respiration\ of\ BSA\ with\ Eto)$
Maximal Respiration due to utilization of endogenous FAs	$= (Maximal\ Respiration\ of\ BSA\ without\ Eto) - (Maximal\ Respiration\ of\ BSA\ with\ Eto)$

Table 2. *Methods for calculating parameters obtained by fatty acid oxidation assay*.

Calculations used for determining different parameters are present under "Equations for calculations". Measurements obtained from specific treatment steps during the assay are displayed in brackets.

2.8 Immunoprecipitation and Western blots

Protein extracted from heart tissue was immunoprecipitated using Protein A Dynabeads® (Invitrogen) as per manufacturer protocol. For western blotting experiments, 20 µg of protein was loaded in each well of a 10% SDS-PAGE gel. The gels were transferred overnight on a polyvinylidene fluoride (PVDF) membrane (Bio-Rad) in a buffer containing 25 mM Tris, 190 mM Glycine, and 20% methanol. All membranes were blocked at room temperature for 1-hour

in Tris-buffered saline (TBST) containing 1 M Tris, 290 mM NaCl, 0.1% Tween 20, pH 7.4, and 5% non-fat dry milk. Primary antibodies were incubated overnight at 4^{o}C with 5% bovine serum albumin (BSA). Membranes were washed 5 times for 5 min each in TBST prior to adding the appropriate horseradish peroxidase labeled secondary antibody (Jackson) in a 1:10,000 dilution in TBST with 5% non-fat dry milk. Membranes were shaken slowly at room temperature for 1-hour while incubating with secondary antibody followed by 5 washes for 5 min each with TBST. Membranes were treated with BM Chemiluminescence Western Blotting Kit (Roche) and developed using autoradiography films (HyBlot CL and GE Healthcare). Bands on the autoradiography films were scanned using Gel Doc System (Bio-Rad), and quantified by densitometry using Image Lab software v.4.0.1 (Bio-Rad). Membranes were stripped (25 mM glycine, 10% SDS and pH 2.2 in dH_2O) and reprobed with different antibodies. All primary antibodies which were used are indicated in a table below along with corresponding dilutions.

2.9 WGA Staining

NMCM cultured cells were cooled to 4°C followed by washing with ice cold PBS. Cells were then incubated with 10µg/mL WGA conjugated to Alexa Fluor® 647 (Thermofisher) in PBS for 10 minutes at 4°C. Cells were then washed with ice cold PBS and immediately fixed with 4% paraformaldehyde for 10 minutes at 4°C. Fixed cells were put under low permiabilzation conditions in order to preserve membranes by placing in 0.01 M PBS, 3% BSA, 0.025% Triton-X-100 for 10 minutes, followed by blocking in 0.01 M PBS with 3% BSA for 30 minutes. Cells were then incubated with 1:300 GLUT4 (Sigma) diluted in 0.01 M PBS with 3% BSA overnight. Cells were then washed and then incubated with donkey anti-rabbit Alexa Fluor® 488 (Invitrogen) at a concentration of 1:300 in 0.01 M PBS with 3% BSA for 45 minutes at 37°C. Slides were washed again with PBS followed by addition of Vectashield mounting media with

DAPI (Vector) and placement of coverslip. Deconvoluted widefield microscopy pictures were taken with Zeiss Axio Observer D1 microscope and rendered using AxioVision Rel. 4.8 software.

2.10 Immunostaining

NMCM cultured cells were fixed to glass slides using 4% Paraformaldehyde solution in PBS. Slides were then blocked and permiabilized with permiabilization blocking solution (0.01 M PBS, 3% BSA, 0.3% Triton-X-100) for 35 minutes at room temperature. This was followed by 3 subsequent washes with PBS solution and addition of primary antibodies in corresponding blocking solution overnight at 4^0C. Slides were washed again twice with PBS, followed by incubation at 37^0C with secondary antibodies donkey anti-mouse Alexa Fluor® 488 and donkey anti-rabbit Alexa Fluor® 568 (Invitrogen) at a concentration of 1:300 in blocking solution. Slides were washed again with PBS followed by addition of Vectashield mounting media with DAPI (Vector) and placement of coverslip. Widefield and deconvolution microscopy pictures were taken with Zeiss Axio Observer D1 microscope and rendered using AxioVision Rel. 4.8 software. Confocal microscopy pictures were taken with Zeiss LSM 510 Axio Imager M1 Confocal and rendered with ZEN 2009 software.

2.11 Quantitative PCR

Total mRNA from mouse hearts was extracted using the Tripure isolation kit (Roche) (Pierce & Wangh, 2007). The concentration and purity of the obtained mRNA was determined by measurement of 260/230 nm absorbance ratio and 280/260 absorbance ratio (Bustin, 2002) using NanoDrop 2000 UV-Vis Spectrophotometer (Thermo Scientific). RNA was used as a template to generate cDNA using SuperScript II reverse transcription protocol following the manufacturer's guidelines (Invitrogen). Equal amounts of cDNA were utilized in real-time PCR using primers

for GLUT4 (forward 5'- GCA GAT CGG CTC TGA CGA TG-3', reverse 5'- GCC ACG TTG CAT TGT AGC TC-3'), Akt1 (forward 5'- ATA ACG GAC TTC GGG CTG TG -3', reverse 5'- CTC GAA CAG CTT CTC GTG GT -3'), Akt2 (forward 5'- CGC CAG CAC TGC CGC -3', reverse 5'- CAG CAT TCA CAC GCT GTC AC -3'), and Actin (forward 5'- ACC CAG GCA TTG CTG ACA GGA T -3', reverse 5'- CGC AGC TCA GTA ACA GTC CGC -3'). Fold change was calculated using the ΔΔCt method.

2.12 Statistical Analyses

Glucose treatments were analyzed using one-way ANOVA. All other comparisons between wildtype and transgenic groups were performed using using two-tailed Student's T-test. All values and points on graphs represent mean values obtained from multiple experiments. All error bars presented in graphs are represented using the standard error of the mean. All sample size values (n) represent biological replicates (different hearts for westerns or different pools of hearts for NMCM culture). All immunofluorescence co-localization values were obtained counting 10 cells each from 3 different pools of neonatal hearts containing 3 hearts each for a total of 30 cells counted.

Antibody	Manufacturer	Application (Dilution)
SLMAP (anti-rabbit)	Proteintech (25220-1-AP)	IP (1:100)
SLMAP (anti-rabbit)	NovusBio (NBP1-81397)	IF (1:100
SLMAP (anti-mouse)	Abnova (H00007871-M08)	IF (1:100)
Myc	Roche (11667149001)	IF (1:300)
GLUT4	Sigma (G4173)	WB (1:1000), IF (1:100)
α-Tubulin	Abcam (ab176560)	WB (1:5000)
Rab5	Cell Signaling Technology (3547)	WB (1:1000), IF (1:100)
Rab4	Abcam (ab1352)	IF (1:100)
Clathrin	Abcam (ab21679)	IF (1:100)
EEA1	Cell Signalling Technology (3288)	IF (1:100), WB (1:1000)
VAMP2	Abcam (ab3347)	IF (1:100), WB (1:1000)
Syntaxin-4	Abcam (ab77037)	IF (1:100), WB (1:1000)
SNAP23	Abcam (ab3340)	IF (1:100), WB (1:1000)
RABEP1/Rabaptin-5	Proteintech (14350-1-AP)	IF (1:300), WB (1:5000)
Rabbit IGG	Sigma (011-000-003)	IP (50ng/uL)

Table 3. *List of antibodies used in this study.* All antibodies used in this study are listed with the corresponding distributor, catalog number, and dilution used for each application.

Immunofluoresence is abbreviated to IF and immunoprecipitation is abbreviated to IP

CHAPTER 3: Results

3.1 SLMAP1 non-transcriptionally regulates GLUT4

The SLMAP gene undergoes extensive splicing to generate many splice variants in myocardium. All SLMAP isoforms contain two leucine zipper coiled-coils through which they homodimerize and a 21 amino acid c-terminal sequence (with an alternative exon) which targets subcellular membranes. Changes in SLMAP1 expression have been correlated to dysfunction in hyperglycemic diabetic mouse models (Chen & Ding, 2011; Ding, et al., 2005) and knockdown studies showed siRNA targeting SLMAP1 lead to a decrease in glucose uptake within adipose tissue (Chen & Ding, 2011). We focused our studies on SLMAP1 with the generation of transgenic mice with cardiac specific overexpression of SLMAP1-TM2. These mice present with marked changes in subcellular membrane structure characterized by enlarged vesicles and mild cardiac deficits (Nader, et al., 2012). In order to define the composition of intracellular membranes effected by SLMAP1 overexpression as well as study how SLMAP1 dysregulation lead to decreased glucose uptake, we examined hearts for expression of GLUT4, a major regulator of glucose uptake in the heart. We found transgenic hearts contained increased levels of GLUT4 (160% ± 39%, n=6, $P<0.01$) compared to wildtype littermates (**Figure 4**). We went on to investigate any if SLMAP1 expression was effecting Akt2, an important regulator of GLUT4 trafficking through GSVs (**Figure 5**). While total levels of Akt2 were significantly increased in SLMAP1-Tg hearts, levels of Phospho-Akt2 were unchanged between wildtype and transgenic hearts. When analyzing the relative phosphorylation, we noted a trend towards decreased phosphorylation in SLMAP1-Tg hearts, suggesting that traffic GLUT4 traffic was most likely not moving through this pathway. Analysis of transcript levels through qPCR analysis between wildtype and transgenic hearts was performed in order to elucidate if SLMAP1 may be

mediating GLUT4 expression transcriptionally. The mRNA levels of GLUT4, Akt1, and Akt2 in adult mouse hearts were analyzed and no significant changes in mRNA expression were found (**Figure 6**). Together, this data suggests that changes in protein expression were not due to upstream changes in mRNA levels, suggesting an alternate mechanism of regulation. We then examined if the increased GLUT4 resulted in a corresponding change in glucose uptake and metabolic parameters of isolated neonatal cardiomyocytes.

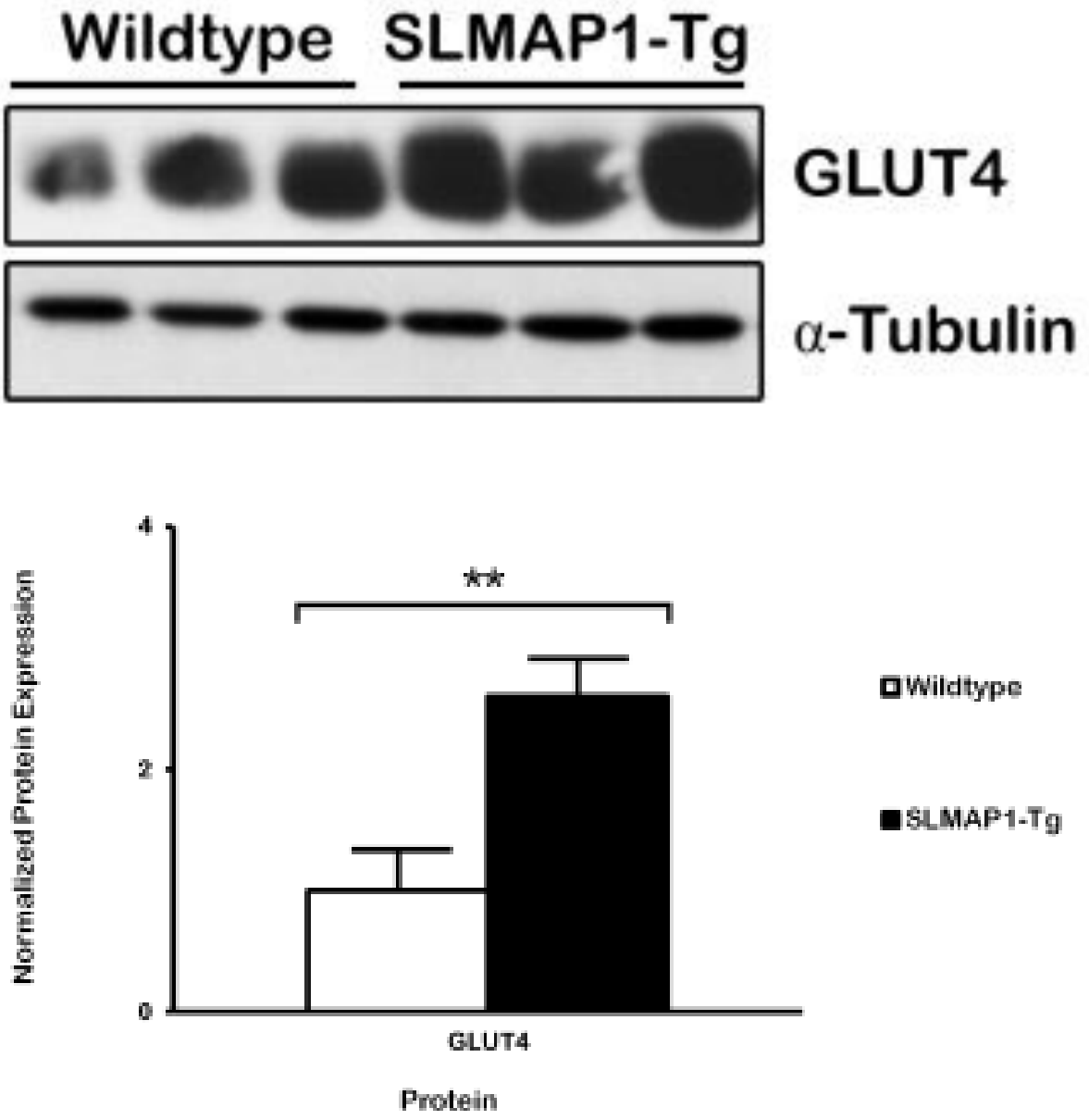

Figure 4. *SLMAP1 regulates GLUT4 expression in mouse hearts.* Protein extracted from adult mouse hearts was quantified using Western Blot densitometry analysis with α-tubulin as a loading control. Anti-GLUT4 was used to probe for GLUT4 expression and anti-α-tubulin was used to quantify α-tubulin expression. GLUT4 expression was increased in transgenic hearts (160% ± 39%, n=6 adult hearts, $P<0.01$ using two-tailed t-test) compared to wildtype littermates.

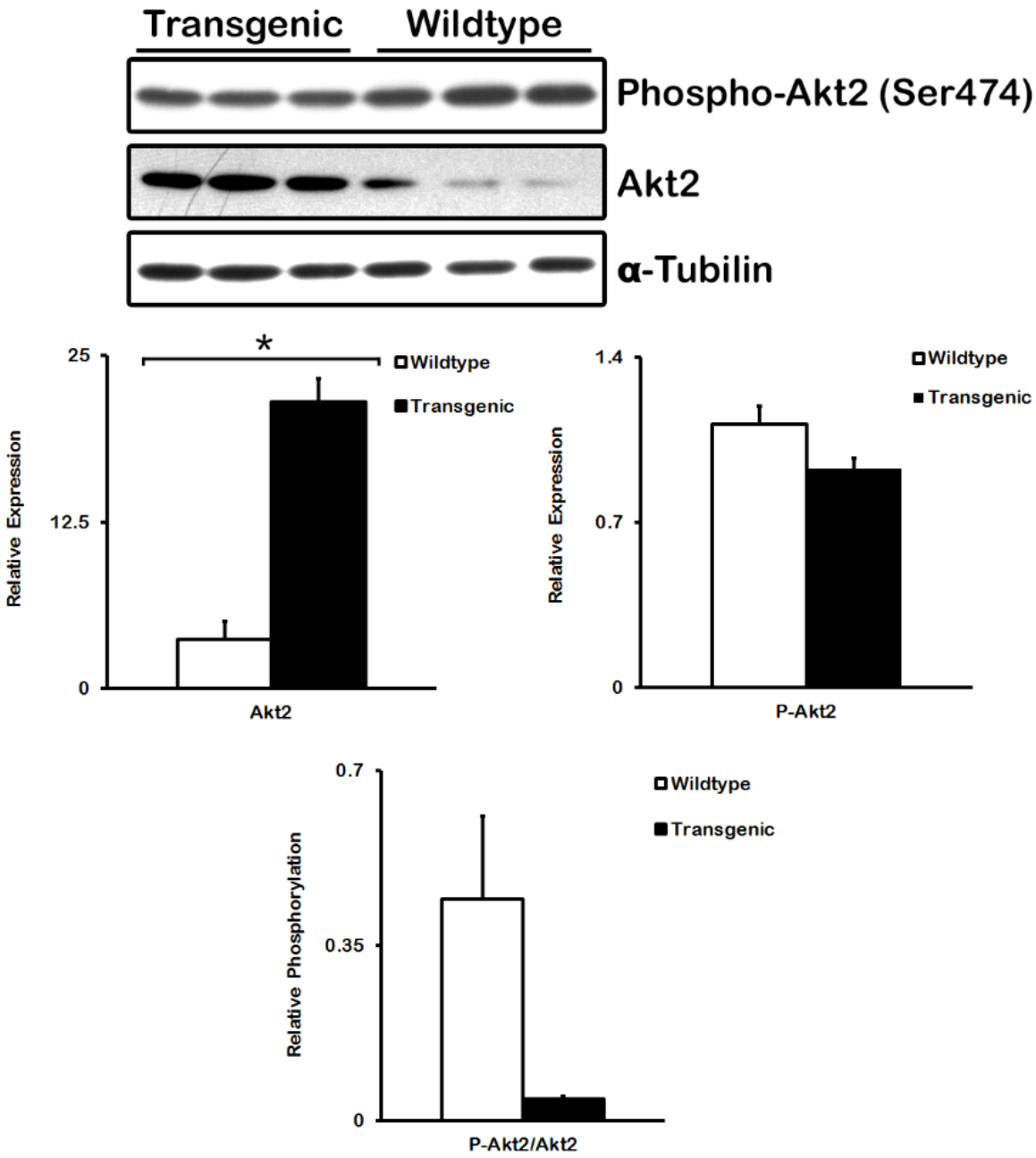

Figure 5. *Total Akt2 upregulation and decreased phosphorylation in SLMAP1-Tg hearts.* Protein extracted from adult mouse hearts was quantified using Western Blot densitometry analysis with α-tubulin as a loading control. Anti-Akt2, anti-Phospho-Akt2, and anti-α-tubulin was used to quantify Akt2, Phospho-Akt2, α-tubulin expression respectively. Akt2 expression was increased

in transgenic hearts (773.7% ± 41.0%, n=3, P<0.05) and total Phospho-Akt2 expression was slightly decreased (-31.47% ± 8.22%, n=3, P=0.12) compared with hearts from wildtype littermates. Overall phosphorylation of Akt2 at Ser474 showed a large decrease in phosphorylation in transgenic hearts (-85.87% ± 8.14%, P=0.16). Asterisk denotes significance of P<0.05.

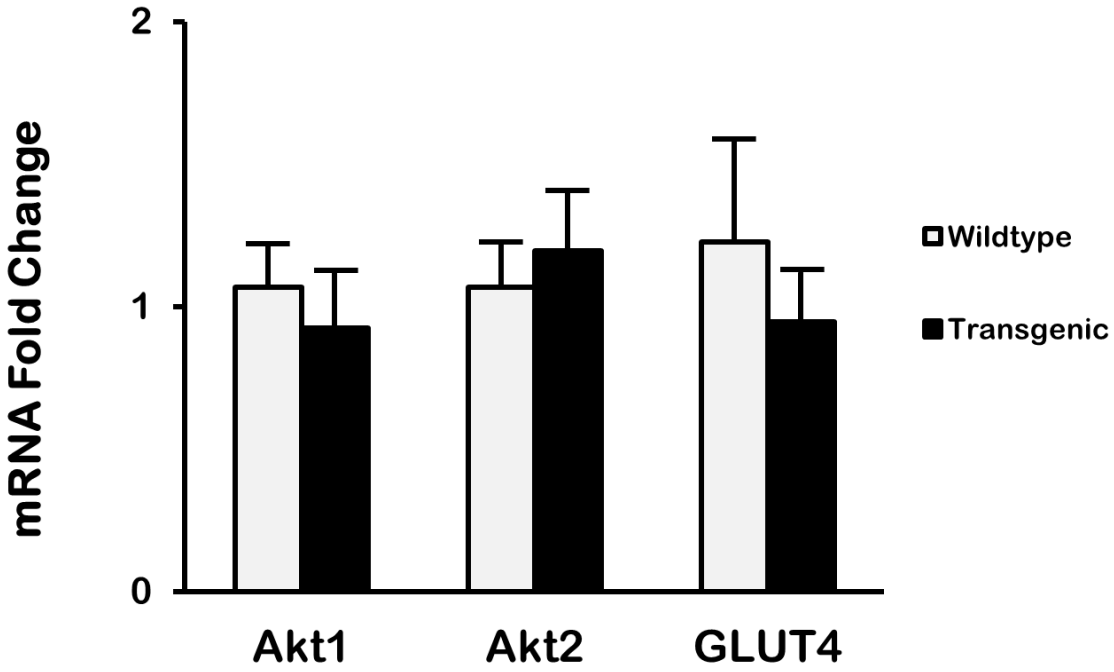

Figure 6. *SLMAP1 expression alters protein expression without changing transcript levels.* Heart tissue mRNA from wildtype and transgenic adult mice was subject to qPCR analysis. Fold change was calculated using Actin as the normalizing control. Transgenic hearts did not show any significant change in mRNA expression of Akt1 (0.92 ± 0.20 fold change, n=7, P=0.59), Akt2 (1.20 ± 0.21, n=7, P=0.54), or GLUT4 (0.95 ± 0.17 fold change, n=7, P=0.56).

3.2 SLMAP1 Expression Regulates Glucose and Fatty Acid Metabolism

The increase in GLUT4 protein expression suggested that there may be increased uptake of glucose. This was analyzed by incubating cells with the glucose analog 2-deoxy-glucose followed by extraction and measurement using a colorimetric assay (Saito, et al., 2011). The SLMAP1 transgenic cardiomyocytes displayed significantly increased 2DG uptake (93% ± 25%, n=5, P<0.01) compared to cardiomyocytes from wildtype littermates (**Figure 7**).

With glucose uptake being one of the rate limiting steps in glycolysis (Guo, et al., 2012), we hypothesized the increased glucose uptake would lead to a downstream increases in glycolysis. In order to measure these changes, we used an Extracellular Flux Analyzer from Seahorse Bioscience to track changes in pH during glycolysis from lactate acid production. Using this method, coupled with sequential treatment of the cells with pharmacological modulators of metabolism, the corresponding changes in the extracellular acidification rate (ECAR) can be used as a measure of the relative amount of glycolysis occurring in the cells (Das, 2013). Cardiomyocytes were sequentially treated with 10mM glucose, 2ug/mL oligomycin, and 100mM 2-deoxy-glucose (2DG) and the corresponding ECAR readings were plotted after each treatment. Glycolytic parameters were calculated from these readings with basal glycolysis indicating ECAR upon addition of glucose (Zannella, et al., 2011), maximal glycolysis indicating ECAR upon addition of glucose and oligomycin (Zhang, et al., 2012; Hao, et al., 2010), and glycolytic reserve indicating the difference between maximal glycolysis and basal glycolysis (Das, 2013; Chibalina, et al., 2007) (**Figure 8**). Transgenic cardiomyocytes displayed significantly increased levels of basal glycolysis (92 ± 40%, n=5, P<0.05) and maximal glycolysis (75 ± 31%, n=5, P<0.05) compared to wildtype cardiomyocytes, although the transgenic cardiomyocytes did not display a significant change in glycolytic reserve compared to wildtype cardiomyocytes.

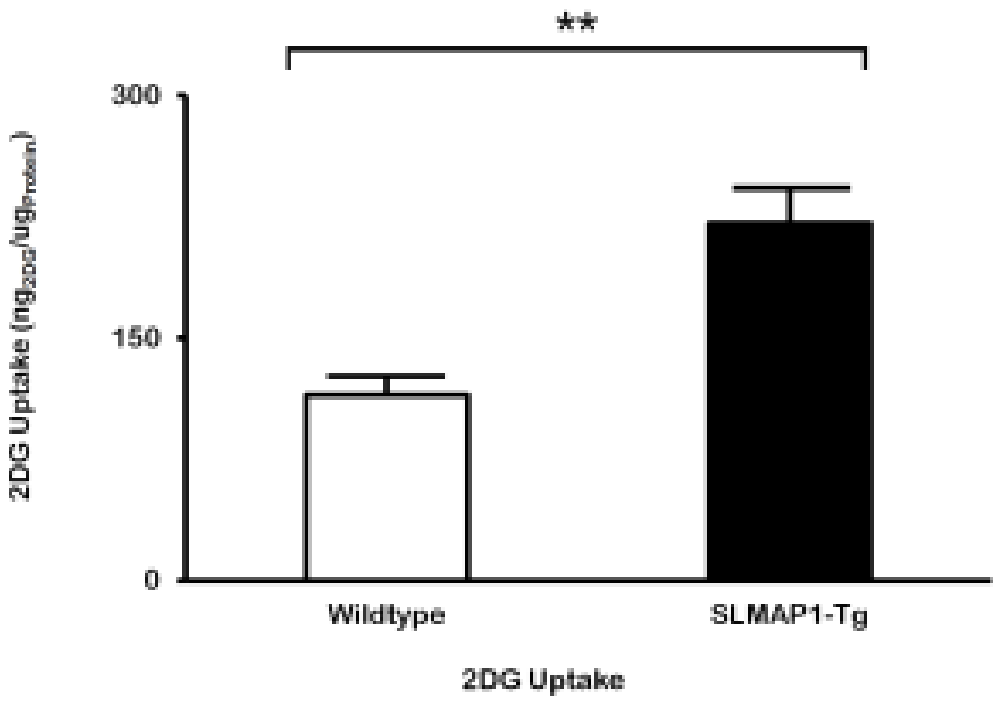

Figure 7. *Enhanced glucose uptake in SLMAP1-Tg neonatal mouse cardiomyocytes.* 2-deoxy-glucose uptake assay was performed on cardiomyocytes isolated from neonatal mouse hearts and allowed to adhere for 48 hours. On day of experiment, cells were starved in a DMEM solution containing 2mM glutamine without glucose or FBS for one hour followed by addition of 2-deoxy-glucose (2DG) for 20 minutes. 2DG was measured by use of a colorimetric enzymatic assay. Transgenic cardiomyocytes displayed increased uptake of 2DG (221 ± 23.4 $ng_{2DG}/\mu g_{protein}$, n=5 pools of neonatal hearts containing 3 hearts each, $P<0.05$ using two-tailed t-test) compared to wildtype cardiomyocytes (115 ± 11.9 $ng_{2DG}/\mu g_{protein}$, n=5 pools of neonatal hearts containing 3 hearts each).

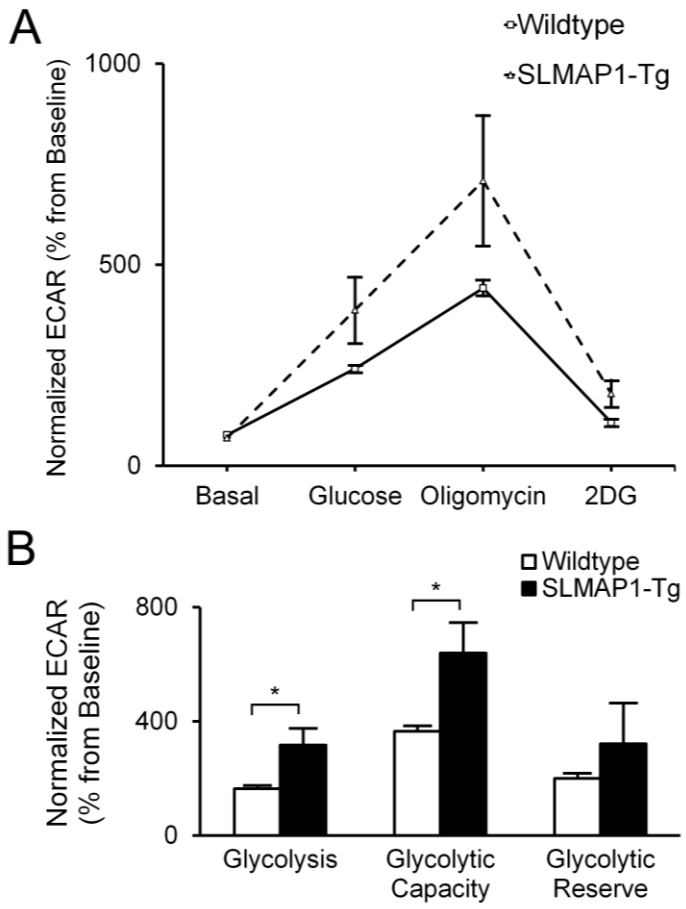

Figure 8. *SLMAP1 overexpression enhances glucose metabolism in neonatal mouse cardiomyocytes.* (**A**) Neonatal cardiomyocytes were sequentially treated with 20mM glucose, 2mg/mL oligomycin, and 100mM 2-deoxy-glucose and the corresponding extracellular acidification rate (ECAR) was measured following each of the treatments (n=4 pools of neonatal hearts containing 3 hearts each) and presented as the relative percent increase from the basal measurement (ECAR prior to any treatment). (**B**) Metabolic parameters were calculated using the ECAR measurements from **A**. Glycolysis was calculated as the glucose treatment ECAR minus the basal treatment, glycolytic capacity was calculated as the oligomycin measurement minus the basal measurement of ECAR, and glycolytic reserve was calculated as the oligomycin measurement minus the glucose measurement. Transgenic cardiomyocytes displayed increased glycolysis (317% ± 101%, $P<0.05$ using two-tailed t-test) compared to wildtype cardiomyocytes (165% ± 20.7%, $P<0.05$ using two-tailed t-test). Transgenic cardioymyocytes displayed increased glycolytic capacity (639% ± 181%, $P<0.05$ using two-tailed t-test) compared to wildtype cardiomyocytes (365% ± 32.7%, $P<0.05$ using two-tailed t-test). Finally, glycolytic reserve was not significantly altered in

transgenic cardioymyocytes (322% ± 251%) compared to wildtype cardiomyocytes (200% ± 194%).

While neonatal cardiomyocytes primarily utilize glucose in order to meet metabolic demands, previous studies revealed SLMAP localization to the mitochondria (Byers, et al., 2009). In order to gain a greater understanding of SLMAP1's role in overall energy metabolism, we measured Oxygen Consumption Rate (OCR) in order to quantify fatty acid oxidation in neonatal cardiomyocytes. Cardiomyocytes were either treated or untreated with etomoxir, an irreversible inhibitor of carnitine palmitoyltransferase-1 (CPT-1) (Kruszynska & Sherratt, 1987). Following this, cells were treated with either BSA vehicle or palmitate conjugated to BSA. By treating cells with these pharmacological reagents, cells could be separated into 4 different treatment profiles in which changes in OCR would represent different metabolic parameters. Changes in OCR of cells which were uninhibited and treated with palmitate represent changes in endogenous and exogenous metabolism of fatty acids, whereas changes in the uninhibited BSA treated cells represent changes in endogenous fatty acid metabolism only. Further, inhibited palmitate treated cells display changes in respiration produced from the uncoupling caused by the presence of palmitate and the inhibited BSA treated cells display changes in respiration not produced by fatty acid metabolism. All four treatment groups were then subjected to a mitochondrial stress test through sequential treatment with oligomycin to inhibit ATP production, FCCP in order to uncouple mitochondria and drive maximal respiration, and Antimycin A in order to inhibit cytochrome c reductase (complex III) and shut down mitochondrial respiration completely. Using OCR values obtained from these treatments, various metabolic parameters can be calculated, these parameters are outlined in **Table 2**. Transgenic cardiomyocytes showed significantly increased basal and maximal respiration upon treatment with palmitate (**Figure 9A**). Changes in respiration were alleviated upon addition of the CPT-1 inhibitor etomoxir (**Figure 9B**). Further, spare capacity was also significantly increased in transgenic

cardiomyocytes treated with palmitate compared to wildtype cardiomyocytes treated with palmitate. This suggests transgenic cardiomyocytes have enhanced utilization of fatty acids under stressed metabolic states. Further, transgenic cardiomyocytes treated with palmitate showed significantly higher ATP production than wildtype cardiomyocytes treated with palmitate. This suggests greater ATPase activity in transgenic cardiomyocytes when fatty acids are present, further supporting a role for SLMAP1 in substrate utilization.

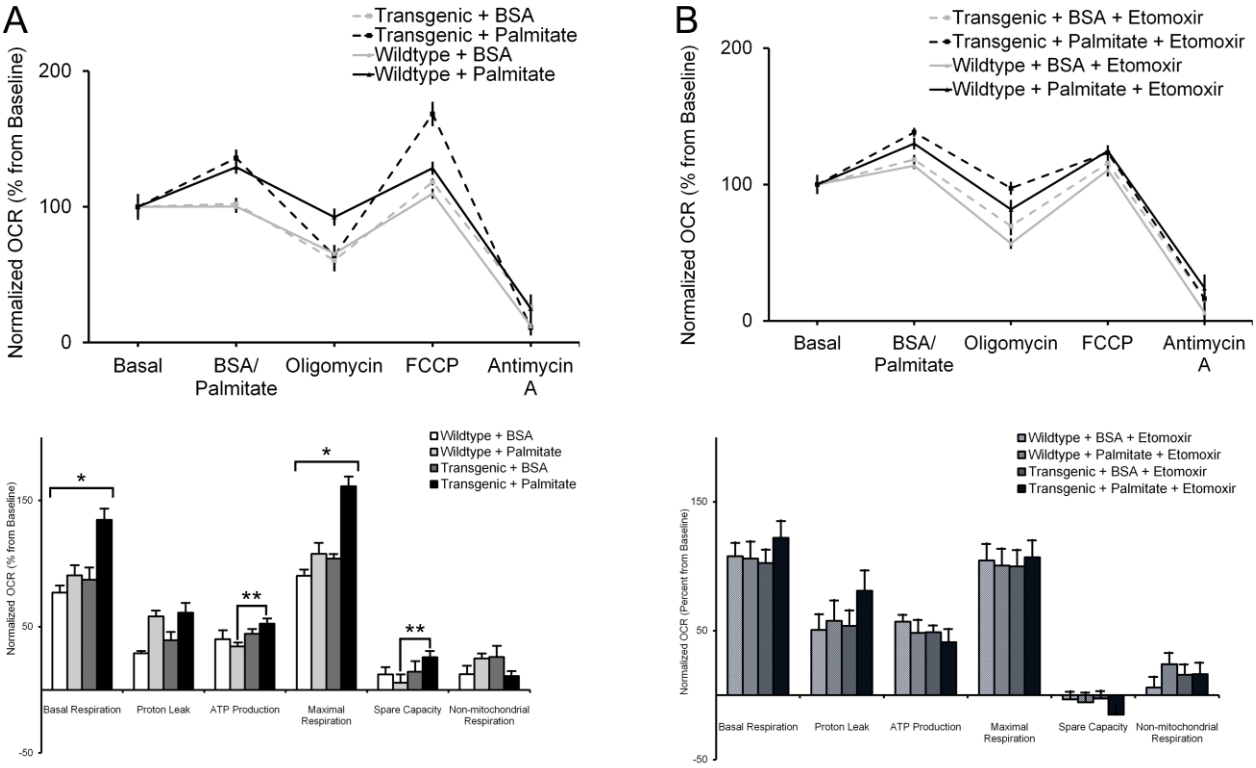

Figure 9. *SLMAP1 regulates fatty acid oxidation in neonatal mouse cardiomyocytes.* Neonatal cardiomyocytes were sequentially treated with 100 µM palmitate conjugated to 17µM BSA or 17µM BSA, 2mg/mL oligomycin, 1uM FCCP, and 1µM Antimycin A and the corresponding oxygen consumption rate (OCR) was measured following each treatment and presented as a relative percent change from the pre-treatment measurement. Cells were either untreated with etomoxir (**A**) or treated with 40µM etomoxir (**B**). Single asterisks denote significance of $P<0.01$ calculated by one-way ANOVA. Double asterisks denote significance of $P<0.05$ calculated by two tailed t-test. Transgenic cardiomyocytes treated with palmitate showed significantly increased basal and maximal respiration compared to transgenic cardiomyocytes treated with BSA, as well as wildtype cardiomyocytes treated with palmitate or with BSA. ATP production in transgenic cardiomyocytes treated with palmitate was also significantly increased compared to wildtype cardiomyocytes treated with palmitate. Spare capacity was also significantly increased in transgenic cardiomyocytes treated with palmitate compared to wildtype cardiomyocytes

treated with palmitate. No significant changes were found in proton leak or non-mitochondrial respiration between groups in cells without etomoxir. Cells treated with etomoxir also did not show significant changes between groups in all parameters.

3.3 Expression of SLMAP1 Increases Size of GLUT4 vesicles

In previous studies from our group, we had found SLMAP1 overexpression lead to an expansion of vesicles and membrane remodelling in the myocardium (Nader, et al., 2012). In order to assess the effects of SLMAP1 expression on GLUT4 containing membranes, we performed immunofluorescence staining on neonatal cardiomyocytes. We used a GLUT4 antibody to track distribution of GLUT4 throughout the cell and an SLMAP antibody to track distribution of all SLMAP isoforms within the cell (**Figure 10**). We performed wide-field microscopy to visualize cells using fluorescent and DIC imaging in order to track changes in membrane structures within cells. Imaging of wildtype cardiomyocytes showed co-localization of GLUT4 and SLMAP within small vesicle compartments within the cell (Pearson R-Value 0.63 ± 0.087) (**Figure 11**). However, upon imaging of transgenic cardiomyocytes, vastly enlarged vesicle compartments were noted (43 fold ± 5 fold in diameter, n=3 pools of neonatal hearts containing 3 hearts each with 43 cells counted total, $P<0.05$). These enlarged vesicles, as presented with arrowheads in **Figure 10**, also presented as regions of co-localization between SLMAP and GLUT4. These transgenic cardiomyocytes also presented with significantly increased co-localization of SLMAP and GLUT4 (Pearson R-Value 0.87 ± 0.01). Interestingly, only vesicles which showed colocalization with SLMAP displayed an increase in size, while all GLUT4 vesicles not containing SLMAP remained similar in size to wildtype counterparts. Further, upon merging DIC pictures with immunofluorescence pictures, the enlarged membrane compartments were shown to be areas of co-localization between GLUT4 and SLMAP. In order to specifically confirm the presence of SLMAP1 within these vesicles, we used a Myc antibody in order to perform isoform specific labelling of SLMAP1. Anti-myc imaging with anti-GLUT4 revealed presence of SLMAP1 within these enlarged vesicles co-localizing with GLUT4. This data

suggested that these were in fact enlarged vesicle compartments, and that SLMAP1 expression mediated expansion of these compartments. We further confirmed the co-localization of SLMAP1 with GLUT4 inside enlarged vesicle compartments with Z-stack imaging using confocal microscopy and maximum intensity projection imaging using Zeiss imaging software (**Figure 11**). Enlarged vesicle compartments showing co-localization of SLMAP1 with GLUT4 was further confirmed in confocal microscopy images. Presence of separate populations of GLUT4 vesicles which did not co-localize with SLMAP1 was also noted, as well as membrane compartments with SLMAP1 but no GLUT4. Again, confocal microscopy showed that GLUT4 vesicles which did not co-localize with SLMAP1 were the same size as GLUT4 vesicles from wildtype hearts.

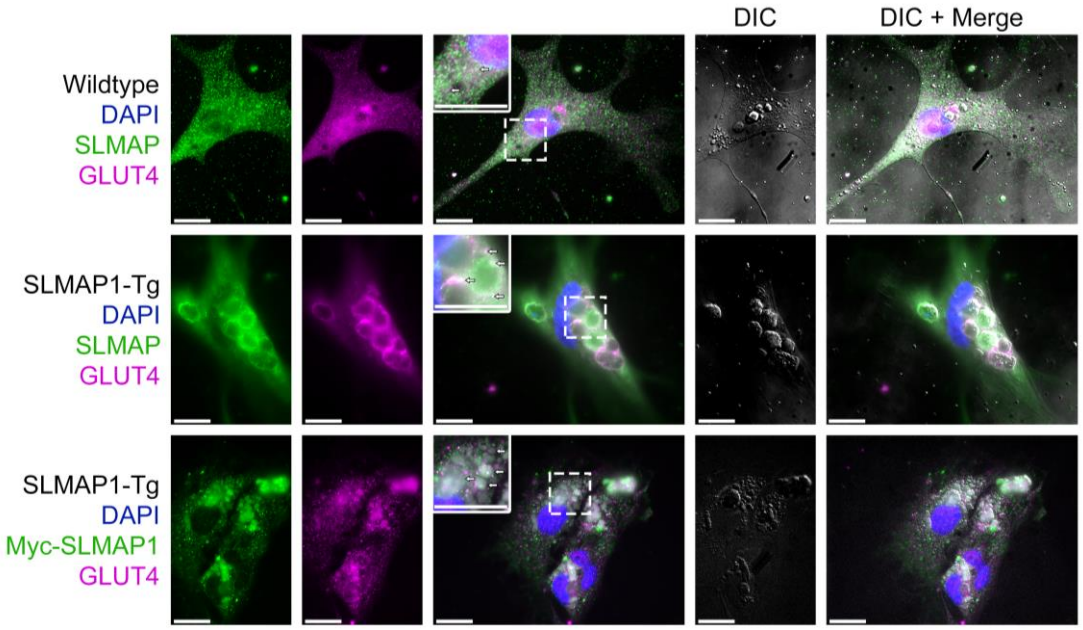

Figure 10. *Expansion of vesicles containing GLUT4 and SLMAP1 in transgenic cardiomyocytes.* Cardiomyocytes isolated from one day old hearts were visualized with Anti-GLUT4 (magenta), SLMAP (green), and Myc (green) antibodies to track localization of GLUT4, all SLMAP isoforms, and overexpressed SLMAP1 respectively. Widefield microscopy showed co-localization of SLMAP1 with GLUT4 in transgenic cardiomyocytes. Wildtype cardiomyocytes displayed significantly smaller GLUT4 vesicles compared to transgenic littermates. DIC imaging revealed presence of enlarged vesicle compartments in transgenic cardiomyocytes, which were significantly larger than wildtype counterparts. Merged DIC images revealed enlarged vesicle compartments to be locations of co-localization between GLUT4 and SLMAP. Arrows in zoomed images indicate areas of colocalization in wildtype and transgenic cardiomyocytes. Analysis with Anti-Myc shows overexpressed SLMAP1 being targeted to enlarged vesicles containing GLUT4.

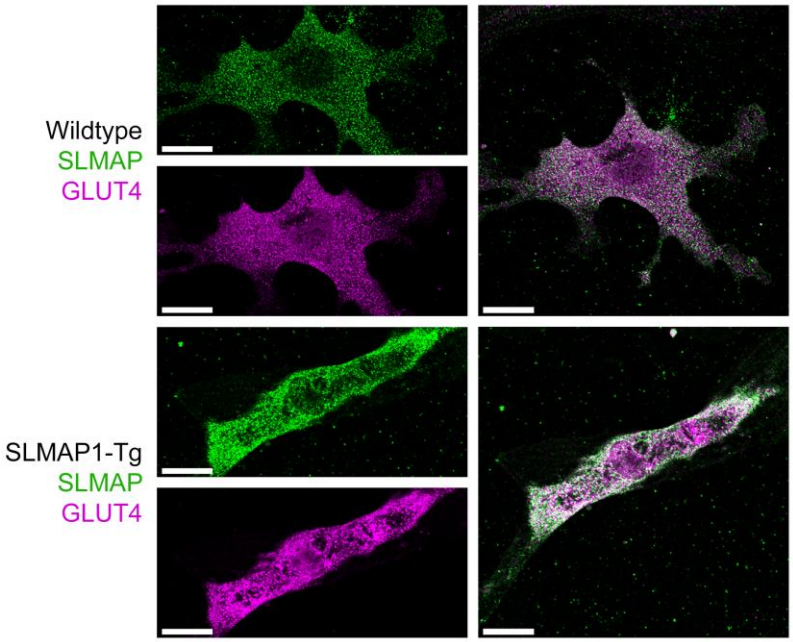

Figure 11. *Co-localization of SLMAP1 and GLUT4 in expanded vesicles.* Confocal microscopy images were taken of cardiomyocytes isolated from one day old hearts visualized with Anti-GLUT4 (red) and SLMAP (magenta) antibodies to track localization of GLUT4 and SLMAP isoforms. Confocal images confirm co-localization noted in widefield imagery between SLMAP proteins and GLUT4 in wildtype cardiomyocytes in peripheral and perinuclear vesicles. Further analysis in transgenic cardiomyocytes shows myc-tagged SLMAP1 co-localizes with GLUT4 in membranes of expanded vesicle compartment.

3.4 SLMAP1 localization to early endosomes

In order to elucidate the mechanism by which SLMAP1 overexpression leads to an upregulation of GLUT4, we first investigated if there may be alterations to GLUT4 trafficking and post-translational stability. The data showing enlarged GLUT4 vesicles at compartments where SLMAP1 and GLUT4 co-localized suggested that SLMAP1 overexpression may be leading to changes in a particular trafficking step, the upregulation of GLUT4 suggested that this step may be during degradation. Further, Akt2 data suggested that SLMAP1 expression did not impact GSV sorting, so our focus moved towards studying if SLMAP1 expression had effects on endosomal sorting. We used antibodies specific to proteins involved in specific trafficking steps; clathrin for imaging clathrin-coated vesicles (CCV), Rab5 for imaging of early and sorting endosomes, Rab4 for imaging of sorting endosomes, and Rab11 for imaging the endosomal recycling compartment (Sönnichsen, et al., 2000; Woodman, 2000; Shen, et al., 2014). Our results show that SLMAP1 does not co-localize in CCVs (Pearson R-Value -0.14 ± 0.040), although it was noted that CCVs did show a trend of surrounding enlarged SLMAP1 containing vesicles. This suggested that SLMAP1 did not play any role in the endocytosis of GLUT4, although the trend of surrounding CCVs indicated that the CCVs may be getting trafficked and fused into the enlarged vesicles (**Figure 12**), suggesting that these vesicles may be endosomal.

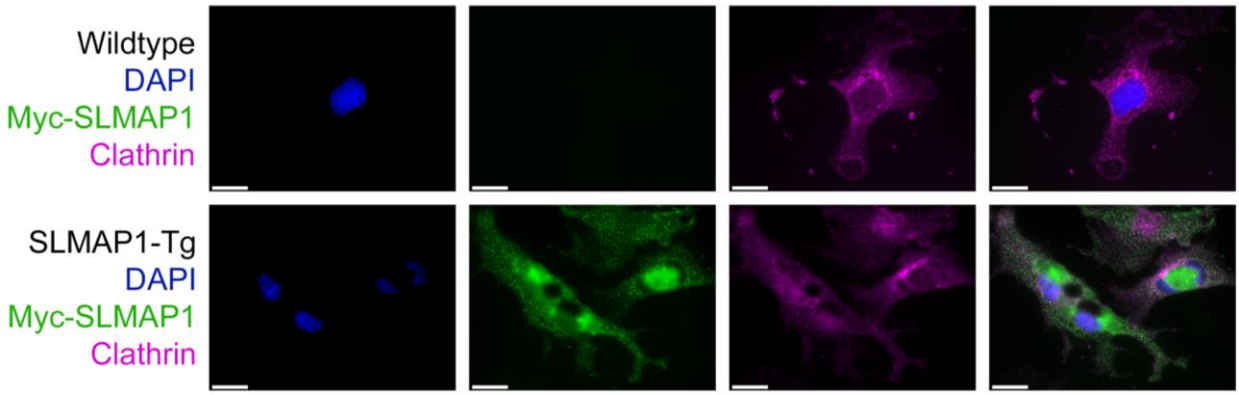

Figure 12. *SLMAP1 overexpression leads to expansion of early endosomes*.

Immunofluorescence co-staining of Clathrin with SLMAP1 using anti-Clathrin (magenta) and anti-Myc (green) antibodies in neonatal cardiomyocytes extracted from day one-old hearts. Clathrin showed no co-localization within enlarged SLMAP1 vesicles, but did show a distinct concentration in regions surrounding enlarged SLMAP1 containing vesicles.

We then moved onto co-staining of Rab5, an early endosome marker, and SLMAP1 (**Figure 13**). We found that there was significant co-localization between SLMAP1 and Rab5 within transgenic cardiomyocytes (Pearson R-Value of 0.89 ± 0.01). This confirmed our beliefs that these enlarged vesicles were in fact endosomes. We also stained with a general SLMAP antibody in order to see if SLMAP co-localized in Rab5 vesicles within wildtypes. We found significant co-localization in wildtype cardiomyocytes between Rab5 and SLMAP (Pearson R-Value of 0.62 ± 0.11). Further, we imaged SLMAP with another early endosome marker known as EEA1 (**Figure 14**), which is involved in the fusion of early endosomes. Similar to Rab5, SLMAP showed significant co-localization with EEA1 in wildtype cardiomyocytes (Pearson R-Value 0.52 ± 0.063) with an increase in co-localization found in transgenic cardiomyocytes (Pearson R-Value 0.81 ± 0.029).

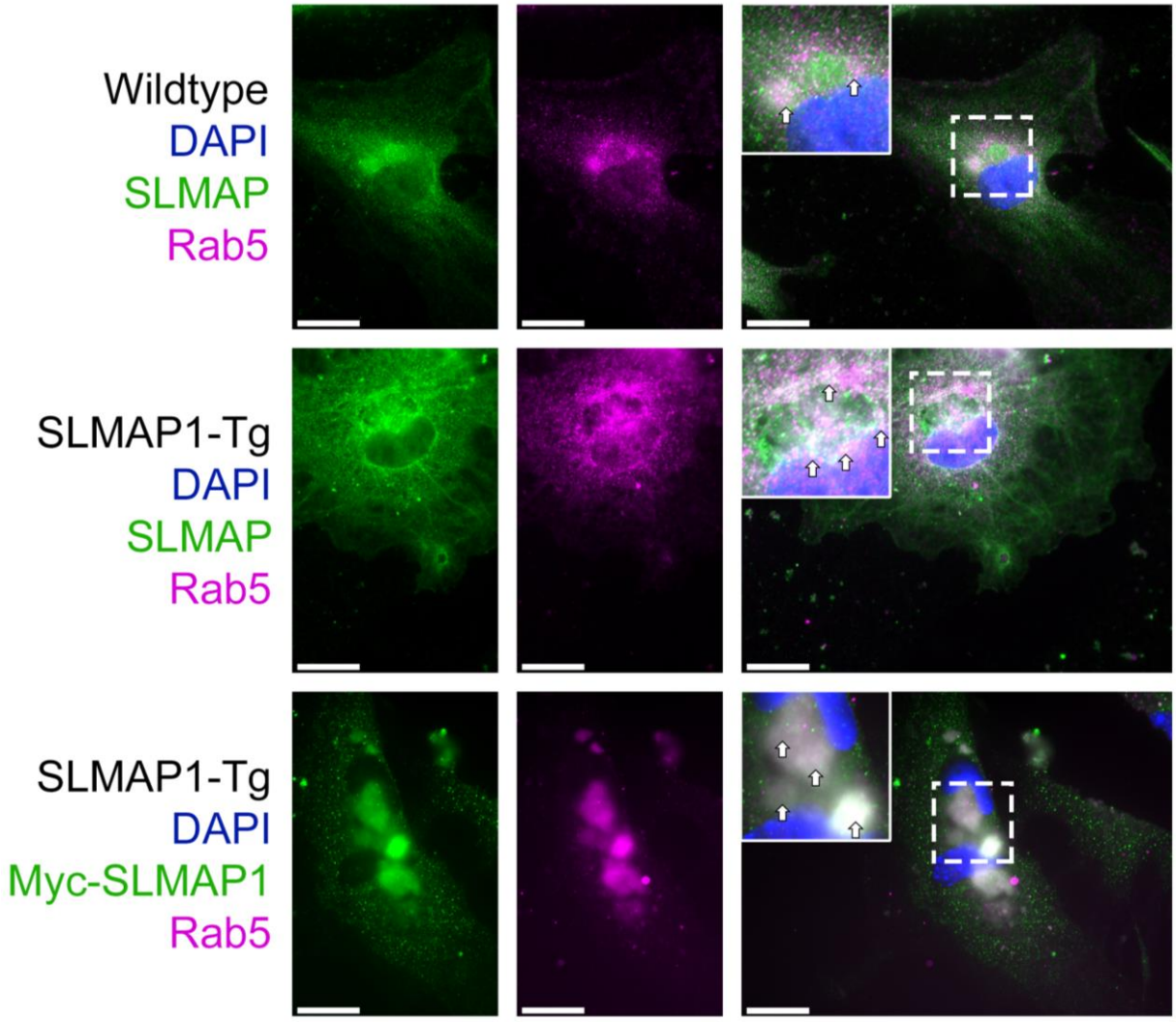

Figure 13. *Co-localization of SLMAP1 in in early endosomes.* Immunofluoresence co-staining of neonatal cardiomyocytes from day one-old hearts visualizing Rab5, all SLMAP isoforms, and SLMAP1 using anti-Rab5 (magenta), anti-SLMAP (green in wildtype), and anti-Myc (green in SLMAP1-Tg) antibodies respectively. Rab5 showed significant colocalization with SLMAP in wildtypes, which increased in transgenic cardiomyocytes. Co-localization with overexpressed SLMAP1 was also noted when stained with anti-Myc. White boxes are shown to depict zoomed in regions, arrows denote regions of co-localization.

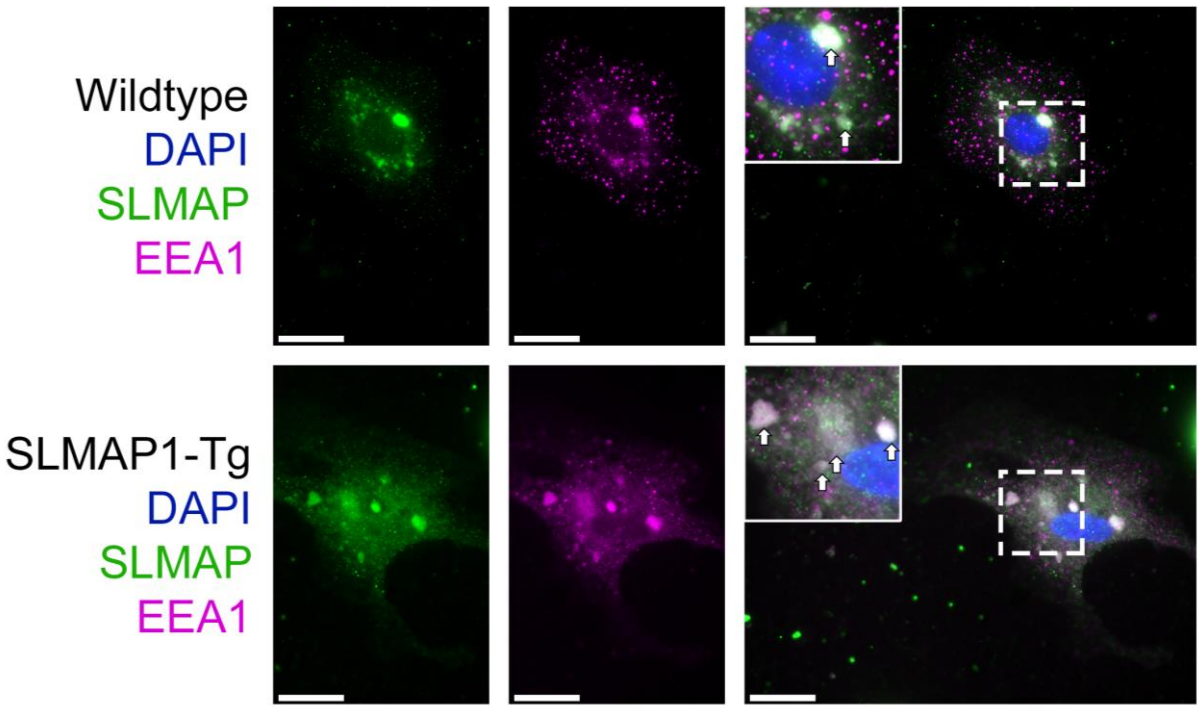

Figure 14. *Co-localization of SLMAP1 with EEA1*. Immunofluoresence co-staining of neonatal cardiomyocytes from day one-old hearts visualizing EEA1, all SLMAP isoforms, and SLMAP1 using anti-EEA1 (magenta), anti-SLMAP (green in wildtype), and anti-Myc (green in SLMAP1-Tg) antibodies respectively. EEA1 showed significant colocalization with SLMAP in wildtypes. Co-localization with overexpressed SLMAP1 was also noted when stained with anti-Myc. White boxes are shown to depict zoomed in regions, arrows denote regions of co-localization. Reprinted with permission from Taha Rehmani. Copyright (2016) of Balwant Tuana laboratory at the University of Ottawa.

In order to obtain further understanding in which subdomain of the endosome SLMAP1 was targeting to, we performed imaging of Myc alongside Rab4 (**Figure 15**), a Rab GTPase present in sorting endosomes. We found that Rab4 and SLMAP1 had a characteristic distribution similar to Clathrin, such that, Rab4 vesicles showed a trend of surrounding SLMAP1 containing vesicles, but did not co-localize significantly (Pearson R-Value -0.026 ± 0.020). This suggested vesicle traffic was diverting away from sorting endosomes. While Rab4 was not found in these endosomes, Rab11, another member of the Rab family of GTPases primarily involved in slow recycling of endosomes to the plasma membrane from the endosomal recycling compartment (Takahashi, et al., 2012), was found to be concentrated in these enlarged early endosomal structures (**Figure 16**). While Rab11 was present within these vesicles, it did not co-localize greatly with SLMAP1 (Pearson R-Value 0.10 ± 0.05). This suggested that while Rab11 was recruited to these structures, it was present within a separate compartment of these endosomes. A proteomic screen also revealed a novel interaction between SLMAP1 and Myosin VI (Hauri, et al., 2013), one of the molecular motors involved in recycling of Rab11 vesicles to the plasma membrane (Chibalina, et al., 2007). Imaging of Wheat germ agglutinin (WGA) and GLUT4 revealed increased localization of GLUT4 at the sarcolemma in SLMAP1-Tg cardiomyocytes compared to wildtype littermates (**Figure 17**). This data suggests SLMAP1 may enhance recycling processes from the ERC to the plasma membrane. In order to elucidate a mechanism for this vesicular traffic redirection we followed up this data by performing immunoprecipitation of SLMAP on wildtype mouse hearts (**Figure 18**). We found a complex between SLMAP and Myosin VI was formed in cardiac tissue. Interactions between SLMAP and Myosin VI also suggest a role SLMAP in recruiting Myosin VI in order to recycle Rab11 vesicles from this enlarged endosomal recycling compartment.

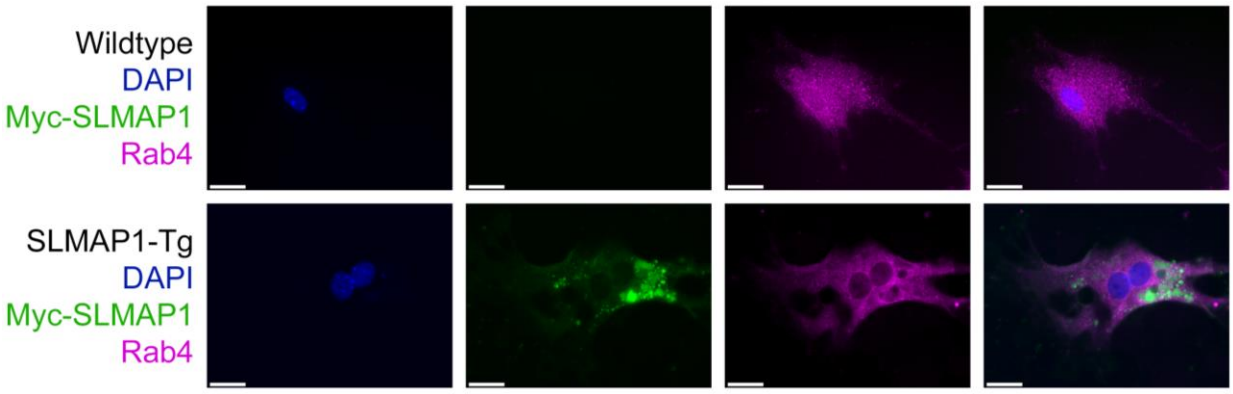

Figure 15. *Early endosome traffic redirected away from sorting endosomes.* Immunofluoresence co-staining of neonatal cardiomyocytes from day one-old hearts visualizing Rab4 and SLMAP1 using anti-Rab4 (magenta) and anti-Myc (green) antibodies respectively. Co-staining of SLMAP1 with Rab4 reveals that Rab4 is not present within expanded endosomes and the two proteins do not co-localize.

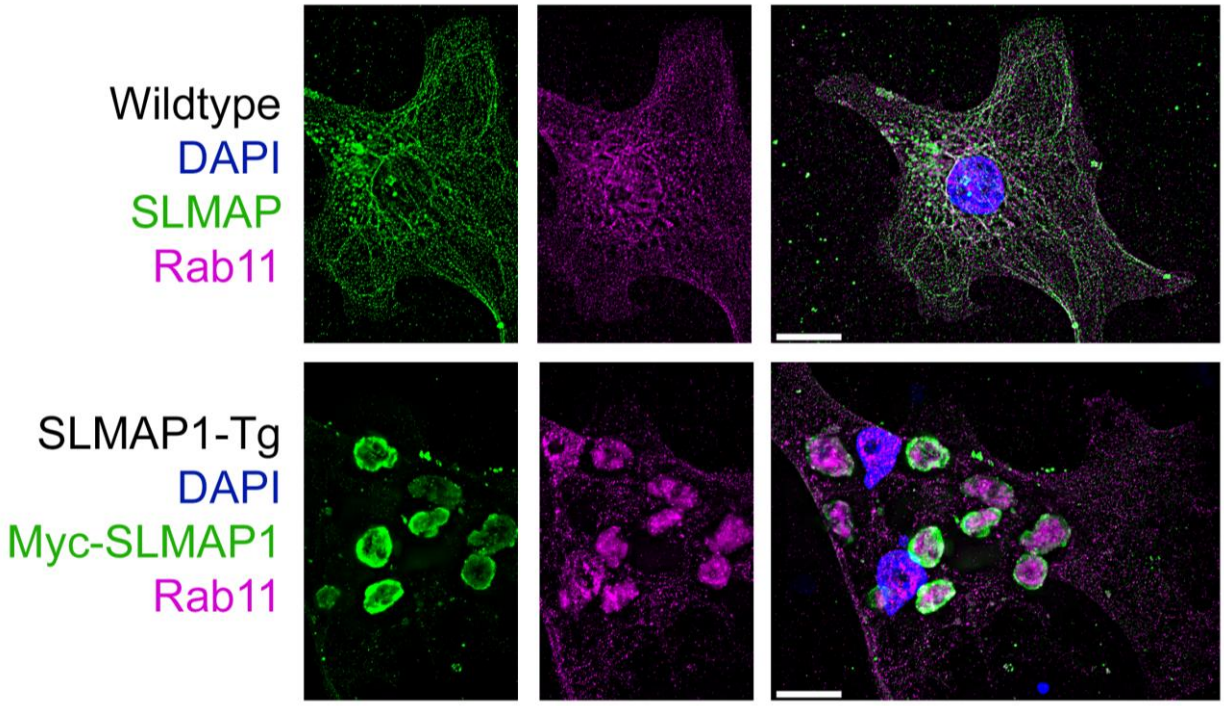

Figure 16. *Redirection of endosomal traffic into the endosomal recycling compartment.* Deconvoluted microscopy of neonatal cardiomyocytes from day one-old hearts visualizing Rab11, all SLMAP isoforms, and SLMAP1 using anti-Rab11 (magenta), anti-SLMAP (green in wildtype), and anti-Myc (green in SLMAP1-Tg) antibodies respectively. Staining with Rab11 and SLMAP1 shows that while proteins do not co-localize, Rab11 concentrates inside enlarged endosomes, while SLMAP1 concentrates around the periphery.

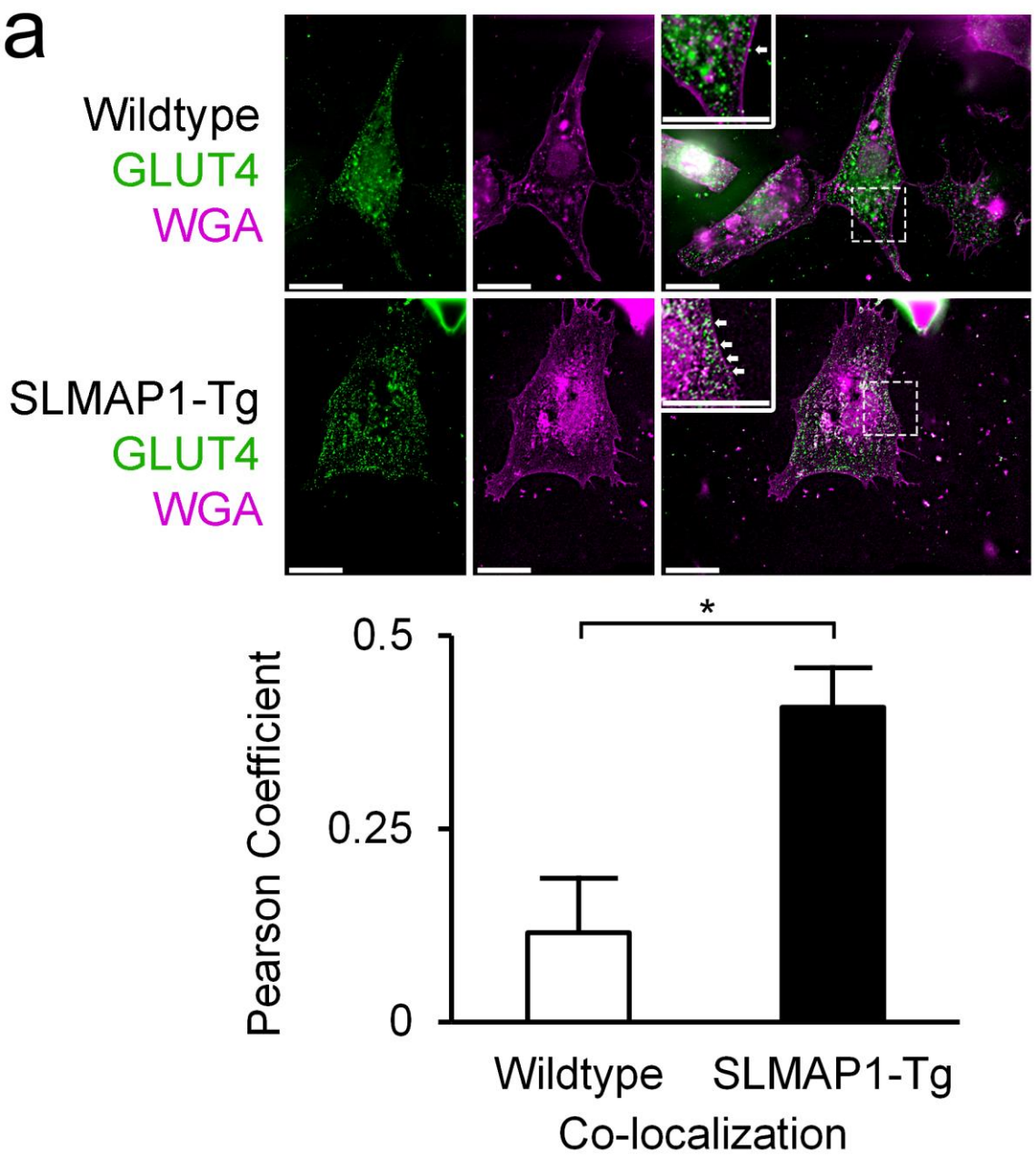

Figure 17. *Increase in plasma membrane GLUT4 content in SLMAP1-Tg neonatal cardiomyocytes.* Deconvoluted microscopy of wheat germ agglutinin (WGA) and GLUT4 in neonatal cardiomyocytes isolated from day one mouse hearts. GLUT4 was visualized using anti-GLUT4 (green) while plasma membranes were visualized using WGA (magenta). Plasma membranes were selected as regions of interest and co-localization values between WGA and

GLUT4 were obtained from these regions. Scale bar represents 20μm. SLMAP1-Tg cardiomyocytes displayed increased localization of GLUT4 to the plasma membrane (Pearson R-Value 0.41 ± 0.05) compared to wildtype littermates (Pearson R-Value 0.12±0.07). Asterisk denotes significance value of $P<0.05$ using T.Test statistical analysis and n=30 cells from 3 different experiments.

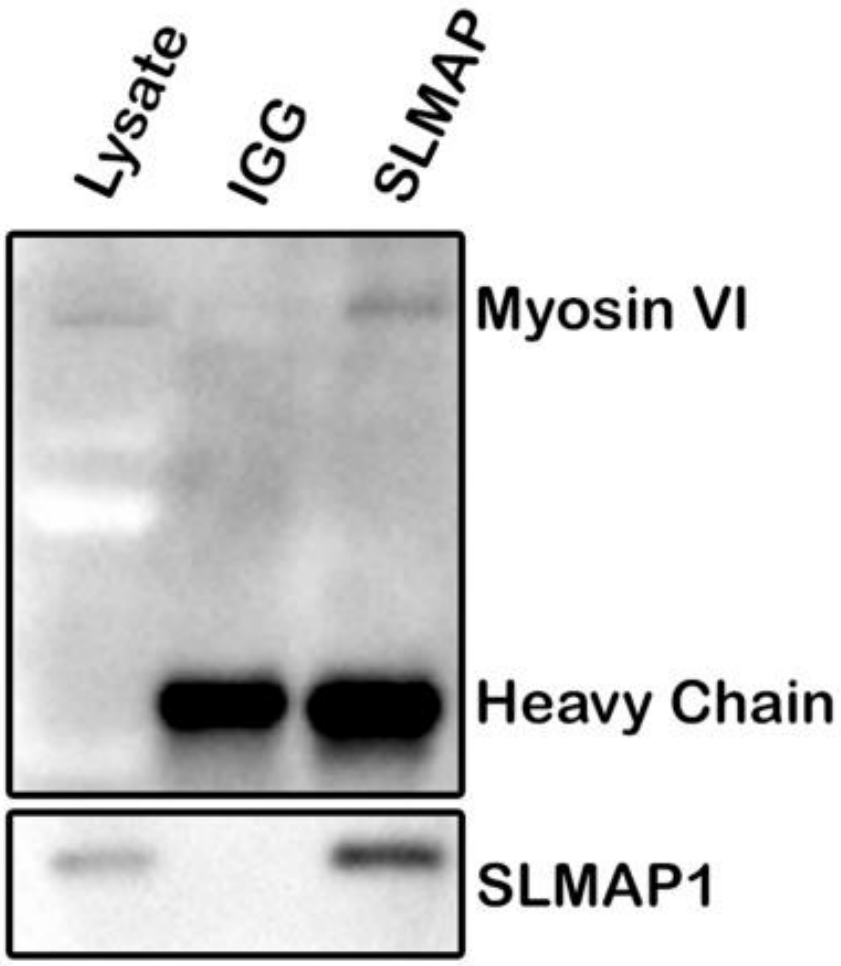

Figure 18. *SLMAP proteins form a complex with motor proteins involved in direction of endosomal traffic.* Protein lysate obtained from adult mouse hearts were immunoprepitated for complexes containing SLMAP proteins using anti-SLMAP and anti-IGG as a control. Immunoprecipitation of SLMAP from wildtype hearts pulls down Myosin VI, suggesting complex formation between Myosin VI and SLMAPs.

3.5 Recruitment of fusion proteins to early endosomes

Co-localization of SLMAP1 in a specific subcompartment of early endosomes with EEA1 and Rab5 suggested a potential role for this protein in the fusion of early endosomes. Within cardiomyocytes, endosomal fusion is mediated by the formation of the SNARE complex by SNAP23, Syntaxin-4, and VAMP-2 (Peters, et al., 2006). We first looked at localization of these proteins to see if SLMAP co-localized with SNARE complex proteins within enlarged endosomes of cardiomyocytes. We found significant co-localization between SLMAP1 and t-SNARE proteins SNAP23 (Pearson R-Value of 0.90 ± 0.02) and Syntaxin-4 (Pearson R-Value of 0.91 ± 0.02). When visualizing the v-SNARE protein VAMP-2, significant co-localization was not found, instead localization was mutually exclusive (Pearson R-Value of -0.20 ± 0.06) (**Figure 19A**). Although it should be noted, that VAMP2 did show concentrated localization around the enlarged endosomes, suggesting a role for it as the v-SNARE in fusing vesicles into this compartment. When protein expression levels of these SNARE proteins were assessed, it was found that transgenic hearts contained increased levels of SNAP23 (187% ± 60.3%, n=6, $P<0.05$), Syntaxin-4 (133% ± 53.04%, n=4, $P<0.01$), and VAMP2 (96.14% ± 26.2%, n=5, $P<0.05$). Further, the expression of vesicle tether EEA1, which initiates and recruits the SNARE complex, was also increased in transgenic hearts (168.26% ± 44.19%, n=4, $P<0.01$) (**Figure 19B**), suggesting SLMAP1 levels may be regulating endosomal sorting and fusion through the expression and recruitment of the SNARE complex.

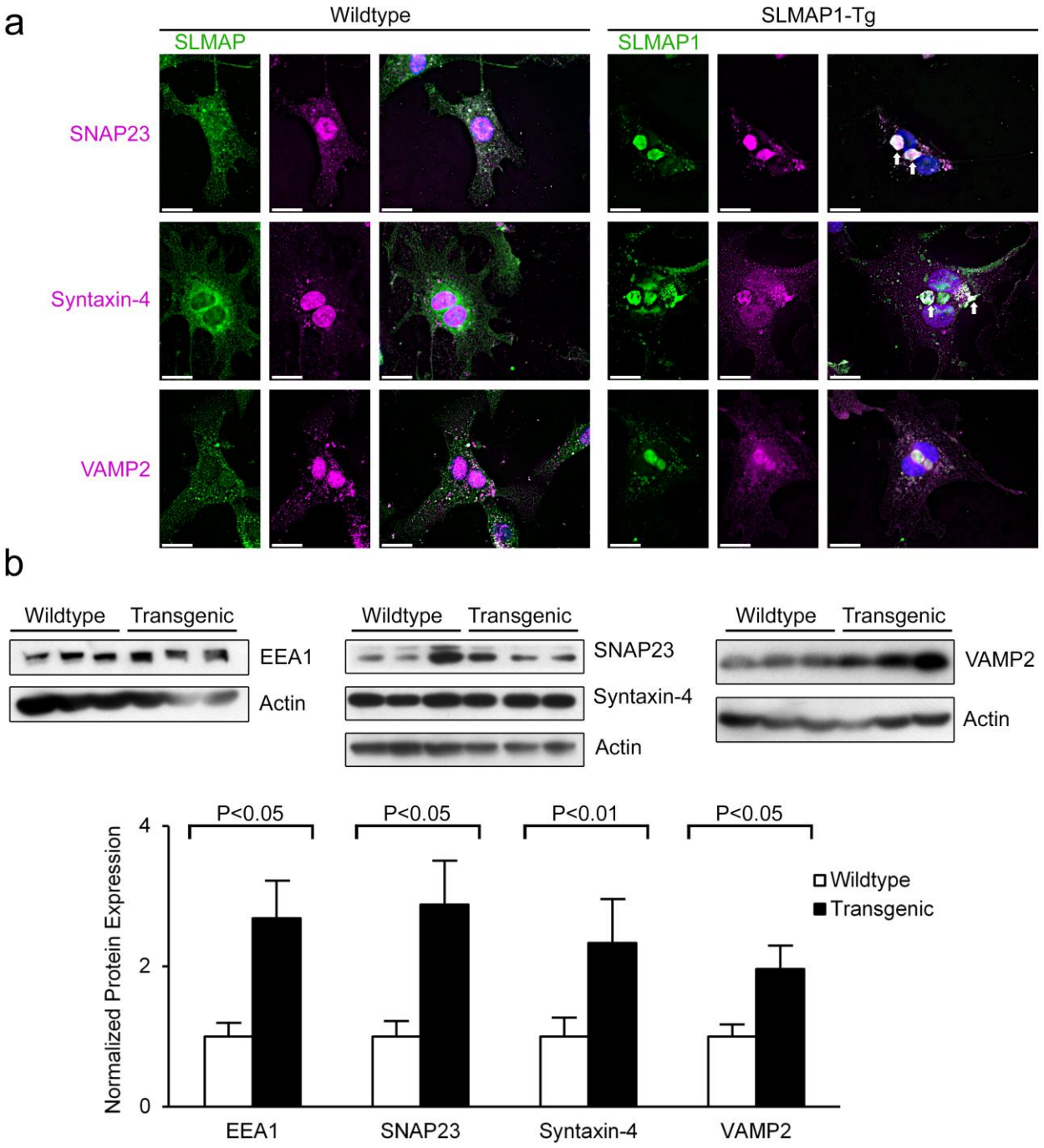

Figure 19. *SLMAP1 overexpression recruits SNARE complex to endosomes.* (**A**) Deconvoluted maximum intensity projection microscopy of neonatal cardiomyocytes from day one-old hearts visualizing SNARE proteins, all SLMAP isoforms, and SLMAP1. SNAREs were visualized using anti-Syntaxin-4, anti-SNAP23, and anti-VAMP2 (magenta). Anti-SLMAP (green in wildtype) was used for visualization of SLMAP proteins in wildtype cardiomyocytes and anti-

Myc (green in SLMAP1-Tg) was used for visualization of SLMAP1 in SLMAP1-Tg cardiomyocytes. Trangenic cardiomyocytes showed recruitment of SNARE complex proteins to SLMAP1-enlarged endosomes. While the t-SNAREs Syntaxin-4 and SNAP23 showed significant colocalization with SLMAP1 (indicated by arrowheads), the v-SNARE VAMP2 was mutually exclusive with SLMAP1, although VAMP2 showed concentration in areas surrounding endosomes. Localization suggests SLMAP1 to be a recruiter of t-SNAREs in order to fuse membranes with v-SNARE containing vesicles. (**B**) Western Blot analysis of SNARE proteins shows upregulation of SNAREs in mouse myocardium. Protein expression was assessed by Western Blot analysis and quantified using densitometry with actin as a loading control. EEA1 (168% ± 44.2%, n=4 adult hearts, $P<0.01$ using two-tailed t-test), SNAP23 (187% ± 60.3%, n=6 adult hearts, $P<0.05$ using two-tailed t-test), Syntaxin-4 (133% ± 53.04%, n=4 adult hearts, $P<0.01$ using two-tailed t-test) and, VAMP2 (96.13% ± 26.2%, n=5 adult hearts, $P<0.05$ using two-tailed t-test) was increased in transgenic hearts compared to wildtype littermates. Reprinted with permission from Taha Rehmani. Copyright (2016) of Balwant Tuana laboratory at the University of Ottawa.

In order for Rab5 to initiate the endosomal fusion process and recruit tethers and SNAREs, binding from the effector protein Rabaptin-5 is required. In a previous proteomic screen, it was proposed that there may be a potential interaction between Rabaptin-5 and SLMAP-(Hauri, et al., 2013). In order to further study if SLMAP1 overexpression had downstream effects on Rabaptin-5, we performed immunofluorescence analysis of Rabaptin-5 and SLMAP in both wildtype and transgenic neonatal cardiomyocytes. While wildtype cardiomyocytes showed significant co-localization between SLMAP and Rabaptin-5 (Pearson R-Value 0.70 ± 0.07), upon overexpression of SLMAP1, this co-localization increased (Pearson R-Value 0.94 ± 0.01, $P<0.05$). This co-localization was considerably concentrated around enlarged endosomal structures (**Figure 20).** Upon western blot analysis of Rabaptin-5 expression in wildtype and transgenic mouse hearts (**Figure 21**), it was found that expression of Rabaptin-5 was increased in transgenic hearts (124.6% ± 36.6, n=5, $P<0.05$). Further, upon immunoprecipitation of SLMAP from wildtype heart lysate, it was found that a complex is formed between SLMAP and Rab5, the protein to which Rabaptin-5 acts as an effector protein (**Figure 22**). The data here suggests a mechanism by which SLMAP1 may act as a recruiter for Rabaptin-5 in order to mediate endosomal fusion.

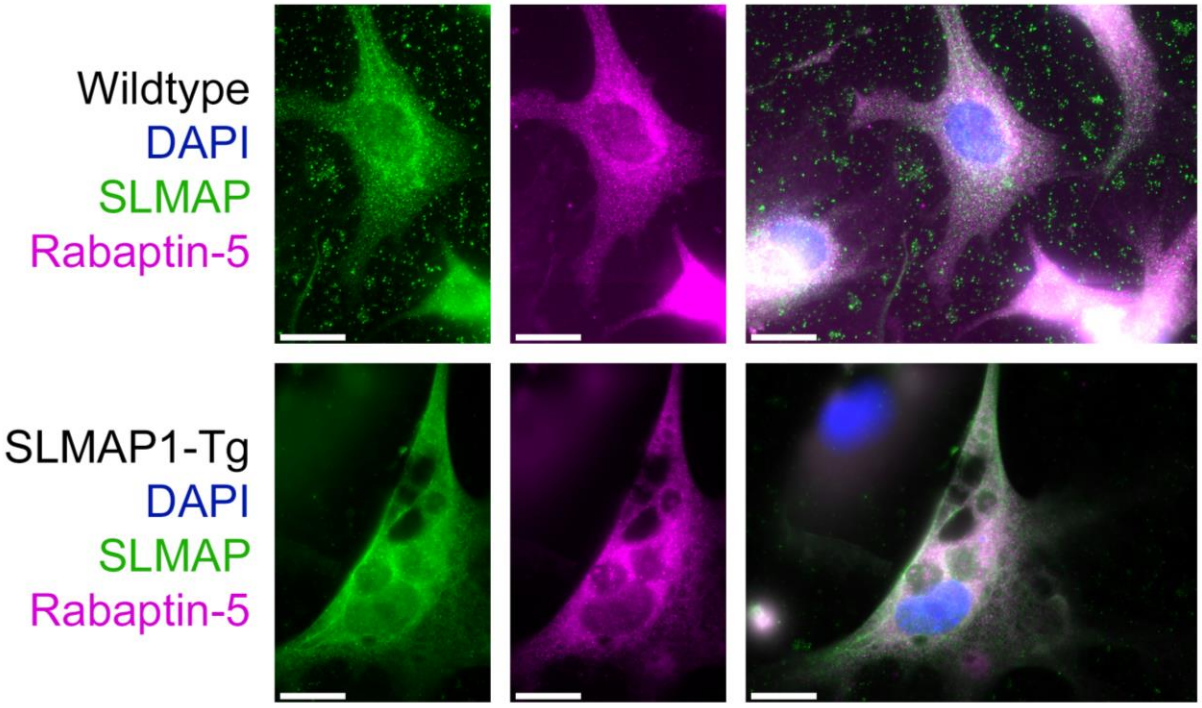

Figure 20. *SLMAP1 expression recruits Rabaptin-5 to early endosomes.* Cardiomyocytes isolated from one day old hearts were visualized with Anti-Rabaptin-5 (magenta) and anti-SLMAP (green) antibodies to track localization of Rabaptin-5 and SLMAP isoforms. SLMAPs co-localized with Rabaptin-5 in wildtype cardiomyocytes and this co-localization increased in SLMAP1-Tg cardiomyocytes alongside increased presence of Rabaptin-5 at membranes of expanded early endosome.

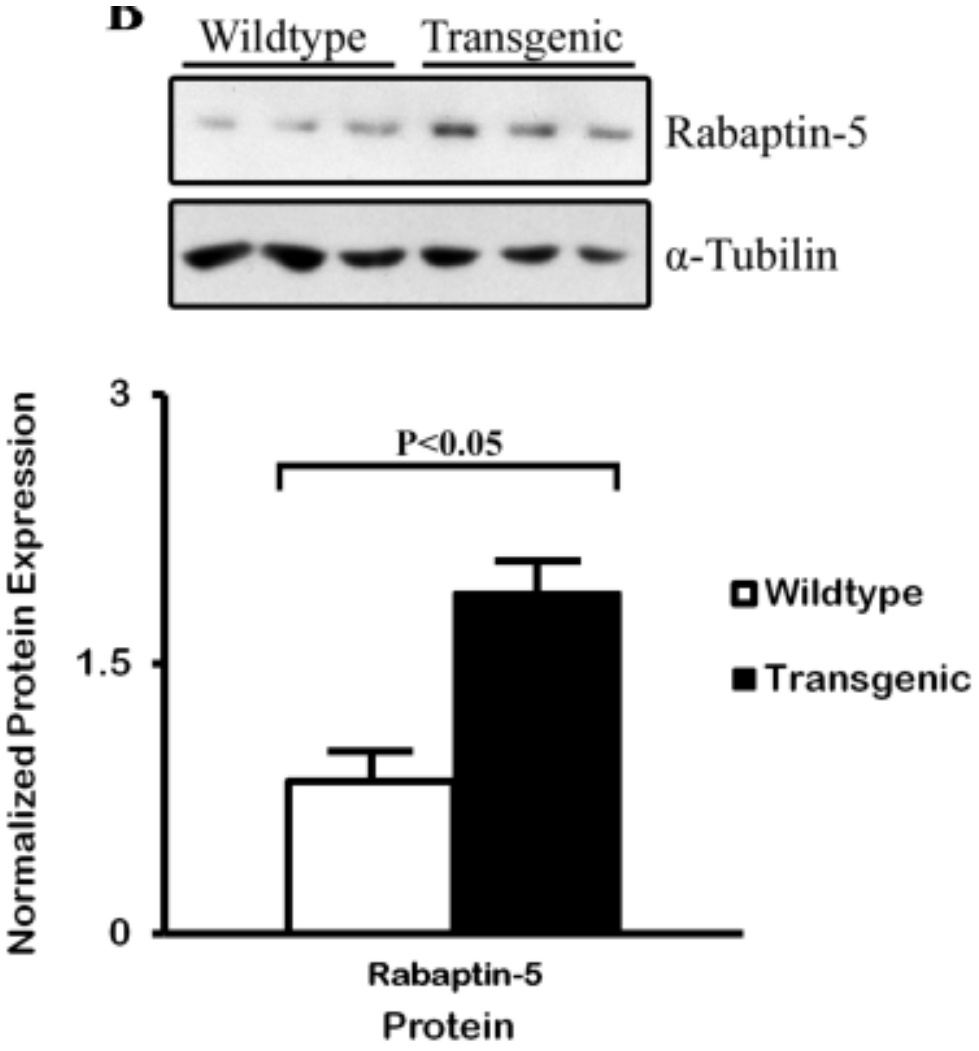

Figure 21. *SLMAP1 expression regulates Rabaptin*-5. Protein extracted from adult mouse hearts was quantified using Western Blot densitometry analysis with α-tubulin as a loading control. Anti-Rabaptin-5 was used to probe for Rabaptin-5 expression and anti-α-tubulin was used to quantify α-tubulin expression. Rabaptin-5 was significantly upregulated in SLMAP1-Tg hearts (125 ±37%, n=5 adult hearts, $P<0.05$ using two-tailed t-test) compared to wildtype littermates.

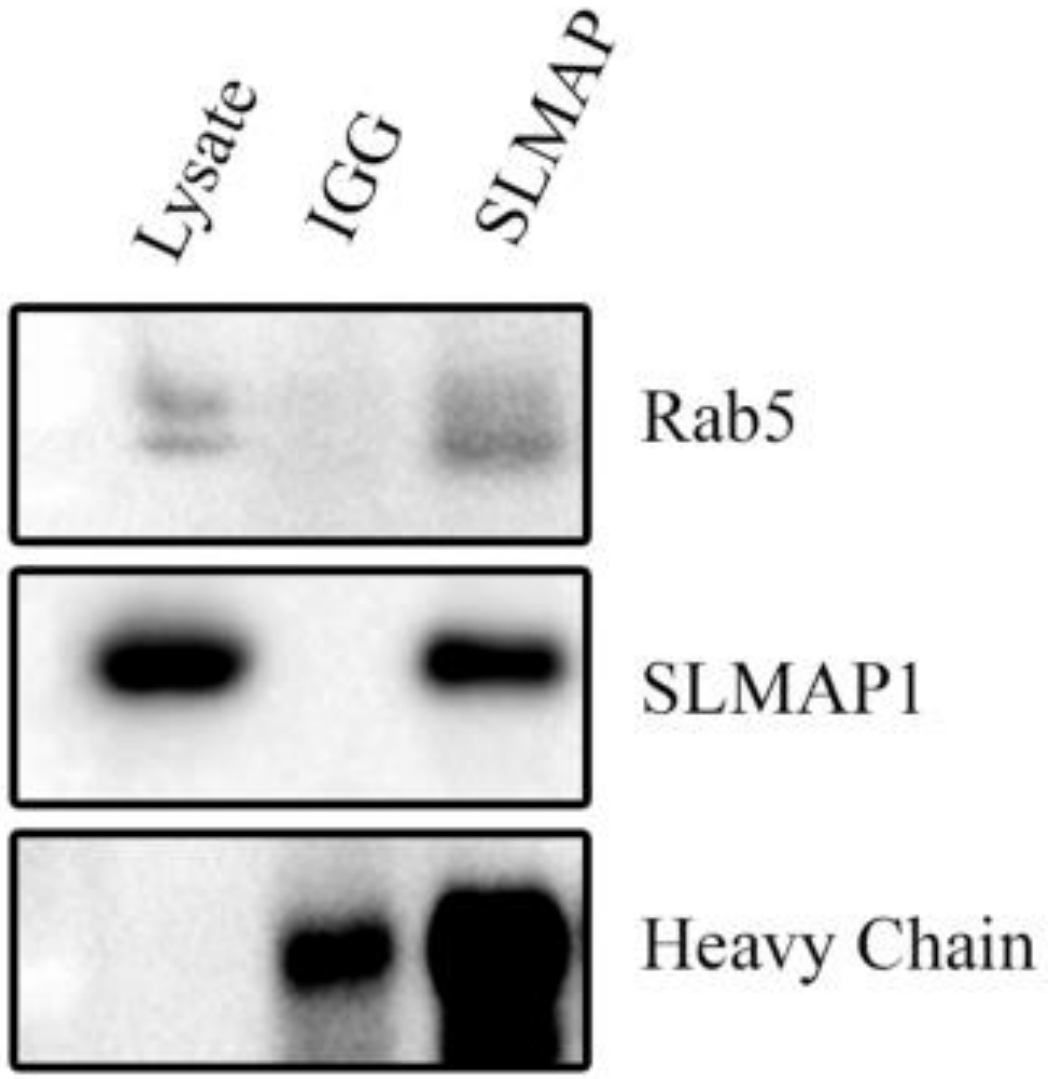

Figure 22. *SLMAPs form complexes with a regulator of endosomal trafficking and fusion*. Protein lysate obtained from adult mouse hearts were immunoprepitated for complexes containing SLMAP proteins using anti-SLMAP and anti-IGG as a control. SLMAP immunoprecipitation pulls down Rab5 proteins, suggesting complex formation between SLMAPs and Rab5.

CHAPTER 4: Discussion

The results here support a role for SLMAP1 as a novel regulatory mechanism of glucose metabolism in the myocardium through a unique mechanism involved in GLUT4 trafficking. We previously noted that increasing SLMAP1 expression in postnatal myocardium lead to an increase in vesicle/vacoule formation and subcellular membrane remodeling (Nader, et al., 2012). While the identity of these membrane vesicles was largely unknown, the data here suggests they are not clathrin-coated vesicles (CCVs) due to the absence of clathrin within these vesicles. We also noted that these were not part of sorting endosomes, do the lack of Rab4. We concluded by identifying these vesicles as part of the endosomal recycling compartment (ERC) due to the presence of Rab5, EEA1, and Rab11. Further, the SLMAP1 expression mediated the expansion of the ERC, as all ERC vesicles containing SLMAP1 showed drastic size expansion. We noted here a complex between SLMAPs and Rab5 in cardiac tissue, which is further supported by proteomic data noting the presence of protein complexes containing SLMAPs and Rabaptin-5 in HEK293 cells (Hauri, et al., 2013). Rabaptin-5 is a Rab5 effector protein which initiates endosomal fusion processes by positioning Rab5 containing vesicles in order to initiate the fusion process (Lippé, et al., 2001). We noted SLMAP1 expression caused a marked upregulation of Rabaptin-5, as well as recruitment to early endosomal membranes. In this regard, Rabaptin-5 has also been noted to be sufficient in mediating the size expansion of early endosomes (Stenmark, et al., 1995), suggesting a potential mechanism by which SLMAP1 may mediate size expansion of vesicles. The fusion proteins EEA1, SNAP23 and Syntaxin-4 were also found to be concentrated in endosomal regions with SLMAP1, suggesting SLMAP1 may be recruiting fusion proteins to mediate membrane fusion processes. Taken together, this data suggests a regulatory role for SLMAP1 in the initiation of early endosomal fusion.

Rab11 was also present within the enlarged endosomes, although it localized in distinct regions compared to SLMAP1. Further, we noted a complex between SLMAPs and Myosin VI, the myosin motor involved in movement of early endosome traffic to the ERC. This data suggests that SLMAP1 not only plays a role in the fusion of early endosomes, but also may be involved in recruiting Myosin VI, in order to direct early endosome traffic away from lysosomal degradation and towards the ERC for recycling. Further, fusion events mediated by Rab5 may occur at different sites from fission (recycling) events mediated by Rab11, due to the concentrating of these proteins within different membrane regions. Indeed, the membrane proteins EEA1, SNAP23, VAMP2, and Syntaxin-4 all showed a marked upregulation in the SLMAP1-Tg myocardium. Redirection of endosomal traffic towards recycling pathways suggests a unique mechanism by which SLMAP1 may be regulating levels of proteins involved in vesicle transport.

GLUT4 has the highest affinity to glucose out of all glucose transporters and is rate limiting in its uptake into heart (Leto & Saltiel, 2012). We noted a marked upregulation of GLUT4, although qPCR analysis revealed no change in transcript levels, suggested that increased GLUT4 protein expression was not due to changes in transcription, but rather an alternate mechanism. Upon further analysis, we noted expression of SLMAP1 altered the intracellular distribution of GLUT4 from an even distribution throughout the cell, to concentration within the ERC. This suggests that GLUT4 traffic was being redirected from being stored in insulin-sensitive GSVs, to the constitutively recycling ERC. This is further exemplified by the SLMAP1-Tg myocardium displaying decreased in phosphorylation of Akt2, a known regulator of GLUT4 traffic through GSVs. While our studies focused on the insulin-independent effects of SLMAP1 on GLUT4 trafficking, the large upregulation of total Akt2 levels by SLMAP1 suggests that these cells may

be more insulin sensitive, although this needs to be examined in future experiments. Interestingly, Akt2 transcript levels were unaltered, suggesting that SLMAP1 expression can regulate the stability of cytosolic proteins, as well as membrane proteins, potentially through changes to lysosomal degradation. Thus, future studies should focus on the role of SLMAP1 in lysosome and degradation of proteins.

Increased SLMAP1 levels lead to a redirection of GLUT4 traffic towards intracellular localization at the ERC. The presence of GLUT4 at the plasma membrane was also increased by SLMAP1 expression, leading to enhanced glucose uptake. This data is further supported by evidence showing siRNA mediated downregulation of SLMAP1 led to a decrease in glucose uptake (Chen & Ding, 2011), suggesting a central role for SLMAP1 in regulating glucose entry into cells. This could implicate SLMAP1 as a potential target in diabetes where there is dysregulation of GLUT4 trafficking to sarcolemma leads to diabetic cardiomyopathy (Goldin, et al., 2006). Our metabolic data supports the notion that SLMAP1 enhanced substrate availability for glycolytic enzymes through enhanced glucose uptake, leading to enhanced glycolysis. Results from the fatty acid oxidation assay also implicate SLMAP1 in the regulation of fatty acid metabolism. The neonatal heart primarily uses glucose metabolism to meet energy demands (Scholz & Segar, 2008; Calmettes, et al., 2013) and SLMAP1 is highly expressed in the developing myocardium to potentially direct GLUT4 function (Guzzo, et al., 2005). While substrate flexibility is paramount to cardiovascular health (Kolwicz, et al., 2013; Byrne, et al., 2016; Shao & Tian, 2015), the data showing SLMAP1 can also impact fatty acid oxidation under stressed conditions suggests that SLMAP1 may be regulating the cardiomyocyte's metabolic flexibility to maximally utilize available substrates to support function.

Based on the data here, we propose the model outlined in **Figure 23** where SLMAP1 levels regulate glucose metabolism through the expression and localization of pertinent proteins via redirection of endosomal traffic towards recycling pathways and away from lysosomal degradation. In this model, SLMAP1 is targeted to the endosome by its tail anchor and serves to recruit proteins involved in the fusion and direction of endosomal traffic. Through this mechanism, SLMAP1 would enhance recycling of membrane proteins, and impact metabolism through increased uptake of glucose by GLUT4 at the plasma membrane. This hugely implicates SLMAP1 in both cardiac membrane biology and metabolism. Previous studies from our group noted drastic remodeling of subcellular membranes brought on by SLMAP1 expression in the postnatal heart with little negative impact on cardiac function. Taken together, this novel role for SLMAP1 in the endosomal regulation of GLUT4 suggests a protective role for SLMAP1 in diseases in which GLUT4 expression and trafficking is altered, such as diabetes. Indeed, recent studies have implicated SLMAP mutations as a prognostic marker for the development of diabetic retinopathy in diabetic populations (Upadhyay, et al., 2015). These findings combined with previous studies suggest a role for SLMAP as a protective factor in diabetes, and future studies should be commenced in order to study its protective effects in diabetic cardiomyopathy.

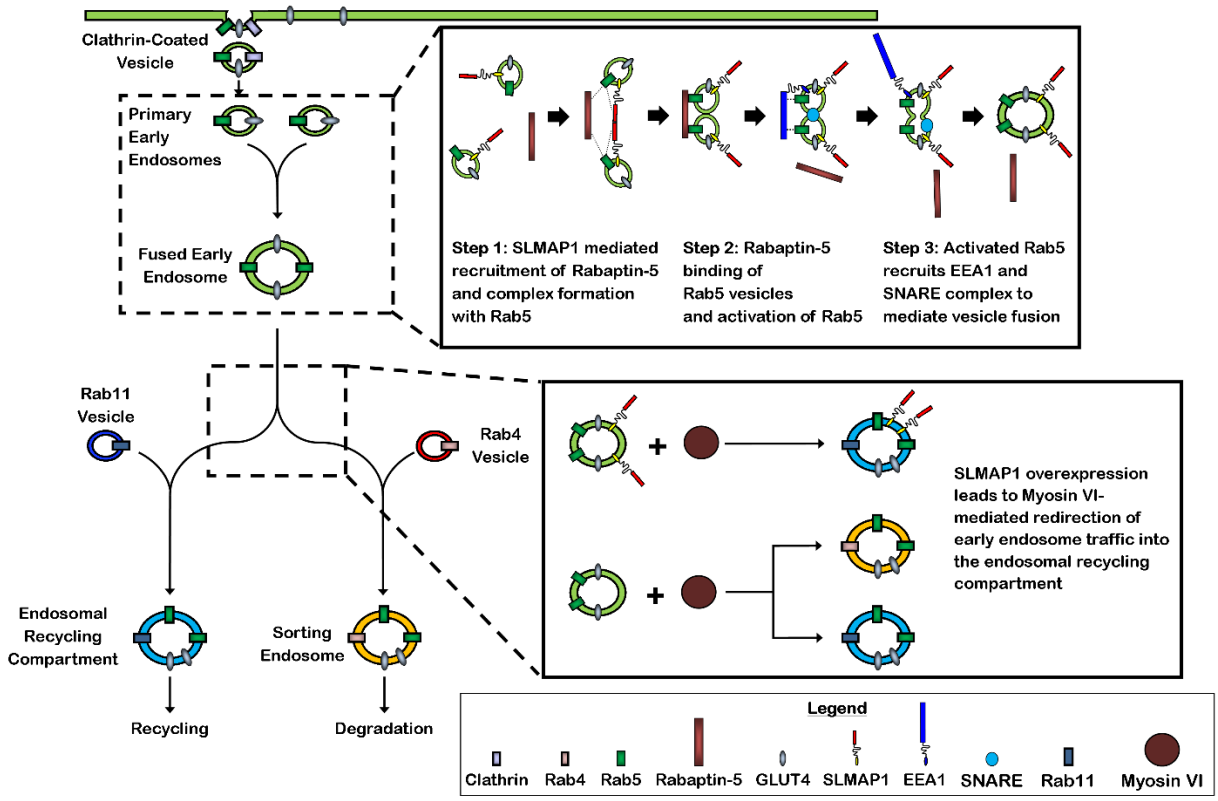

Figure 23. *Schematic representation of the role of SLMAP1 in vesicle trafficking.* The data predicts that SLMAP1 plays several key roles in the trafficking of endosomes and regulating expressing and localization of membrane proteins like GLUT4. First, SLMAP1 may serve to recruit Rabaptin-5 and fusion proteins in order to initiate early endosomal fusion. Second, SLMAP1 may redirect early endosomal traffic into the endosomal recycling compartment, potentially via assembly with Myosin VI. Finally, redirection to the endosomal recycling compartment would lead to increased recycling of endosomes, and thus recycling of GLUT4 to the sarcolemma, leading to enhanced glucose uptake and metabolism. Through this mechanism, SLMAP1 regulates the levels of membrane proteins like GLUT4 and SNAREs.

CHAPTER 5: References

Ai, X. et al., 2005. Ca2+/calmodulin-dependent protein kinase modulates cardiac ryanodine receptor phosphorylation and sarcoplasmic reticulum Ca2+ leak in heart failure. *Circulation Research,* 97(12), pp. 1314-22.

Aledo, J. C. et al., 1997. Identification and characterization of two distinct intracellular GLUT4 pools in rat skeletal muscle: evidence for an endosomal and an insulin-sensitive GLUT4 compartment. *Biochem J,* 325(Pt 3), pp. 727-732.

Anderson, E. J. et al., 2009. Substrate-specific derangements in mitochondrial metabolism and redox balance in the atrium of the type 2 diabetic human heart. *J Am Coll Cardiol,* 54(20), pp. 1891-1898.

Aniento, F., Gu, F., Parton, R. G. & Gruenberg, J., 1996. An endosomal beta COP is involved in the pH-dependent formation of transport vesicles destined for late endosomes. *J Cell Biol,* 133(1), pp. 29-41.

Antonescu, C. N. et al., 2008. Clathrin-dependent and independent endocytosis of glucose transporter 4 (GLUT4) in myoblasts: regulation by mitochondrial uncoupling. *Traffic,* 9(7), pp. 1173-1190.

Antonescu, C. N., Foti, M., Sauvonnet, N. & Klip, A., 2009. Ready, set, internalize: mechanisms and regulation of GLUT4 endocytosis. *Biosci Rep,* 29(1), pp. 1-11.

Balteau, M. et al., 2011. NADPH oxidase activation by hyperglycaemia in cardiomyocytes is independent of glucose metabolism but requires SGLT1. *Cardiovasc Res,* 92(2), pp. 237-246.

Band, A. M. et al., 2002. Endogenous plasma membrane t-SNARE syntaxin 4 is present in rab11 positive endosomal membranes and associates with cortical actin cytoskeleton. *FEBS Lett,* 531(3), pp. 513-519.

Baskin, K. K. et al., 2014. MED13-dependent signaling from the heart confers leanness by enhancing metabolism in adipose tissue and liver. *EMBO Mol Med,* 6(12), pp. 1610-1621.

Baskin, K. K., Winders, B. R. & Olson, E. N., 2015. Muscle as a "mediator" of systemic metabolism. *Cell Metab,* 21(2), pp. 237-248.

Bernhardt, U. et al., 2009. A dual role of the N-terminal FQQI motif in GLUT4 trafficking. *Biol Chem,* 390(9), pp. 883-892.

Birault, V., Solari, R., Hanrahan, J. & Thomas, D. Y., 2013. Correctors of the basic trafficking defect of the mutant F508del-CFTR that causes cystic fibrosis. *Curr Opin Chem Biol,* 17(3), pp. 353-360.

Blot, V. & McGraw, T. E., 2006. GLUT4 is internalized by a cholesterol-dependent nystatin-sensitive mechanism inhibited by insulin. *EMBO J,* 25(24), pp. 5648-5658.

Bogan, J. S., 2012. Regulation of glucose transporter translocation in health and diabetes. *Annu Rev Biochem,* Volume 81, pp. 507-532.

Borgese, N., Colombo, S. & Pedrazzini, E., 2003. The tale of tail-anchored proteins: coming from the cytosol and looking for a membrane. *J Cell Biol,* 161(6), pp. 1013-1019.

Boudina, S. & Adel, E., 2007. Diabetic cardiomyopathy revisited.. *Circulation,* Volume 115, p. 3213–23.

Bryant, N., Govers, R. & James, D., 2002. Regulated transport of the glucose transporter GLUT4. *Nature Rev Mol Cell Biol,* 3(4), pp. 267-277.

Bryant, N. J. & Gould, G. W., 2011. SNARE proteins underpin insulin-regulated GLUT4 traffic. *Traffic,* 12(6), pp. 657-664.

Bugger, H. & Abel, E. D., 2014. Molecular mechanisms of diabetic cardiomyopathy. *Diabetologia,* 57(4), pp. 660-671.

Bustin, S. A., 2002. Quantification of mRNA using real-time reverse transcription PCR (RT-PCR): trends and problems. *J Mol Endocrinol,* 29(1), pp. 23-29.

Byers, J. T., Guzzo, R. M., Salih, M. & Tuana, B. S., 2009. Hydrophobic profiles of the tail anchors in SLMAP dictate subcellular targetting. *BMC Cell Biol,* 10(48), pp. 1-18.

Byrne, N. J. et al., 2016. Normalization of Cardiac Substrate Utilization and Left Ventricular Hypertrophy Precede Functional Recovery in Heart Failure Regression. *Cardiovasc Res,* p. [Epub ahead of print].

Calmettes, G., John, S. A., Weiss, J. N. & Ribalet, B., 2013. Hexokinase–mitochondrial interactions regulate glucose metabolism differentially in adult and neonatal cardiac myocytes. *J Gen Physiol,* 142(4), pp. 425-36.

Candido, R. et al., 2003. A breaker of advanced glycation end products attenuates diabetes-induced myocardial structural changes. *Circulation Research,* 92(7), pp. 785-792.

Caplan, S., Dell'Angelica, E. C., Gahl, W. A. & Bonifacino, J. S., 2000. Trafficking of major histocompatibility complex class II molecules in human B-lymphoblasts deficient in the AP-3 adaptor complex. *Immunol Lett,* 72(2), pp. 113-117.

Chen, D. & Whiteheart, S. W., 1999. Intracellular localization of SNAP-23 to endosomal compartments. *Biochem and Biophys Res Commun,* 255(2), pp. 340-346.

Chen, X. & Ding, H., 2011. Increased expression of the tail-anchored membrane protein SLMAP in adipose tissue from type 2 Tally Ho diabetic mice. *Exp Diabetes Res,* 2011(421982), pp. 1-10.

Chibalina, M. V. et al., 2007. Myosin VI and its interacting protein LMTK2 regulate tubule formation and transport to the endocytic recycling compartment. *J Cell Sci,* 120(Pt 24), pp. 4278-4288.

Cho, H. et al., 2001. Insulin resistance and a diabetes mellitus-like syndrome in mice lacking the protein kinase Akt2 (PKB beta). *Science,* 292(5522), pp. 1728-1731.

Choi, H., Tostes, R. C. & Webb, R. C., 2011. Mitochondrial aldehyde dehydrogenase prevents ROS-induced vascular contraction in angiotensin-II hypertensive mice. *J Am Soc Hypertens,* 5(3), pp. 154-160.

Christoforidis, S., McBride, H., Burgoyne, R. & Zerial, M., 1999 . The Rab5 effector EEA1 is a core component of endosome docking. *Nature,* 397(6720), pp. 621-5.

Cobbold, C., Monaco, A. P., Sivaprasadarao, A. & Ponnambalam, S., 2003. Aberrant trafficking of transmembrane proteins in human disease. *Trends Cell Biol,* 13(12), pp. 639-647.

Condorelli, G. et al., 2002. Akt induces enhanced myocardial contractility and cell size in vivo in transgenic mice. *Proceedings of the National Academy of Sciences of the United States of America,* 99(19), pp. 12333-12338.

Czech, M. P. & Corvera, S., 1999. Signaling mechanisms that regulate glucose transport. *Journal of Biological Chemistry,* 274(4), pp. 1865-1868.

Das, K. C., 2013. Hyperoxia decreases glycolytic capacity, glycolytic reserve and oxidative phosphorylation in MLE-12 cells and inhibits complex I and II function, but not complex IV in isolated mouse lung mitochondria. *PLoS One,* 8(9), p. e73358.

de Simone, G. et al., 2010. Diabetes and incident heart failure in hypertensive and normotensive participants of the Strong Heart Study. *Journal of Hypertension,* 28(2), pp. 353-360.

Desrois, M. et al., 2004. Initial steps of insulin signaling and glucose transport are defective in the type 2 diabetic rat heart.. *Cardiovasc Res,* 61(2), pp. 288-296.

Devereux, R. B. et al., 2000. Impact of diabetes on cardiac structure and function: the strong heart study. *Circulation,* 101(19), pp. 2271-2276.

Ding, H. et al., 2005. Endothelial dysfunction in type 2 diabetes correlates with deregulated expression of the tail-anchored membrane protein SLMAP. *Am J Physiol Heart Circ Physiol,* 289(1), pp. 206-211.

Doherty, G. J. & McMahon, H. T., 2009. Mechanisms of endocytosis. *Annu Rev Biochem,* Volume 78, pp. 857-902.

Dunn, K. W., McGraw, T. E. & Maxfield, F. R., 1989. Iterative fractionation of recycling receptors from lysosomally destined ligands in an early sorting endosome. *J Cell Biol,* 109(6), pp. 3303-3314.

Dyck, J. R. & Lopaschuk, G. D., 2006. AMPK alterations in cardiac physiology and pathology: enemy or ally?. *J Physiol,* 574(Pt 1), pp. 95-112.

Elahi, M. M., Kong, Y. X. & Matata, B. M., 2009. Oxidative stress as a mediator of cardiovascular disease. *Oxid Med Cell Longev,* 2(5), pp. 259-269.

Erickson, J. R. et al., 2013. Diabetic hyperglycaemia activates CaMKII and arrhythmias by O-linked glycosylation. *Nature,* 502(7471), pp. 372-376.

Fang, Z. Y. et al., 2005. Screening for heart disease in diabetic subjects. *American Heart Journal,* 149(2), pp. 349-354.

Fasshauer, D., 2003. Structural insights into the SNARE mechanism. *Biochim Biophys Acta,* 164(2-3), pp. 87-97.

Fasshauer, D. et al., 1997. Structural changes are associated with soluble N-ethylmaleimide-sensitive fusion protein attachment protein receptor complex formation. *J Biol Chem,* 272(44), pp. 28036-28041.

Fazakerley, D. J. et al., 2010. Kinetic evidence for unique regulation of GLUT4 trafficking by insulin and AMP-activated protein kinase activators in L6 myotubes. *J Biol Chem,* 285(3), pp. 1653-1660.

Foley, K., Boguslavsky, S. & Klip, A., 2011. Endocytosis, recycling, and regulated exocytosis of glucose transporter 4. *Biochemistry,* 50(15), pp. 3048-3061.

Foster, L. J., Li, D., Randhawa, V. K. & Klip, A., 2001. Insulin accelerates inter-endosomal GLUT4 traffic via phosphatidylinositol 3-kinase and protein kinase B. *J Biol Chem,* 276(47), pp. 44212-44221.

Fujita, H. et al., 2010. Identification of Three Distinct Functional Sites of Insulin-mediated GLUT4 Trafficking in Adipocytes Using Quantitative Single Molecule Imaging. *Mol Biol Cell,* 21(15), pp. 2721-2731.

Fukuda, M., 2011. TBC proteins: GAPs for mammalian small GTPase Rab?. *Bioscience Reports,* 31(3), pp. 159-168.

Gadsby, D. C., Vergani, P. & Csanády, L., 2006. The ABC protein turned chloride channel whose failure causes cystic fibrosis. *Nature,* 440(7083), pp. 477-483.

Gertz, E. W., Wisneski, J. A., Stanley, W. C. & Neese, R. A., 1988. Myocardial substrate utilization during exercise in humans. Dual carbon-labeled carbohydrate isotope experiments. *J Clin Invest,* 82(6), pp. 2017-2025.

Goldin, A., Beckman, J. A., Schmidt, A. M. & Creager, M. A., 2006. Advanced glycation end products: sparking the development of diabetic vascular injury. *Circulation,* 114(6), pp. 597-605.

Grant, B. D. & Donaldson, J. G., 2009. Pathways and mechanisms of endocytic recycling. *Nat Rev Mol Cell Biol,* 10(9), pp. 597-608.

Grueter, C. et al., 2012. A cardiac microRNA governs systemic energy homeostasis by regulation of MED13. *Cell,* 149(3), pp. 671-683.

Guo, X. et al., 2012. Glycolysis in the control of blood glucose homeostasis. *Acta Pharm Sin B,* 2(4), pp. 358-367.

Guzzo, R. M., Salih, M., Moore, E. D. & Tuana, B. S., 2005. Molecular properties of cardiac tail-anchored membrane protein SLMAP are consistent with structural role in arrangement of excitation-contraction coupling apparatus. *American Journal of Physiology: Heart and Circulatory Physiology,* 288(4), pp. 1810-1819.

Guzzo, R. M., Sevinc, S., Salih, M. & Tuana, B. S., 2004. A novel isoform of sarcolemmal membrane-associated protein (SLMAP) is a component of the microtubule organizing centre. *J Cell Sci,* 117(Pt 11), pp. 2271-2281.

Guzzo, R. M. et al., 2004. Regulated expression and temporal induction of the tail-anchored sarcolemmal-membrane-associated protein is critical for myoblast fusion. *Biochem J,* 381(3), pp. 599-608.

Hafstad, A. D., Nabeebaccus, A. A. & Shah, A. M., 2013. Novel aspects of ROS signalling in heart failure. *Basic Res Cardiol,* 108(4), p. 359.

Hanson, P., Heuser, J. & Jahn, R., 1997. Neurotransmitter release—four years of SNARE complexes. *Curr Opin Neurobiol,* 7(3), pp. 310-315.

Hao, W., Chang, C. P., Tsao, C. C. & Xu, J., 2010. Oligomycin-induced bioenergetic adaptation in cancer cells with heterogeneous bioenergetic organization. *J Biol Chem,* 285(17), pp. 12647-12654.

Haucke, V., Neher, E. & Sigrist, S. J., 2011. Protein scaffolds in the coupling of synaptic exocytosis and endocytosis. *Nature Rev Neurosci,* 12(3), pp. 127-138.

Hauri, S. et al., 2013. Interaction proteome of human Hippo signaling: modular control of the co-activator YAP1. *Mol Sys Biol,* 9(713), pp. 1-16.

Hay, J. & Scheller, R., 1997. SNAREs and NSF in targeted membrane fusion. *Curr Opin Cell Biol,* 9(4), pp. 505-512.

Heather, L. C. & Clarke, K., 2011. Metabolism, hypoxia and the diabetic heart.. *J Mol Cell Cardiol,* 50(4), pp. 598-605.

Hindi, S. M., Tajrishi, M. M. & Kumar, A., 2013. Signaling Mechanisms in Mammalian Myoblast Fusion. *Sci Signal,* 6(272), pp. 1-18.

Houten, S. M. & Wanders, R. J. A., 2010. A general introduction to the biochemistry of mitochondrial fatty acid β-oxidation. *J Inherit Metab Dis,* 33(5), pp. 469-477.

How, O. et al., 2006. Increased myocardial oxygen consumption reduces cardiac efficiency in diabetic mice.. *Diabetes,* 55(2), pp. 466-473.

Huang, J., Imamura, T. & Olefsky, J. M., 2001. Insulin can regulate GLUT4 internalization by signaling to Rab5 and the motor protein dynein. *Proc Natl Acad Sci U S A,* 98(23), pp. 13084-13089.

Huang, S. & Czech, M. P., 2007. The GLUT4 glucose transporter. *Cell Metab,* 5(4), pp. 237-252.

Huss, J. M. & Kelly, D. P., 2004. Nuclear receptor signaling and cardiac energetics. *Circ Res,* 95(6), pp. 568-578.

Ikemoto, S. et al., 1995. High fat diet-induced hyperglycemia: prevention by low level expression of a glucose transporter (GLUT4) minigene in transgenic mice. *Proc Natl Acad Sci U S A,* 92(8), pp. 3096-3099.

IMS Brogan, 2011. *Canadian pharmaceutical trends. Top 10 dispensed therapeutic classes in Canada,* Canada: s.n.

Ishikawa, T. et al., 2012. A novel disease gene for Brugada syndrome: sarcolemmal membrane-associated protein gene mutations impair intracellular trafficking of hNav1.5. *Circ Arrhythm Electrophysiol,* 5(6), pp. 1098-1107.

Ishikura, S. & Klip, A., 2008. Muscle cells engage Rab8A and myosin Vb in insulin-dependent GLUT4 translocation. *Am J Physiol Cell Physiol,* 295(4), pp. 1016-1025.

Jahn, R. & Su¨dhof, T., 1999. Membrane fusion and exocytosis. *Ann Rev Biochem,* Volume 68, pp. 863-911.

Jedrychowski, M. P. et al., 2010. Proteomic analysis of GLUT4 storage vesicles reveals LRP1 to be an important vesicle component and target of insulin signaling. *J Biol Chem,* 285(1), pp. 104-114.

Jhun, B. H. et al., 1992. Effects of insulin on steady state kinetics of GLUT4 subcellular distribution in rat adipocytes. Evidence of constitutive GLUT4 recycling. *J Biol Chem,* 267(25), pp. 17710-17715.

Johnson, L. S., Dunn, K. W., Pytowski, B. & McGraw, T. E., 1993. Endosome acidification and receptor trafficking: bafilomycin A1 slows receptor externalization by a mechanism involving the receptor's internalization motif. *Mol Biol Cell,* 4(12), pp. 1251-1266.

Jordens, I. et al., 2010. Insulin-regulated aminopeptidase is a key regulator of GLUT4 trafficking by controlling the sorting of GLUT4 from endosomes to specialized insulin-regulated vesicles. *Mol Biol Cell,* 21(12), pp. 2034-2044.

Kaddai, V., Marchand-Brustel, Y. L. & Cormont, M., 2008. Rab proteins in endocytosis and Glut4 trafficking. *Acta Physiol (Oxf),* 192(1), pp. 75-88.

Kane, S. et al., 2002. A method to identify serine kinase substrates. Akt phosphorylates a novel adipocyte protein with a Rab GTPase-activating protein (GAP) domain. *Journal of Biological Chemistry,* 277(25), pp. 22115-22118.

Kannel, W. B. & McGee, D. L., 1979. Diabetes and cardiovascular disease. The Framingham study. *JAMA,* 241(19), pp. 2035-2038.

Karim, Z. A. et al., 2013. IκB kinase phosphorylation of SNAP-23 controls platelet secretion. *Blood,* 121(22), pp. 4567-4574.

Karylowski, O., Zeigerer, A., Cohen, A. & McGraw, T. E., 2004. GLUT4 is retained by an intracellular cycle of vesicle formation and fusion with endosomes. *Mol Biol Cell,* 15(2), pp. 870-882.

Kawaguchi, T. et al., 2010. The t-SNAREs syntaxin4 and SNAP23 but not v-SNARE VAMP2 are indispensable to tether GLUT4 vesicles at the plasma membrane in adipocyte. *Biochem Biophys Res Commun,* 391(3), pp. 1336-1341.

Kerner, J. & Hoppel, C., 2000. Fatty acid import into mitochondria. *Biochim Biophys Acta,* 1486(1), pp. 1-17.

Kioumourtzoglou, D., Gould, G. W. & Bryant, N. J., 2014. Insulin stimulates syntaxin4 SNARE complex assembly via a novel regulatory mechanism. *Mol Cell Biol,* 34(7), pp. 1271-1279.

Kolwicz, S. C., Purohit, S. & Tian, R., 2013. Cardiac metabolism and its interactions with contraction, growth, and survival of cardiomyocytes. *Circ Res,* 113(3), pp. 603-616.

Kondoh, H., Lleonart, M. E., Bernard, D. & Gil, J., 2007. Protection from oxidative stress by enhanced glycolysis; a possible mechanism of cellular immortalization. *Histol Histopathol,* 22(1), pp. 85-90.

Kranstuber, A. L. et al., 2012. Advanced glycation end product cross-link breaker attenuates diabetes-induced cardiac dysfunction by improving sarcoplasmic reticulum calcium handling. *Frontiers in Physiology,* Volume 3, p. 292.

Kruszynska, Y. T. & Sherratt, H. S., 1987. Glucose kinetics during acute and chronic treatment of rats with 2[6(4-chloro-phenoxy)hexyl]oxirane-2-carboxylate, etomoxir. *Biochem Pharmacol,* 36(22), pp. 3917-3921.

Kuang, M. et al., 2004. Fatty acid translocase/CD36 deficiency does not energetically or functionally compromise hearts before or after ischemia. *Circulation,* 109(12), pp. 1550-1557.

Kupriyanova, T. A., Kandror, V. & Kandror, K. V., 2002. Isolation and characterization of the two major intracellular Glut4 storage compartments. *J Biol Chem,* 277(11), pp. 9133-9138.

Kutay, U., Hartmann, E. & Rapoport, T. A., 1993. A class of membrane proteins with a C-terminal anchor. *Trends Cell Biol,* 3(3), pp. 72-75.

Lampson, M. A. et al., 2001. Insulin-regulated release from the endosomal recycling compartment is regulated by budding of specialized vesicles. *Mol Biol Cell,* 12(11), pp. 3489-3501.

Lee, J. H., Bassel-Duby, R. & Olson, E. N., 2014. Heart- and muscle-derived signaling system dependent on MED13 and Wingless controls obesity in Drosophila. *Proc Natl Acad Sci U S A,* 111(26), pp. 9491-9496.

Leto, D. & Saltiel, A. R., 2012. Regulation of glucose transport by insulin: traffic control of GLUT4. *Nat Rev Mol Cell Biol,* 13(6), pp. 383-396.

Liao, M.-H.et al., 2013. The disturbance of hippocampal CaMKII/PKA/PKC phosphorylation in early experimental diabetes mellitus. *CNS Neurosci Ther,* 19(5), pp. 329-336.

Lin, S. X., Grant, B., Hirsh, D. & Maxfield, F. R., 2001. Rme-1 regulates the distribution and function of the endocytic recycling compartment in mammalian cells. *Nat Cell Biol,* 3(6), pp. 567-572.

Lippé, R. et al., 2001. Functional synergy between Rab5 effector Rabaptin-5 and exchange factor Rabex-5 when physically associated in a complex. *Mol Biol Cell,* 12(7), pp. 2219-2228.

Liu, M. et al., 1993. Transgenic mice expressing the human GLUT4/muscle-fat facilitative glucose transporter protein exhibit efficient glycemic control. *Proc Natl Acad Sci U S A,* 90(23), pp. 11346-11350.

Luo, W.-j. & Chang, A., 2000. An Endosome-to-Plasma Membrane Pathway Involved in Trafficking of a Mutant Plasma Membrane ATPase in Yeast. *Mol Biol Cell,* 11(2), pp. 579-592.

Martin, S. et al., 1996. The glucose transporter (GLUT-4) and vesicle-associated membrane protein-2 (VAMP-2) are segregated from recycling endosomes in insulin-sensitive cells. *J Cell Biol,* 134(3), pp. 625-635.

Martin, S. et al., 1996. The glucose transporter (GLUT-4) and the vesicle-associated membrane protein-2 (VAMP-2) are segregated from recycling endosomes in insulin-sensitive cells. *J Cell Biol,* 134(3), pp. 625-635.

Masure, S. et al., 1999. Molecular cloning, expression and characterization of the human serine/threonine kinase Akt-3. *European Journal of Biochemistry,* 265(1), pp. 353-360.

Maxfield, F. & McGraw, T., 2004. Endocytic Recycling. *Nat Rev Mol Cell Biol,* Volume 5, pp. 121-132.

Mayor, S., Presley, J. F. & Maxfield, F. R., 1993. Sorting of membrane components from endosomes and subsequent recycling to the cell surface occurs by a bulk flow process. *J Cell Biol,* 121(6), pp. 1257-1269.

McClave, S. A. & Snider, H. L., 2001. Dissecting the energy needs of the body. *Curr Opin Clin Nutr Metab Care,* 4(2), pp. 143-147.

McGarry, J., 2002. Banting lecture 2001: dysregulation of fatty acid metabolism in thecetiology of type 2 diabetes. Volume 51, pp. 7-18.

Mehta, A. D. et al., 1999. Myosin-V is a processive actin-based motor. *Nature,* 400(6744), pp. 590-593.

Ménard, S. et al., 2010. Abnormal in vivo myocardial energy substrate uptake in diet-induced type 2 diabetic cardiomyopathy in rats.. *Am J Physiol Endocrinol Metab,* 298(5), pp. 1049-1057.

Montaigne, D. et al., 2014. Myocardial contractile dysfunction is associated with impaired mitochondrial function and dynamics in type 2 diabetic but not in obese patients. *Circulation,* 130(7), pp. 554-564.

Moore, R. H. et al., 2004. Rab11 regulates the recycling and lysosome targeting of beta2-adrenergic receptors. *J Cell Sci,* 117(Pt 15), pp. 3107-3117.

Morgan, B. J., Chai, S. Y. & Albiston, A. L., 2011. GLUT4 associated proteins as therapeutic targets for diabetes. *Recent Pat Endocr Metab Immune Drug Discov,* 5(1), pp. 25-32.

Muretta, J. M., Romenskaia, I. & Mastick, C. C., 2008. Insulin releases Glut4 from static storage compartments into cycling endosomes and increases the rate constant for Glut4 exocytosis. *J Biol Chem,* 283(1), pp. 311-323.

Nader, M. et al., 2012. Tail-anchored membrane protein SLMAP is a novel regulator of cardiac function at the sarcoplasmic reticulum. *Am J Physiol Heart Circ Physiol,* 302(5), pp. 1138-1145.

Nakamura, S., 2004. Glucose activates H(+)-ATPase in kidney epithelial cells. *Am J Physiol Cell Physiol,* 287(1), pp. 97-105.

Norton, G. R., Candy, G. & Woodiwiss, A. J., 1996. Aminoguanidine prevents the decreased myocardial compliance produced by streptozotocin-induced diabetes mellitus in rats. *Circulation,* 93(10), pp. 1905-1912.

Oh, E., Stull, N. D., Mirmira, R. G. & Thurmond, D. C., 2014. Syntaxin 4 up-regulation increases efficiency of insulin release in pancreatic islets from humans with and without type 2 diabetes mellitus. *J Clin Endocrinol Metab,* 99(5), pp. 866-870.

Patel, N., Khayat, Z. A., Ruderman, N. B. & Klip, A., 2001. Dissociation of 5' AMP-activated protein kinase activation and glucose uptake stimulation by mitochondrial uncoupling and hyperosmolar stress: differential sensitivities to intracellular Ca2+ and protein kinase C inhibition. *Biochem Biophys Res Commun,* 285(4), pp. 1066-1070.

Paulson, D. J., Ward, K. M. & Shug, A. L., 1984. Malonyl CoA inhibition of carnitine palmityltransferase in rat heart mitochondria. *FEBS Lett,* 176(2), pp. 381-384.

Perera, H. K. et al., 2003. Syntaxin 6 regulates Glut4 trafficking in 3T3-L1 adipocytes. *Molecular Biology of the Cell,* 14(7), pp. 2946-2958.

Peters, C. G., Miller, D. F. & Giovannucci, D. R., 2006. Identification, localization and interaction of SNARE proteins in atrial cardiac myocytes. *J Mol Cell Cardiol,* 40(3), pp. 361-374.

Pierce, K. E. & Wangh, L. J., 2007. Linear-after-the-exponential polymerase chain reaction and allied technologies. Real-time detection strategies for rapid, reliable diagnosis from single cells. *Methods Mol Med,* Volume 132, pp. 65-85.

Planas, J. V., Capilla, E. & Gutierrez, J., 2000. Molecular identification of a glucose transporter from fish muscle. *FEBS Lett,* 481(3), pp. 266-270.

Ploug, T. et al., 1998. Analysis of GLUT4 distribution in whole skeletal muscle fibers: identification of distinct storage compartments that are recruited by insulin and muscle contractions. *J Cell Biol,* 142(6), pp. 1429-1446.

Presley, J. F. et al., 1997. Bafilomycin A1 treatment retards transferrin receptor recycling more than bulk membrane recycling. *J Biol Chem,* 272(21), pp. 13929-13936.

Public Health Agency of Canada, 2009. *Tracking Heart Disease and Stroke in Canada,* Canada: s.n.

Public Health Agency of Canada, 2011. *Unpublished analysis using 2008/09 data from the Canadian Chronic Disease Surveillance System,* s.l.: s.n.

Ramm, G., Slot, J. W., James, D. E. & Stoorvogel, W., 2000. Insulin recruits GLUT4 from specialized VAMP2-carrying vesicles as well as from the dynamic endosomal/trans-golgi network in rat adipocytes. *Mol Biol Cell,* 11(12), pp. 4079-4091.

Ren, J. M. et al., 1993. Evidence from transgenic mice that glucose transport is rate-limiting for glycogen deposition and glycolysis in skeletal muscle. *J Biol Chem,* 268(22), pp. 16113-16115.

Rothman, J., 1994. Mechanisms of intracellular protein transport. *Nature,* 372(6501), pp. 55-63.

Rubler, S. et al., 1972. New type of cardiomyopathy associated with diabetic glomerulosclerosis. *American Journal of Cardiology,* Volume 30, pp. 595-602.

Saito, K. et al., 2011. An enzymatic photometric assay for 2-deoxyglucose uptake in insulin-responsive tissues and 3T3-L1 adipocytes. *Anal Biochem,* 412(1), pp. 9-17.

Sakamoto, T., Amitani, I., Yokota, E. & Ando, T., 2000. Direct observation of processive movement by individual myosin V molecules. *Biochem Biophys Res Commun,* 272(2), pp. 586-590.

Sargeant, R. J. & Pâquet, M. R., 1993. Effect of insulin on the rates of synthesis and degradation of GLUT1 and GLUT4 glucose transporters in 3T3-L1 adipocytes. *Biochem J,* 290(Pt 3), pp. 913-919.

Schafer, J. C. et al., 2014. Rab11-FIP2 interaction with MYO5B regulates movement of Rab11a-containing recycling vesicles. *Traffic,* 15(3), pp. 292-308.

Schertzer, J. D. et al., 2009. A transgenic mouse model to study glucose transporter 4myc regulation in skeletal muscle. *Endocrinology,* 150(4), pp. 1935-1940.

Scheuermann-Freestone, M. et al., 2003. Abnormal cardiac and skeletal muscle energy metabolism in patients with type 2 diabetes. *Circulation,* 107(24), pp. 3040-3046.

Scholz, T. D. & Segar, J. L., 2008. Cardiac Metabolism in the Fetus and Newborn. *NeoReviews,* 9(3), pp. 109-118.

Schwenk, R. W. & Eckel, J., 2007. A novel method to monitor insulin-stimulated GTP-loading of Rab11a in cardiomyocytes. *Cell Signal,* 19(4), pp. 825-830.

Serpillon, S. et al., 2009. Superoxide production by NAD(P)H oxidase and mitochondria is increased in genetically obese and hyperglycemic rat heart and aorta before the development of cardiac dysfunction. The role of glucose-6-phosphate dehydrogenase-derived NADPH. *Am J Physiol Heart Circ Physiol,* 297(1), pp. 153-162.

Shao, D. & Tian, R., 2015. Glucose Transporters in Cardiac Metabolism and Hypertrophy. *Compr Physiol,* 1(331-351), p. 6.

Shen, Y., Rosendale, M., Campbell, R. E. & Perrais, D., 2014. pHuji, a pH-sensitive red fluorescent protein for imaging of exo- and endocytosis. *J Cell Biol,* 207(3), pp. 419-432.

Shewan, A. M. et al., 2003. GLUT4 recycles via a trans-Golgi network (TGN) subdomain enriched in Syntaxins 6 and 16 but not TGN38: involvement of an acidic targeting motif. *Mol Biol Cell,* 14(3), pp. 973-986.

Shibata, H., Omata, W. & Kojima, I., 1997. Insulin stimulates guanine nucleotide exchange on Rab4 via a wortmannin-sensitive signaling pathway in rat adipocytes. *J Biol Chem,* 272(23), pp. 14542-14546.

Shigematsu, S., Watson, R. T., Khan, A. H. & Pessin, J. E., 2003. The adipocyte plasma membrane caveolin functional/structural organization is necessary for the efficient endocytosis of GLUT4. *J Biol Chem,* 278(12), pp. 10683-10690.

Shi, J., Kandror & K, V., 2005. Sortilin is essential and sufficient for the formation of Glut4 storage vesicles in 3T3-L1 adipocytes. *Dev Cell,* 9(1), pp. 99-108.

Singh, R., Barden, A., Mori, T. & Beilin, L., 2001. Advanced glycation end-products: a review. *Diabetologia,* 44(2), pp. 129-146.

Sollner, T. et al., 1993. A protein assembly – disassembly pathway in vitro that may correspond to sequential steps of synaptic vesicle docking, activation, and fusion. *Cell,* 75(3), pp. 409-418.

Sollner, T. et al., 1993. SNAP receptors implicated in vesicle targeting and fusion. *Nature,* 362(6418), pp. 318-324.

Sönnichsen, B. et al., 2000. Distinct membrane domains on endosomes in the recycling pathway visualized by multicolor imaging of Rab4, Rab5, and Rab11. *J Cell Biol,* 149(4), pp. 901-914.

Stanley, W. C., Lopaschuk, G. D., Hall, J. L. & McCormack, J. G., 1997. Regulation of myocardial carbohydrate metabolism under normal and ischaemic conditions. Potential for pharmacological interventions. *Cardiovasc Res,* 33(2), pp. 243-257.

Stanley, W. C., Recchia, F. A. & Lopaschuk, G. D., 2005. Myocardial substrate metabolism in the normal and failing heart. *Physiol Rev,* 85(3), pp. 1093-1129.

Statistics Canada, 2014. *Leading causes of death, total population, by age group and sex, Canada, annual,* Canada: CANSIM (database).

Stenmark, H., 2009. Rab GTPases as coordinators of vesicle traffic. *Nat Rev Mol Cell Biol,* 10(8), pp. 513-525.

Stenmark, H., Vitale, G., Ullrich, O. & Zerial, M., 1995. Rabaptin-5 is a direct effector of the small GTPase Rab5 in endocytic membrane fusion. *Cell,* 83(3), pp. 423-432.

Subtil, A., Lampson, M. A., Keller, S. R. & McGraw, T. E., 2000. Characterization of the insulin-regulated endocytic recycling mechanism in 3T3-L1 adipocytes using a novel reporter molecule. *J Biol Chem,* 275(7), pp. 4787-4795.

Sudhof, T. C. & Rothman, J. E., 2009. Membrane fusion: grappling with SNARE and SM proteins. *Science,* 323(5913), pp. 474-477.

Sun, Y., Bilan, P. J., Liu, Z. & Klip, A., 2010. Rab8A and Rab13 are activated by insulin and regulate GLUT4 translocation in muscle cells. *Proc Natl Acad Sci U S A,* 107(46), pp. 19909-19914.

Takahashi, S. et al., 2012. Rab11 regulates exocytosis of recycling vesicles at the plasma membrane. *J Cell Sci,* 125(17), pp. 4049-4057.

Tao, R. et al., 2010. AMPK exerts dual regulatory effects on the PI3K pathway. *J Mol Signal,* 5(1), pp. 1-9.

Tozzo, E., Gnudi, L. & Kahn, B. B., 1997. Amelioration of insulin resistance in streptozotocin diabetic mice by transgenic overexpression of GLUT4 driven by an adipose-specific promoter. *Endocrinology,* 138(4), pp. 1604-1611.

Turke, A. B. et al., 2012. MEK inhibition leads to PI3K/AKT activation by relieving a negative feedback on ERBB receptors. *Cancer Res,* 72(13), pp. 3228-3237.

U.S. Department of Agriculture and U.S. Department of Health and Human Services, 2011. Dietary Guidelines for Americans, 2010. *Advances in Nutrition,* 2(3), pp. 293-294.

Ungvári, Z. et al., 2005. Role of oxidative-nitrosative stress and downstream pathways in various forms of cardiomyopathy and heart failure. *Curr Vasc Pharmacol,* 3(3), pp. 221-229.

Upadhyay, R. et al., 2015. Role of SLMAP genetic variants in susceptibility of diabetes and diabetic retinopathy in Qatari population. *J Transl Med,* 13(61).

Van-Weert, A. W. et al., 1995. Transport from late endosomes to lysosomes, but not sorting of integral membrane proteins in endosomes, depends on the vacuolar proton pump. *J Cell Biol,* 130(4), pp. 821-834.

Wang, J. et al., 2011. Inhibition of aldehyde dehydrogenase 2 by oxidative stress is associated with cardiac dysfunction in diabetic rats. *Mol Med,* 17(3-4), pp. 172-179.

Wang, Z. et al., 2013. Inhibition of protein kinase C βII isoform rescues glucose toxicity-induced cardiomyocyte contractile dysfunction: Role of mitochondria. *Life Sci,* 93(2-3), pp. 116-124.

Ward, E. S. et al., 2005. From Sorting Endosomes to Exocytosis: Association of Rab4 and Rab11 GTPases with the Fc Receptor, FcRn, during Recycling. *Mol Biol Cell,* 16(4), pp. 2028-2038.

Wells, A. L. et al., 1999. Myosin VI is an actin-based motor that moves backwards. *Nature,* 401(6752), pp. 505-508.

Wijesekara, N., Tung, A., Thong, F. & Klip, A., 2006. Muscle cell depolarization induces a gain in surface GLUT4 via reduced endocytosis independently of AMPK. *Am J Physiol Endocrinol Metab,* 290(6), pp. 1276-1286.

Williams, B. & Howard, R. L., 1994. Glucose-induced changes in Na+/H+ antiport activity and gene expression in cultured vascular smooth muscle cells. Role of protein kinase C. *J Clin Invest,* 93(6), pp. 2623-2631.

Williams, D., Hicks, S. W., Machamer, C. E. & Pessin, J. E., 2006. Golgin-160 is required for the Golgi membrane sorting of the insulin-responsive glucose transporter GLUT4 in adipocytes. *Mol Biol Cell,* 17(12), pp. 5346-5355.

Williams, D. & Pessin, J. E., 2008. Mapping of R-SNARE function at distinct intracellular GLUT4 trafficking steps in adipocytes. *J Cell Biol,* 180(2), pp. 375-387.

Wiseman, D. A., Kalwat, M. A. & Thurmond, D. C., 2011. Stimulus-induced S-nitrosylation of Syntaxin 4 impacts insulin granule exocytosis. *J Biol Chem,* 286(18), pp. 16344-16354.

Wisneski, J. A. et al., 1985. Metabolic fate of extracted glucose in normal human myocardium. *J Clin Invest,* 76(5), pp. 1819-1827.

Wisneski, J. A., Gertz, E. W., Neese, R. A. & Mayr, M., 1987. Myocardial metabolism of free fatty acids. Studies with 14C-labeled substrates in humans. *J Clin Invest,* 79(2), pp. 359-366.

Woodman, P. G., 2000. Biogenesis of the sorting endosome: the role of Rab5. *Traffic,* 1(9), pp. 695-701.

Wu, S. B. & Wei, Y. H., 2012. AMPK-mediated increase of glycolysis as an adaptive response to oxidative stress in human cells: implication of the cell survival in mitochondrial diseases. *Biochim Biophys Acta,* 1822(2), pp. 233-247.

Yang, J. & Holman, G. D., 2005. Insulin and contraction stimulate exocytosis, but increased AMP-activated protein kinase activity resulting from oxidative metabolism stress slows endocytosis of GLUT4 in cardiomyocytes. *J Biol Chem,* 280(6), pp. 4070-4078.

Yang, Q. & Li, Y., 2007. Roles of PPARs on regulating myocardial energy and lipid homeostasis. *J Mol Med (Berl),* 85(7), pp. 697-706.

Ye, G. et al., 2004. Catalase protects cardiomyocyte function in models of type 1 and type 2 diabetes. *Diabetes,* 53(5), pp. 1336-1343.

Yoshizaki, T. et al., 2007. Myosin 5a is an insulin-stimulated Akt2 (protein kinase Bbeta) substrate modulating GLUT4 vesicle translocation. *Mol Cell Biol,* 27(14), pp. 5172-5183.

Yu, C., Cresswell, J., Löffler, M. G. & Bogan, J. S., 2007. The glucose transporter 4-regulating protein TUG is essential for highly insulin-responsive glucose uptake in 3T3-L1 adipocytes. *J Biol Chem,* 282(10), pp. 7710-7722.

Zannella, V. E. et al., 2011. AMPK regulates metabolism and survival in response to ionizing radiation. *Radiother Oncol,* 99(3), pp. 293-299.

Zeigerer, A. et al., 2002. GLUT4 retention in adipocytes requires two intracellular insulin-regulated transport steps. *Mol Biol Cell,* 13(7), pp. 2421-2435.

Zerial, M. & McBride, H., 2001. Rab Proteins as Membrane Organizers. *Nat Rev Mol Cell Biol,* 2(2), pp. 107-117.

Zhang, J. et al., 2012. Measuring energy metabolism in cultured cells, including human pluripotent stem cells and differentiated cells. *Nat Protoc,* 7(6), pp. 1068-1085.

Zhou, Q. L. et al., 2004. Analysis of insulin signalling by RNAi-based gene silencing. *Biochemical Society Transactions,* 32(5), pp. 817-821.

Zhu, G. et al., 2004. Structural basis of Rab5-Rabaptin5 interaction in endocytosis. *Nat Struct Mol Biol,* 11(10), pp. 975-983.

Zisman, A. et al., 2000. Targeted disruption of the glucose transporter 4 selectively in muscle causes insulin resistance and glucose intolerance. *Nat Med,* 6(8), pp. 924-928.

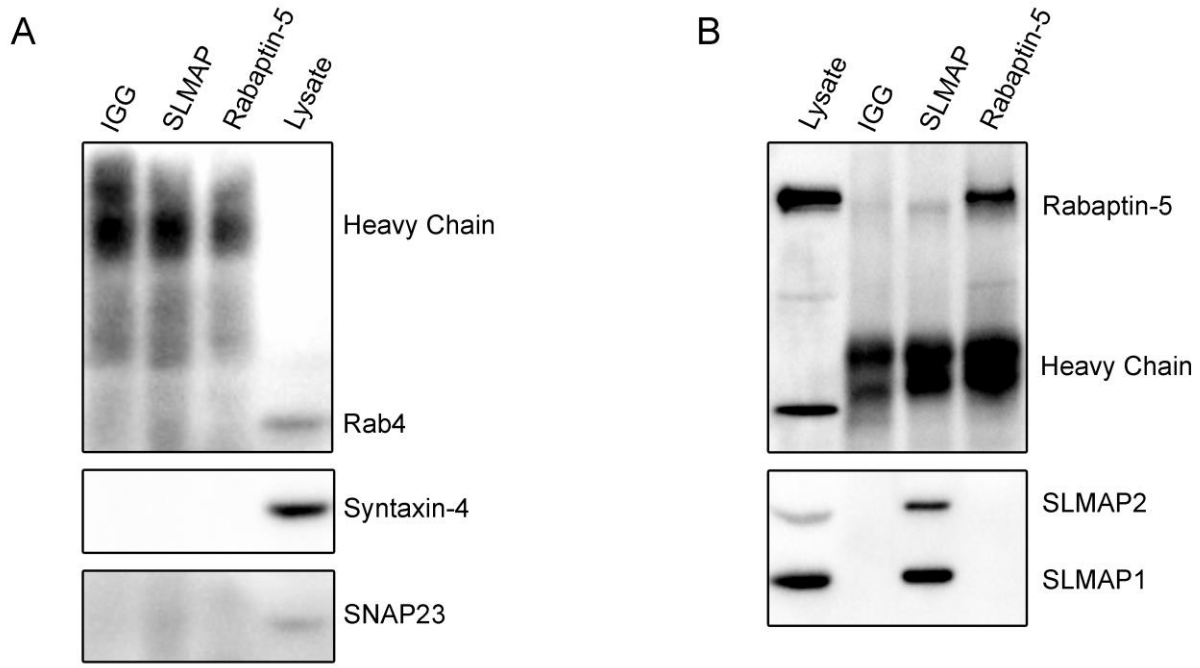

Appendix 1. *Immunoprecipitation of SLMAPs and Rabaptin-5, but not Rab4, Syntaxin-4 or SNAP23*. Protein lysate obtained from adult mouse hearts were immunoprepitated for complexes containing SLMAP and Rabaptin-5 proteins using anti-SLMAP and anti-Rabaptin-5 respectively, with anti-IGG as a control. (**A**) Rab4, Syntaxin-4, and SNAP23 were not present in complexes with SLMAP proteins. (**B**) SLMAP does not present in complex with Rabaptin-5. Rabaptin-5 immunoprecipitation did not contain SLMAP proteins, while SLMAP immunoprecipitation did not contain Rabaptin-5.

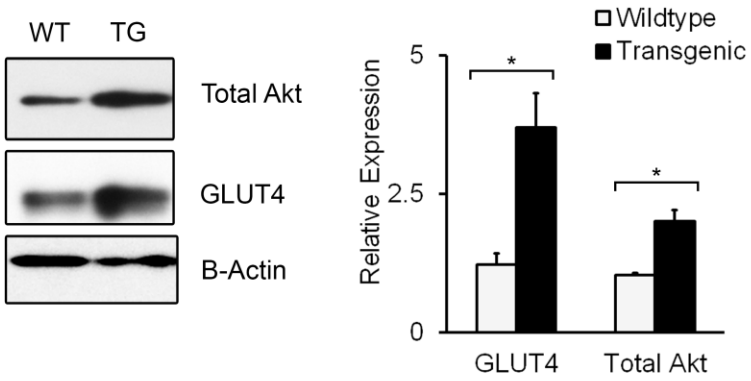

Appendix 2. *GLUT4 and Akt expression in neonatal cardiomyocytes.* Protein extracted from day one old neonatal cardiomyocytes was quantified using Western Blot densitometry analysis with β-actin as a loading control. Anti-GLUT4 and anti-Akt was used to probe for GLUT4 and total Akt expression respectively and anti- β-actin was used to quantify β-actin expression. GLUT4 expression was increased in transgenic cardiomyocytes (200% ± 61%, n=7, $P<0.01$ using two-tailed t-test) compared to wildtype littermates. Total Akt expression was increased in transgenic cardiomyocytes (95% ± 20%, n=7, $P<0.01$ using two-tailed t-test) compared to wildtype littermates.